NAVAL POSTGRADUATE SCHOOL

MONTEREY, CALIFORNIA

THESIS

OXIDATION BEHAVIOR OF OXIDE PARTICULATE REINFORCED TITANIUM COMPOSITES FABRICATED BY SELECTIVE LASER MELTING

by

Andrew J. Reinhart

June 2020

Thesis Advisor: Andy Nieto
Second Reader: Garth V. Hobson

THIS PAGE INTENTIONALLY LEFT BLANK

REPORT DOCUMENTATION PAGE	*Form Approved OMB No. 0704-0188*

1. AGENCY USE ONLY *(Leave blank)*	**2. REPORT DATE** June 2020	**3. REPORT TYPE AND DATES COVERED** Master's thesis

4. TITLE AND SUBTITLE
OXIDATION BEHAVIOR OF OXIDE PARTICULATE REINFORCED TITANIUM COMPOSITES FABRICATED BY SELECTIVE LASER MELTING

5. FUNDING NUMBERS

6. AUTHOR(S) Andrew J. Reinhart

7. PERFORMING ORGANIZATION NAME(S) AND ADDRESS(ES)
Naval Postgraduate School
Monterey, CA 93943-5000

8. PERFORMING ORGANIZATION REPORT NUMBER

9. SPONSORING / MONITORING AGENCY NAME(S) AND ADDRESS(ES)
N/A

10. SPONSORING / MONITORING AGENCY REPORT NUMBER

11. SUPPLEMENTARY NOTES The views expressed in this thesis are those of the author and do not reflect the official policy or position of the Department of Defense or the U.S. Government.

12a. DISTRIBUTION / AVAILABILITY STATEMENT
Approved for public release. Distribution is unlimited.

12b. DISTRIBUTION CODE
A

13. ABSTRACT (maximum 200 words)

This thesis project mixed additive manufacturing (AM) feedstock powders of Ti-6Al-4V with 1% and 3% by volume reinforcements of Al_2O_3 and Ta_2O_5. These powders were printed using the MAE selective laser melting (SLM) printer, after which they were subjected to mechanical testing such as indentation testing and isothermal oxidation testing. Microstructural characterization was conducted using optical microscopes and scanning electron microscope (SEM) capabilities, and energy dispersive x-ray spectroscopy (EDS) maps were produced to determine homogeneity of the composite microstructure. Imaging in the SEM revealed that the sample of Ti-6Al-4V reinforced with 1% by volume of Ta_2O_5 experienced about 50% less oxidation in terms of oxidation layer thickness than the control sample fabricated using only commercial Ti-6Al-4V feedstock powder. Furthermore, this titanium-tantalum oxide composite exhibited a higher hardness and higher elastic modulus during both nano and micro indentation testing when compared to the control sample. Both Ti-6Al-4V Al_2O_5 specimens and the Ta_2O_5 3% sample had worse mechanical properties than the control sample; however, the work spent fabricating these new materials revealed many of the potential pitfalls in composite additive manufacturing and offered insight into how to produce titanium composites via SLM for future work.

14. SUBJECT TERMS additive manufacturing, titanium, oxides, scanning electron microscope, an-isotropic	**15. NUMBER OF PAGES** 123
	16. PRICE CODE

17. SECURITY CLASSIFICATION OF REPORT	**18. SECURITY CLASSIFICATION OF THIS PAGE**	**19. SECURITY CLASSIFICATION OF ABSTRACT**	**20. LIMITATION OF ABSTRACT**
Unclassified	Unclassified	Unclassified	UU

NSN 7540-01-280-5500

Standard Form 298 (Rev. 2-89)
Prescribed by ANSI Std. 239-18

THIS PAGE INTENTIONALLY LEFT BLANK

Approved for public release. Distribution is unlimited.

OXIDATION BEHAVIOR OF OXIDE PARTICULATE REINFORCED TITANIUM COMPOSITES FABRICATED BY SELECTIVE LASER MELTING

Andrew J. Reinhart
Ensign, United States Navy
BSE, United States Naval Academy, 2019

Submitted in partial fulfillment of the
requirements for the degree of

MASTER OF SCIENCE IN MECHANICAL ENGINEERING

from the

NAVAL POSTGRADUATE SCHOOL
June 2020

Approved by: Andy Nieto
Advisor

Garth V. Hobson
Second Reader

Garth V. Hobson
Chair, Department of Mechanical and Aerospace Engineering

THIS PAGE INTENTIONALLY LEFT BLANK

ABSTRACT

This thesis project mixed additive manufacturing (AM) feedstock powders of Ti-6Al-4V with 1% and 3% by volume reinforcements of Al_2O_3 and Ta_2O_5. These powders were printed using the MAE selective laser melting (SLM) printer, after which they were subjected to mechanical testing such as indentation testing and isothermal oxidation testing. Microstructural characterization was conducted using optical microscopes and scanning electron microscope (SEM) capabilities, and energy dispersive x-ray spectroscopy (EDS) maps were produced to determine homogeneity of the composite microstructure. Imaging in the SEM revealed that the sample of Ti-6Al-4V reinforced with 1% by volume of Ta_2O_5 experienced about 50% less oxidation in terms of oxidation layer thickness than the control sample fabricated using only commercial Ti-6Al-4V feedstock powder. Furthermore, this titanium-tantalum oxide composite exhibited a higher hardness and higher elastic modulus during both nano and micro indentation testing when compared to the control sample. Both Ti-6Al-4V Al_2O_5 specimens and the Ta_2O_5 3% sample had worse mechanical properties than the control sample; however, the work spent fabricating these new materials revealed many of the potential pitfalls in composite additive manufacturing and offered insight into how to produce titanium composites via SLM for future work.

THIS PAGE INTENTIONALLY LEFT BLANK

TABLE OF CONTENTS

THIS PAGE INTENTIONALLY LEFT BLANK

LIST OF FIGURES

LIST OF TABLES

THIS PAGE INTENTIONALLY LEFT BLANK

LIST OF ACRONYMS AND ABBREVIATIONS

Al_2O_3	aluminum oxide, commonly known as alumina
AM	additive manufacturing
BCC	body centered cubic
CNC	computer numerical control
EOS	Electro-Optical Systems
GTE	gas turbine engine
HCP	hexagonal close packed
HEBM	high energy ball milling
MCF	matrix coated fiber
MMC	metal matrix composite
PVD	physical vapor deposition
RP	rapid prototyping
SEM	scanning electron microscope
SLM	selective laser melting
STL	stereolithography
Ta_2O_5	tantalum oxide
Ti-6Al-4V	titanium alloy with approximately 6 weight percent aluminum and 4 weight percent vanadium

THIS PAGE INTENTIONALLY LEFT BLANK

ACKNOWLEDGMENTS

First and foremost, I would like to thank my advisor, Dr. Nieto. Working with him on my thesis has been a pleasure. I would like to acknowledge the role Dr. Smith and Mr. Kohlgrueber played in training me on how to use the MAE SLM printer, and then helping me run the printer when I experienced challenges with the novel materials. Additionally, John Mobley and the MAE machine shop were of great assistance in helping me get my samples ready in a timely fashion. Finally, Dr. Ansell and Dr. Chanman helped me through the sample preparation process by assisting me both with polishing and the use of the SEM. Thank you all for your time; I could not have done this without you.

I would also like to thank Dr. Tien Roehling and Captain Baker. The two of them played an instrumental role introducing me to the fields of material science, and additive manufacturing in particular, during my undergraduate study. Their mentorship was what gave me the desire to pursue a master's degree in mechanical engineering with a focus on materials research.

THIS PAGE INTENTIONALLY LEFT BLANK

I. BACKGROUND AND MOTIVATION

A. BACKGROUND OF AM

In traditional manufacturing, parts are made from raw metal through subtractive processes that use machinery such as a mill or a lathe to cut away unwanted material and thereby obtain a desired shape. In additive manufacturing (AM), parts are built from a raw material powder or liquid that is built up layer by layer until an entire piece has been completed.

1. Historic Introduction of AM

AM was first used on the commercial scale in 1987 with the advent of stereolithography (STL) machines. These devices utilized a laser to cure thin layers of ultraviolet-sensitive liquid polymer and create a solid structure [1]. This novel technique offered many advantages over traditional manufacturing, and led to the desire to use AM on metals in addition to plastics. In 1992, selective laser melting machines (SLM) were developed for commercial use, which allowed for the AM of metal powders [1]. SLM is a process where metal powder is deposited on a build plate, then melted in a fast pass by a high energy laser (see Figure 1 for an example). Once the melted powder has fused, another layer of powder is coated onto the build plate and this process is repeated.

SLM was originally commercially used as a way to conduct rapid prototyping (RP). In rapid prototyping, a company creates models of a completed part with no intention of using this same manufacturing method for mass production [2]. Rapid prototyping is conducted to facilitate visualization of the product for both the design team and the potential customers, and to help to detect potential problems ahead of mass production.

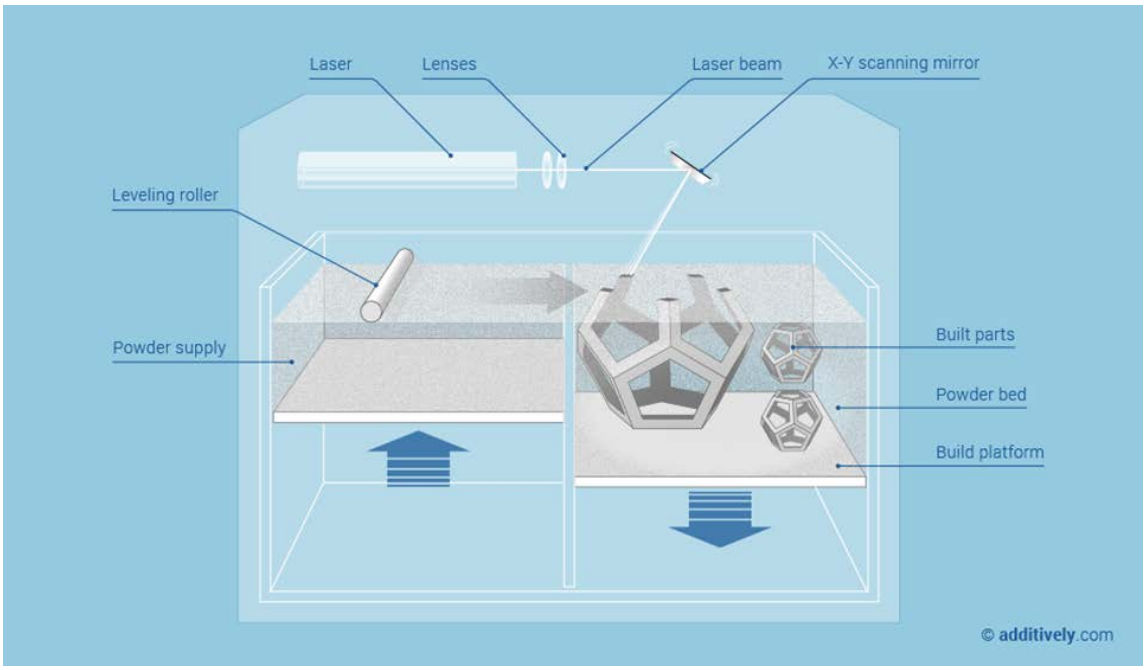

Figure 1. Selective Laser Melting (SLM) Infographic. Source: [3].

2. Current Uses of AM

Two decades after its introduction to commercial use, AM is no longer solely used for RP. Enough research and production have been conducted such that parts have begun to be built for use in load bearing applications. Companies such as General Electric have begun development of AM components for use in applications such as gas turbine engines, and the novel building process has resulted in higher efficiencies through complex new geometries for everything from heat shields to turbine engines [4]. Specifically, additive manufacturing of the titanium-aluminum-vanadium alloy Ti-6Al-4V has dramatically increased as laser sintering technology expanded. This is particularly important for aerospace applications as Ti-6Al-4V has a high strength to weight ratio, and has excellent corrosion resistance at high temperatures like those experienced in a gas turbine engine [5]. AM will continue to expand to be used in a wider variety of high-end applications as the mechanical properties of 3-D printed parts continue to improve.

B. BENEFITS OF AM

AM has many benefits over traditional manufacturing. The following sections outline some of the most commonly cited benefits of AM [6].

1. Versatility in Design

AM offers more freedom than traditional manufacturing as it is not limited to the precision of machining tools, casts, welds, or other manufacturing techniques. Because parts are built layer by layer, they can be designed to have complex internal geometry than would be possible with a traditional manufacturing method. This presents opportunities to reduce a structure's overall weight, which can be critical in many applications. Additionally, internal structures can have specific designs to manage heat loss, or increase airflow, or perform countless other functions [7].

2. Mass Customization

Because AM produces parts one at a time, individual builds can be highly customized to suit the intended application. This contrasts with traditional manufacturing techniques such as casting, as parts would be limited to the molds available and it would be uneconomical to make a different mold for every part. Furthermore, a single AM machine could theoretically produce parts that would normally require multiple traditional manufacturing machines and long work hours from a machinist [8]. In this way, AM can be both a cost-saving measure and a space-saving measure if it eliminates the need for an entire machine shop. Mass customization also has increasing importance in both commercial and military applications as traditional manufacturing has declined in the 21st century; many legacy systems are no longer in production and replacement parts are no longer available. One AM machine could create replacements on an as-needed basis, allowing for continued operation of legacy platforms. This could reduce or eliminate the requirement for a supply chain, and offers potential to build parts on site—a promising feature when replacements could be needed quickly—at a forward operating base, at sea, or in a space application; areas logistically difficult or impossible to reach.

3. Elimination of Waste Product

In SLM, metal powder that is not melted by the laser is collected and can be reused to build new parts without negative effects. A 2017 study conducted by the University of New Brunswick demonstrated that both the microstructure and tensile strength of parts made via SLM using recycled powder were not significantly different from parts made of using fresh powder [9]. The number of cycles which powder can be reused is without negative impacts is a topic that has been extensively researched; some studies have recycled powder over 30 times with no ill effects noted [10]. In contrast, traditional subtractive manufacturing techniques typically cut out parts from sheet metal. The waste sheet metal would need to undergo extensive costly processing in order to be turned into new sheets that could be cut again with similar mechanical properties, and most facilities will scrap the waste material as they lack this capability. This is important not just from an environmental perspective, but also from a cost perspective as some high-performance alloys can be extremely expensive. In traditional manufacturing, up to 98% of the original metal may be discarded as waste during the process of machining the part down to the desired shape [11]. When using high-cost alloys, this waste has a high associated expense; SLM eliminates this expense.

4. Highly Adaptable

One of the chief benefits of developing new techniques with AM is that they can quickly be put into production. Typically, the time between materials development, implementation, and full-scale production can span years if not decades. As mentioned in the general background of AM section, one of the first uses of AM was RP. This is because AM allows for much faster creation of parts than traditional manufacturing. For this same reason, new techniques using as novel materials, laser beam rastering speeds, different shapes of laser beams, and other machine parameters can quickly get put into use at the commercial level as AM is by design highly adaptable. A newly created metal powder with better mechanical properties or a new laser optimization could theoretically go from design and testing to commercial use in the time frame of months to years instead of years to decades with traditional manufacturing. This is part of why the scientific interest in AM is

as high as it currently is—if novel materials are developed for AM, they have increased viability for commercial use as the cost of adapting to employ the new materials is low.

C. DRAWBACKS OF AM

AM is not without drawbacks, however. The following list includes some of the most commonly encountered issues regarding AM.

1. Anisotropic Completed Parts

One of the main issues with components produced via laser sintering is that they tend to have high levels of anisotropy in the direction the part was built, and this can limit their feasibility for use in load-bearing applications [12]. This is almost impossible to avoid with AM, as by the very nature of the AM the parts will be built in layers in the vertical direction. Anisotropy is generally undesirable as it requires knowledge of exactly how the part will be put under stress in order to ensure the stress does not reach endurance or yield limits in the direction with lower mechanical strength. In order to avoid or mitigate anisotropy in the completed part, a significant knowledge base regarding both the SLM machine and the material used is required to optimize the building parameters. Furthermore, the design of the part will require more work to take into account differing material properties in different directions. Figure 2 demonstrates the layer-by-layer build effects, which in turn result in anisotropic material properties.

Figure 2. SEM Imaging of Layer-by-Layer Build Part.
Source: [13].

2. Higher Costs Due to Slow Build Times

Although the cost of a SLM printer can be significantly lower than the price of an entire machine shop, when the versatility of AM is not required a traditional manufacturing technique can be used to make a part for a fraction of the price. For instance, for builds with simple geometries, using AM would not make economic sense as AM machines tend to take a long time to build parts irrespective of geometry. Likewise, where waste minimization is not important, sheet metal for traditional manufacturing techniques is often substantially cheaper than the metal powders required for AM. Furthermore, the long build times associated with AM mean that if producing an identical product on a mass-production scale, AM is often not the cheapest or fastest choice. For these reasons, AM often only makes economic sense for producing complex parts in smaller quantities from expensive, high-performance alloys. When these three conditions are met, however, the specific cost of additive manufacturing can be up to 30% lower than the costs of traditional manufacturing [11].

3. Small Build Volumes

SLM is limited in terms of how large the finalized product can be based on the machine used. For most commercially available AM machines this means that engineers can only construct small parts using AM. For example, the EOS 100 M printer used in this study has a maximum build volume of 100 x 95 mm. This obviously limits the applications in which AM can be effectively used.

4. Post Processing Required

SLM will not result in a high enough quality surface finish for use in load bearing applications, and as a result post processing is required in order to improve the surface finish of the part before it may be used. SLM normally gives a raw surface finish with a roughness of about 8.75 μm [13]. For comparison, a mirror surface finish has a surface roughness of 0.025 μm. This poor finish can lead to worse mechanical properties and/or corrosion issues such as pitting. For parts produced by SLM, numerous processes can be used to improve the surface finish; the best will depend on the intended use of the product

and the requisite surface finish. A few of the processes that are more commonly used include the following:

- abrasive blast
- shot peen
- electrochemical polishing
- optical polishing
- CNC finishing. Source: [13]

D. TITANIUM BACKGROUND

Titanium is a high-performance material used in a variety of industries. This section is designed to give a brief overview of the mechanical properties of this metal, the different microstructures exhibited, and the commercial applications where it is commonly employed.

1. Desirable Mechanical Properties of Titanium Alloys

Titanium alloys are often used for their superior mechanical properties when compared to other aluminum, nickel, or steel alloys. In particular, the main reasons for using titanium are to reduce weight and size, allow for use at higher operating temperatures, increase corrosion resistance, and titanium's high degree of compatibility with composite materials from a galvanic standpoint [14]. Titanium alloys can provide significant weight savings, as titanium has a much higher strength-to-weight ratio. Steel may have a higher strength than titanium, but its much greater density makes it weight prohibitive in many aerospace applications. Titanium has a greater density than aluminum, but its significantly higher strength means that less material can be used, and substantial space savings can be achieved when compared to an aluminum structure bearing the same load. Titanium has a superior ultimate tensile strength when compared to many metals in elevated temperature applications, as seen in Figure 3. Titanium's inherent corrosion resistance is high enough that preventative measures such as paint are unnecessary so long as the titanium is not in contact with aluminum or low alloy steel. Contact between titanium and these metals would drive galvanic corrosion in the contact metal [14]. Titanium has a high degree of compatibility with polymer matrix composites (it will not result in galvanic corrosion when in contact with carbon fibers in composite materials), and this is increasingly important as

more aerospace platforms utilize composite structures. Aluminum and steel, by contrast, would result in galvanic corrosion with these composites.

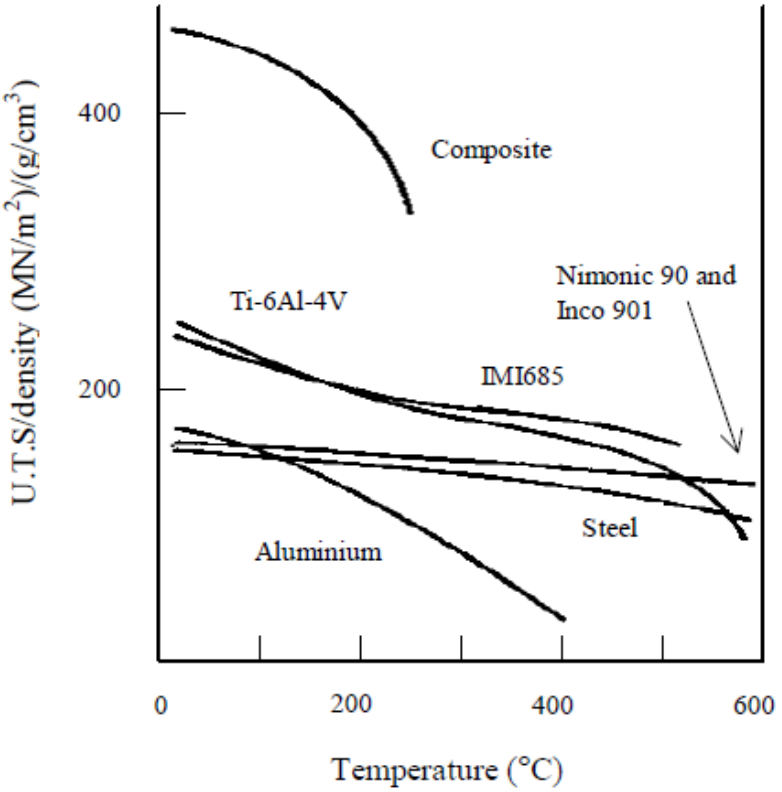

Figure 3. Tensile Strength vs. Temperature for Different Alloys. Source: [15].

2. Titanium Alloy Microstructure

Titanium has two different crystalline structures: hexagonal close packed (hcp, or the α phase) and body center cubic (bcc, or the β phase). Titanium will transition from its α phase to the β phase when treated to temperatures above 882° Celsius [15]. As such, titanium alloys can be divided into three subgroups based on whether they have α phase, β phase, or an α+β phase. Trace elements can be added to titanium to change which phases predominantly occur; those elements that increase the α phase are known as α stabilizers while the elements that increase the β phase are known as β stabilizers. Common α stabilizers include aluminum, oxygen, carbon, and nitrogen. Of these α stabilizers, only aluminum is generally considered desirable while the rest are generally considered

contaminants. This is because small amounts of weight percentages of aluminum can greatly increase the alloy's tensile strength and corrosion resistance, but oxygen, nitrogen and carbon result in microscopic hardening within the alloy. This hardening effect will decrease the ductility of the metal, thereby making it more susceptible to cracking [16]. Additionally, α alloys lack a ductile to brittle fracture behavior (which occurs in β alloys) making them the choice material for use in a cryogenic environment. Vanadium, molybdenum, iron, chromium and manganese are the predominantly used β stabilizers for titanium. β phase titanium, due to its bcc crystalline structure, tends to have better ductility and toughness when compared to α alloys, resulting in greatly improved fabricability [15].

For most manufacturing applications, a combination of the superior corrosion resistance and tensile strength offered by the α phase and the improved fabricability of the β phase is desired. For this reason, the most commonly used titanium alloys are α + β phase alloys. α + β phase alloys can be subjected to specific heat treatments in order to produce the specific phase ratio desired in order to have optimum performance in the intended final application. Ti-6Al-4V, in particular, is the most commonly used of all titanium alloys and "accounts for half of all titanium alloy manufactured" [16]. Table 1 lists some of the more commonly used titanium alloys and which phases they predominantly exhibit.

Table 1. Titanium Alloys and Their Predominant Phase.
Adapted from [15].

Titanium Alloy	**Microstructure**
Pure Titanium Ti-5Al-2.5-Sn	Pure α phase
Ti-8Al-1Mo-1V Ti-6Al-2Sn-4Zr-2Mo	α + β, predominantly α phase
Ti-6Al-4V Ti-6Al-2Sn-6V	α + β phase
Ti-6Al-2Sn-4Zr-6Mo Ti-3Al-10V-2Fe	α + β, predominantly β phase
Ti-13V-11Cr-3Al Ti-8Mo-8V-2Fe-3Al	Pure β phase

3. Industrial Uses of Titanium

As observed above, titanium has excellent, customizable material properties depending on its microstructure and can be processed or alloyed in such a manner as to work well in a wide variety of situations. Thus, the biggest limiting factor for titanium tends to be actually cost rather than lacking the requisite material properties. Titanium machining is significantly more expensive than machining of relatively softer metals (titanium machining is often ten times as expensive when compared to the cost of machining aluminum), and the actual titanium raw material itself can cost up to three times as much as steel or aluminum [14]. For this reason, the use of titanium is generally restricted to high tech applications.

Titanium is primarily used by the aerospace industry. Titanium alloys are often used to make components in aircraft gas turbine engines (GTE) since titanium offers a high strength-to-weight ratio at high operating temperatures. Turbine inlet temperatures can reach temperatures in excess of 1500° C, and even with advanced thermal barrier coatings and cooling designs the effective temperatures that turbine components are exposed to remain high [17]. Additionally, titanium is used in the airframe itself, and makes up about 7% of the total weight in commercial planes and 20–25% of the weight in military aircraft [18].

The use of titanium is not limited to the aerospace industry, however. Titanium is often the material of choice for steam condensers and heat exchangers (both applications where corrosion resistance and strength at high temperatures are essential). Titanium is used in marine engineering and chemical plants for these same reasons. Titanium is also extensively used in the health care industry. Titanium's β phase alloys have a low modulus of elasticity that is similar to that of bone, making β phase alloys excellent for implants in both orthodontics and general medicine [14].

E. ADVANCED METAL MATRIX COMPOSITES

Metal matrix composites (MMCs) have been a research topic of high interest for decades, as these materials theoretically offer much greater mechanical properties in

elevated thermal conditions than traditional alloys. In the past twenty years, these advanced materials have gone from laboratory use to mass production, as industries ranging from the aerospace industry to automobile industry have adopted metal matrix composites for widespread use.

1. MMCs Basic Background

MMCs are specially fabricated materials that include a base metal with a reinforcing constituent added to the metallic matrix. These constituents are usually added to the matrix in one of three ways: either as continuous fibers, short fibers, or particles. These three methods are depicted in Figure 4. These constituents impede the dislocation motion of the metal matrix, resulting in dispersion and/or precipitation hardening in the metal sample. Typically, low volume fractions are used to maintain the ductility of the final product, but in applications requiring high temperature strength and creep resistance, constituents may reach as high as 15% by volume [19]. Specifically, oxide particulates are often used in higher concentrations as these particulates have high thermal stability. Most types of constituents added are ceramics, but refractory metals may also be used in certain applications. [20] MMCs are produced by a variety of methods, including casting, powder metallurgy, and foil-and-fiber pressing techniques. [21]

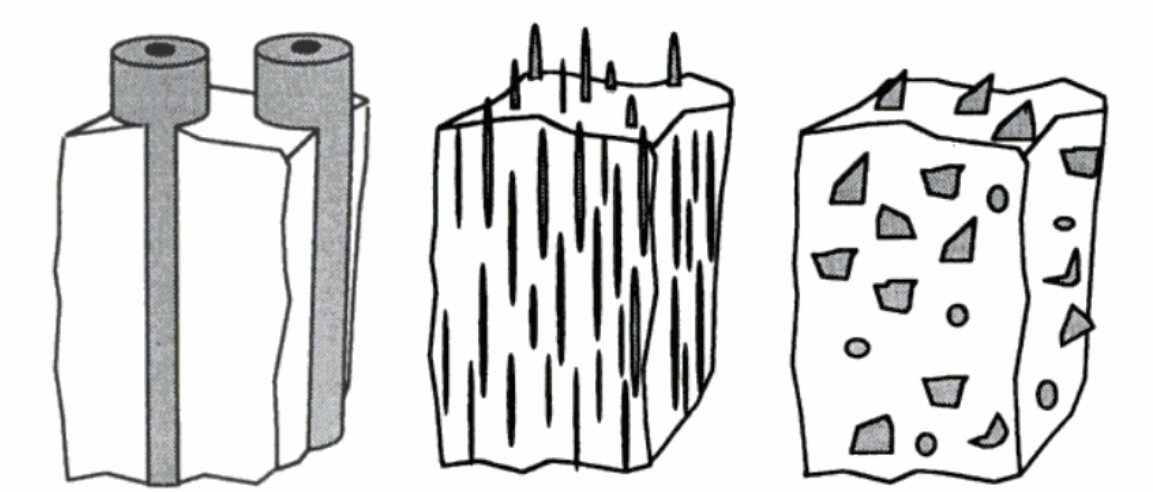

From left to right: monofilaments, whiskers/staple fibers, and particulates

Figure 4. The Three Types of MMCs. Source: [19].

2. Benefits of MMCs

The benefits of MMCs include the following:

- Low Density
- High Specific Strength
- High Specific Modulus
- High Thermal Conductivity
- Good Fatigue Response
- Control of Thermal Expansion
- High Abrasion Resistance
- High Wear Resistance
- Reduced Weight. Source: [20]

In general, MMC are often extremely attractive for use in elevated temperature applications where weight is important design consideration. They offer improved stiffness and strength while reducing weight when compared to traditional metal materials. Figure 5 demonstrates how adding reinforcing phase to metals such as aluminum, titanium, and nickel can greatly increase the specific strength of these materials, particularly when in use at elevated temperatures.

Another extremely important benefit is that MMCs have such a wide variety of capabilities depending on what material is used as a constituent, what type method is used

to create the material, and which form the composite takes within the metal matrix that MMCs can be designed to have exactly the necessary properties for their intended application. For example, a specific part made of an MMC material can have a specific strength and stiffness in one direction as needed for its application, and can have a different coefficient of thermal expansion in a separate direction, in order to best meet the demands of its intended end use [21]. Monolithic materials are generally isotropic, and even when they are anisotropic they still lack the level of customization that is associated with MMC. A final benefit to MMCs is that when the MMCs are created in such a way as to have aligned fibers, the strength and stiffness in the direction of the fibers is often great enough that MMCs may be used directly in components such as stiffeners and struts without requiring any transverse reinforcement due to their much greater strength in the direction the fibers are oriented [21].

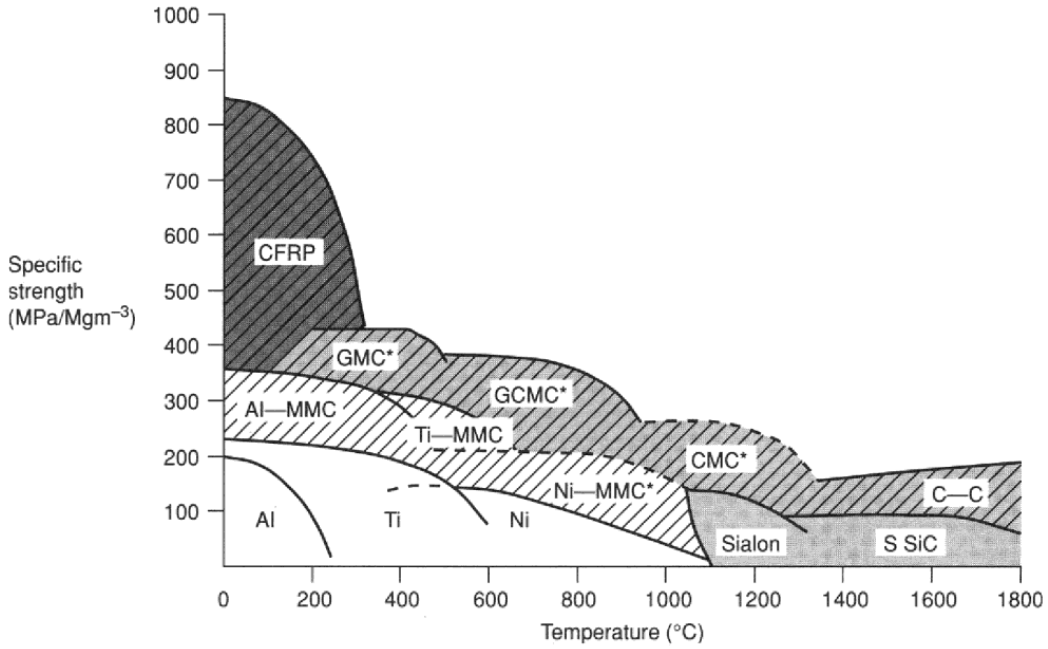

CFRP, carbon fiber reinforced polymers; GMC, glass-matrix composites; GCMC, glass-ceramic matrix composites; CMC; ceramic-matrix composites; MMC; metal-matrix composites; C-C, carbon-carbon composites.

Figure 5. Specific Strengths vs. Temperature for Advanced Composite Materials. Source: [20].

3. Limitations of MMCs

As with almost every advanced engineering material, one of the primary disadvantages associated with MMCs is cost. The reasons for increased costs of MMC are twofold: first, MMCs require the addition of costly composite materials. These materials can take three separate forms: monofilaments, whiskers/staple fibers, or particulates. The monofilaments are the most difficult to produce and therefore the most expensive, the whiskers/staple fibers offer a midrange both in terms of costs and but provide less reinforcement than monofilaments, and the particulates increase properties such as tensile strength the least but have the advantage of also costing less [22]. These expensive added constituents mean than the price of MMCs is often much higher than that of the base material [20]. Secondly, the fabrication and post processing of MMCs can be more difficult and thus expensive due to the increased hardness of MMCs when compared to monolithic materials. Machining of MMCs in particular is a challenge as the high strength of the reinforcements will prevent some traditional methods of machining [21].

MMCs also have several limitations in terms of their mechanical properties when compared to traditional metals. The most prominent of these issues are their reduced ductility and decreased fracture toughness. These drawbacks are factors that limit the adoption of MMCs in numerous applications. Furthermore, the finished products often have anisotropic properties, which may result in low transverse and inter-laminar shear strength [20].

It is worth noting that AM has the potential to help reduce/eliminate some of the drawbacks associated with MMCs, as the parts can be produced via AM powder metallurgy in such a way as to eliminate any machining requirements. This could significantly decrease fabrication costs associated with MMCs, and further increase their usage.

4. High Energy Ball Milling

High energy ball milling, or HEBM, is a mechanical process where an initial base powder (usually a metallic powder, either that of a pure element or an alloy) is mixed with smaller quantities of ceramics, nanocomposites, or even other metals. This powder mixture is placed in a ball mill, and the movement of the mill will result in the powder experiencing

high energy collisions with the balls [23]. An infographic of this interaction is included as Figure 6. HEBM is also known as mechanical alloying, as it can be used to create alloys from two different metal powders. Additionally, HEBM is one of the many methods used to create MMCs.

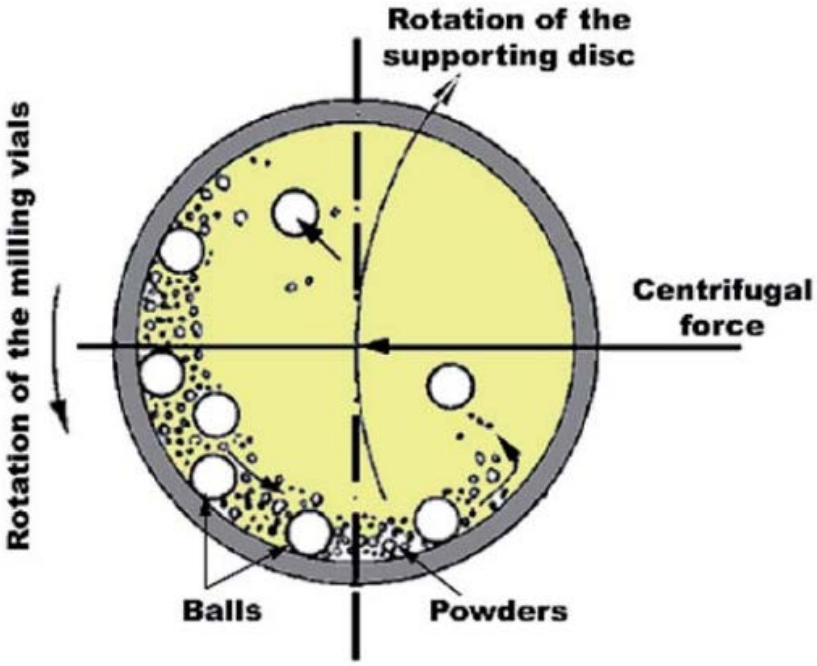

Figure 6. HEBM Infographic. Source: [24].

HEBM can be used to have different effects depending on what is desired. HEBM may be a mechanical process, but it can result in profound chemical changes in the base powder due to the thermal shock, high-speed plastic deformation, mechanical grinding and fracturing, cold welding, and intimate mixing that occur during HEBM [25]. In addition to making alloys, HEBM may be used to reduce the grain size of powder, potentially to either the nano or sub-micron scale. HEBM is often used to construct metal matrix composites since its ability to mechanically reduce the grain size of powders allows for small particles of ceramics, etc., to be added to metals. If alloying is not desired, HEBM can be employed for short durations to ensure a constituent is well-mixed into a base powder.

5. Current State of the Art Applications of MMC

MMCs have reached a stage where they are currently in widespread usage across many industries. MMCs first went into mass production when Toyota and Honda introduced reinforced pistons and engine blocks in the early 1990s [20]. Today, the costs associated with MMCs have decreased enough for them to be utilized across a wide variety of industries. Specialty items such as solar panels, spacecraft or satellite exteriors, nuclear radiation control rods, and catalysts in chemical reactions are now being fabricated from MMCs [26]. Furthermore, MMCs have become the standard material of choice for pistons, cylinders and brakes for the automotive industry, and are in widespread use throughout the aerospace industry. Current military aircraft have structures comprised of almost 1/3 MMCs, and commercial aircraft also employ MMCs to a large extent [26].

F. THESIS OBJECTIVES

The overall goal of this research was to enhance the mechanical properties of Ti-6Al-4V cubes made via AM by adding oxides to the metal matrix. This main goal was subdivided into three individual categories, each with separate metrics:

1. Oxidation Resistance of Ti-6Al-4V Composites

The oxidation resistance of Ti-6Al-4V and Ti-6Al-4V composites were tested on a weight change per surface area basis for varying times at varying temperatures. Specifically, the following test matrix was used for a total of nine independent trials for each composite material and a control sample (Table 2).

Table 2. Oxidation Testing Matrix

Test Matrix	**Temperature**		
Hours	700° C	900° C	1100° C
4	Trial 1	Trial 4	Trial 7
40	Trial 2	Trial 5	Trial 8
400	Trial 3	Trial 6	Trial 9

Temperatures of 700° through 1100° C were used as these are temperatures that gas turbine parts can be expected to be exposed to after experiencing the effects of thermal barrier coatings or advanced cooling airflows. The 4–400 hours tests were designed to show how the samples developed passive layers to help mitigate the effects of oxidation. The oxidation was measured both via the scanning electron microscope (SEM) and weight change results.

The motivation behind the oxidation study was to determine what effect, if any, adding oxides to the base Ti-6Al-4V powder had on the oxidation rates of the completed parts. In traditional manufacturing, MMC can be expected to have much better oxidation rates than monolithic metals. This study was designed to determine if this principle held true for AM, or if irregularities resulting from the addition of oxides in the AM building process actually resulted in increased oxidation for the composite materials.

Part of the reason this study was important from a scientific perspective was that at the time of this writing there were no published results regarding the oxidation properties of oxide reinforced Ti-6Al-4V produced via additive manufacturing. There is published literature regarding both oxide reinforced Ti-6Al-4V and the AM of Ti-6Al-4V, but this study will be the first study regarding the combination of the two approaches. Prior work in the field of direct metal laser sintering of metals enhanced with oxides has been conducted (see [27] for a study of AM stainless steel reinforced with oxide particulates), as well as research into the effects of AM Ti-6Al-4V reinforced with TiN (see [28]). However, there were no published results regarding the AM of Ti-6Al-4V composites using oxides as a reinforcing material. It is worth noting that both of these studies limited their testing to hardness and tensile strength, and that no literature regarding oxidation behavior of SLM Ti-6Al-4V composites currently exists.

2. Effect of Particulate Reinforcement on Mechanical Properties

As mentioned above in the background on MMCs, the effect of the particulate reinforcement in the composite material should be increased overall tensile strength. This study hoped to demonstrate that the composite parts built via SLM had better mechanical

properties than the control samples via hardness testing using both micro and nano indentation.

Again, part of the motivation behind this study was that there are no published results in the area of Ti-6Al-4V oxide-reinforced particulates produced via SLM. However, the study regarding the SLM produced stainless steel reinforced with oxide particulates had completed parts that only had 65% of the tensile strength when compared to the tensile strength of oxide reinforced stainless steel produced via traditional fabrication methods [27]. This study concluded that agglomeration of the added nanoparticles was the most likely reason for the loss of strength.

This research attempted to take preventative measures to ensure the added oxides did not form agglomerations by conducting high energy ball milling (HEBM) of the base Ti-6Al-4V with the added volume percent of oxides desired. This process is discussed further in Chapter III Fabrication and Processing. The comparison between the control sample and the composites was designed to include a comparison between the elastic modulus and the hardness for both samples; again, these parameters were determined via indentation testing.

3. Development of SLM Techniques

Difficulties with the AM of a completely new metal powder are expected, and part of this research was to help determine the optimal parameters for printing the composite powders. As mentioned above, one of the reasons that research in AM is particularly attractive is that is has the potential to go from research to commercial production in a much faster pace than conventional materials development approaches due to AM's highly adaptable and scalable nature. In order for this to occur, the work performed in this research must be repeatable. By documenting the optimized parameters for building composite parts, future work with composite powders should be able to get the exact same results as in this experiment. This in turn will help speed the adoption of new composite powders with enhanced mechanical properties.

Two specific SLM parameters were addressed in this research: laser power and build supports. These two areas were modified as initial failures to build using default

parameters indicated that the default support structure was not sufficient, and sparking indicated that the laser power may have been too high for a specific composite powder composition. For more information regarding these results, refer to Chapter III Fabrication and Processing Section D.

THIS PAGE INTENTIONALLY LEFT BLANK

II. TITANIUM MMCS AND METAL OXIDES OVERVIEW

In Chapter I, a brief background was given regarding both industrial uses and material properties of titanium and metal matrix composites. This section gives a more in-depth explanation regarding the state of the art of current work in both titanium metal matrix composites and oxide reinforced MMCs, in order to serve as a comparison for the titanium metal matrix composites produced in this research. Specifically, both the fabrication methods and the resulting mechanical properties of the end structures will be explored in depth in this chapter.

A. TITANIUM METAL MATRIX COMPOSITES

1. Continuous Fiber Titanium MMC Fabrication

Titanium MMCs have been fabricated in a myriad of different ways. The methods used largely depends on whether the end goal is to have an MMC with continuous fibers or with discrete particulates. When continuous ceramic fibers are desired, the following five methods are most frequently used: foil-fiber, powder cloth method, plasma spray, matrix-coated fiber, and titanium wires. Figure 7 portrays each of these various fabrication methods.

In the foil-fiber fabrication process, alternating layers of metal foil and ceramic fibers are laid on top of each other and hot pressed under inert conditions in order to produce a final product with the desired density. This process may use a titanium ribbon cross-weave or an organic binder in order to ensure the foil and the fibers are held in place during the hot press [29]. In the powder cloth method, a cloth-material is synthesized by mixing metal alloy powders with organic binder to form a substitute for a true metal foil, and then the foil fiber method is applied. The organic binder will later be removed via vacuum degassing. This method was designed to decrease cost as the manufacture of a true metal foil for titanium alloys can be extremely expensive. The titanium wire method consists of a ceramic fiber and a small diameter titanium wire that are hot pressed together to make a final product. The titanium alloy wires are expensive and difficult to fabricate, so this method does not offer a financial advantage over the foil-fiber method, and has the

added difficulty of requiring some sort of supporting matrix to insure the complex lay-up of the titanium wires and ceramic fibers maintain their precise positions during the hot press. In the plasma sprayed process, metal is sprayed onto a fiber array. This method avoids the manufacturing expenses associated with manufacture of a titanium foil or wire, but has problems associated with the metal spraying process—often this process results in a metal with high porosity and fiber damage from the thermal shook associated with the plasma powder [29]. In the matrix coated fiber method (MCF), electron beam physical vapor deposition (PVD) is used to coat the ceramic fibers with the titanium alloy. These coated fibers then are solid-state consolidated in order to form a finalized product [29]. Figure 8 is a schematic of the electron beam apparatus used in the PVD process [30].

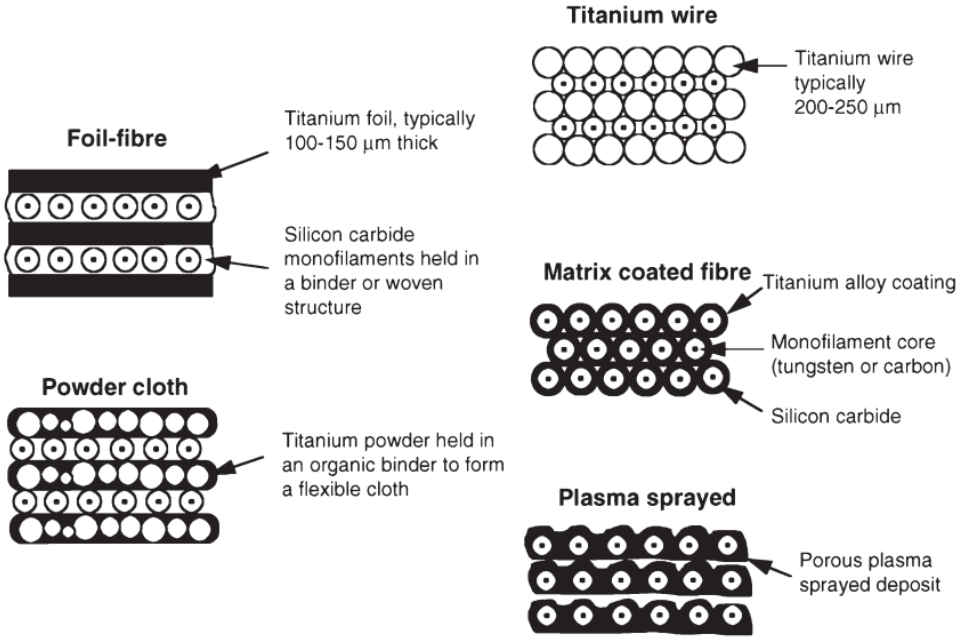

Figure 7. Fabrication Methods for Continuous Fiber Titanium MMCs. Source: [29].

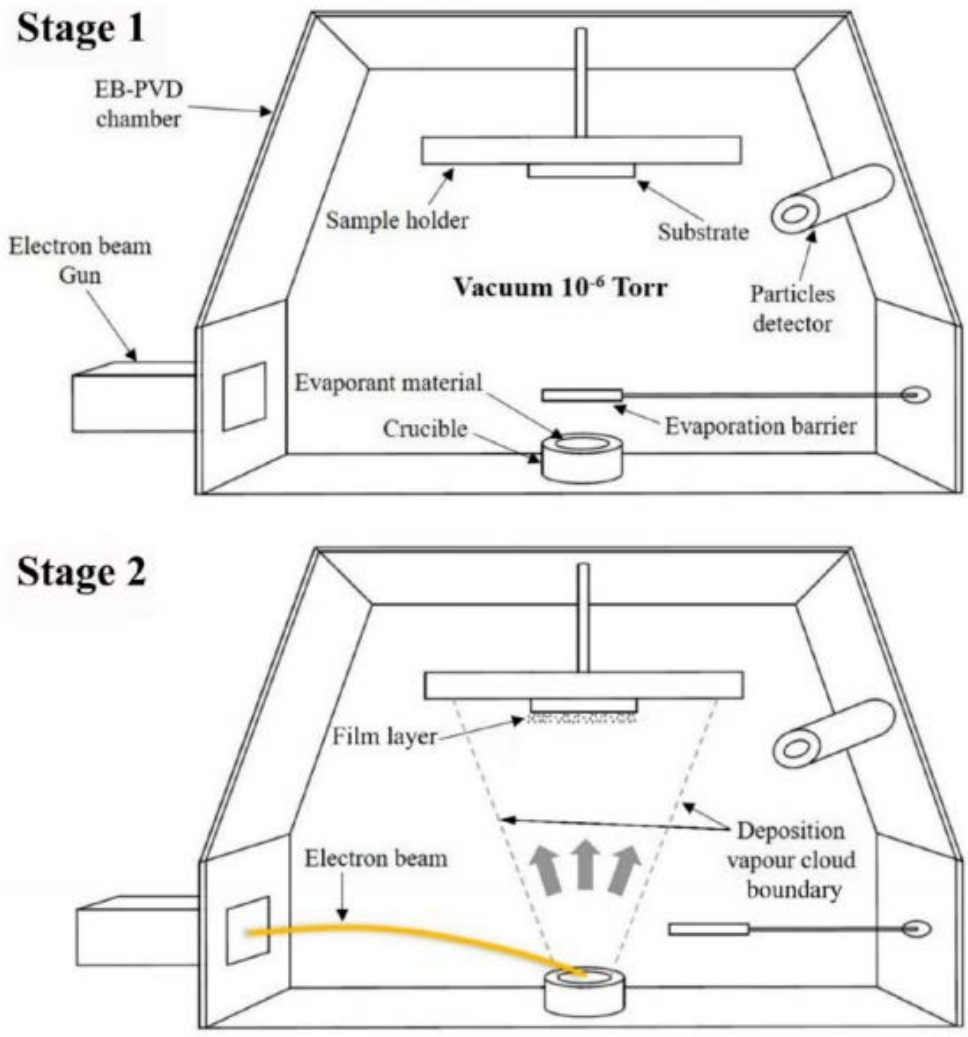

Figure 8. Schematic of Electron Beam Apparatus Used in PVD to Make MCF. Source: [30].

Of the five fabrication methods described above, foil-fiber is the oldest method and as a result it has the most well-established methods. In particular, there is a larger wealth of knowledge regarding how to add ceramic fibers to titanium alloys without having large losses in ductility for the foil-fiber method. Foil-fiber can be used to produce large volumes of titanium MMC sheet metal, and is one of the most commonly used methods due to its comparative reliability. The foil-fiber method has the benefits of a highly controlled microstructure, consistent alloy chemistry, and low impurity levels. There are two main downsides to the foil-fiber method: high cost, and a high degree of difficulty for producing

complex shapes. The foil-fiber method is expensive as the α + β phase alloys such as Ti-6Al-4V and Ti-6Al-2Sn-6V, which are most commonly used titanium alloys in MMCs, are difficult to roll. This means that producing the metal foil required for use in the foil-fiber process is a time-consuming and expensive process. Rolling these alloys typically requires frequent interstate annealing and extremely controlled processing [29]. Additionally, the end state of all parts produced by the foil-fiber method is a sheet metal consisting of the titanium MMC. This type of metal is more difficult to machine in complex shapes—the machining process to make disks, rings, blades, and other curved parts from the extremely hard MMC sheet metal requires special tooling. This further increases the overall cost of the end product produced by the foil-fiber method.

The second most commonly used method for producing titanium metal matrix composites is the MCF method. The MCF method has numerous advantages:

- the ceramic fibers are well distributed without overlapping
- the consolidation requirements for multiple layers of MCF are lower than for MMCs made by the foil-fiber method or any of the other continuous fiber methods
- minimal disturbance in the interface region between the ceramic fibers and the metal alloys
- any metal matrix alloy can be used
- no foils or powders are necessary
- well suited for production of round shapes such as rings, discs, or shafts as it can be easily used as filament winding
- up to 80% volume fraction of ceramic fibers is possible
- the metal coating serves as a protective layer for the ceramic fibers during consolidation process and in any other post-processing work or machining. Adapted from [29]

The MCF method is not without downsides, however. The implementation of the PVD step can be difficult for alloys with refractory elements. Specifically, MCF can result in variable alloy chemistry within the metal coating. This can resultant in material defects in the end product. The MCF method is also not as easily scaled up as the foil-fiber method, so for large economies of scale the foil-fiber method may actually be cheaper. However, the current aerospace market generally lacks the scale required to make the foil-fiber method cost efficient compared to the MCF as large quantities of sheet metal MMC is not

desired since the aerospace industry is currently focusing using these materials in turbine components rather than generic paneling [29].

2. Discontinuous or Discrete Fiber Titanium MMC Fabrication

When discrete ceramic particles are desired rather than continuous fibers, different fabrication methods are used to create MMCs. As mentioned in Chapter I, discrete particles are generally used when a more isotropic end material is desired—the continuous fibers will result in a higher tensile strength than the discrete particles, but only in the direction of the fibers [31]. Conventional ingot metallurgy processes will not work for the fabrication of discontinuous fiber titanium MMCs due to titanium's high chemical reactivity. For this reason, discontinuous fiber titanium MMCs are normally fabricating using rapid solidification or powder metallurgy [31].

Rapid solidification is not a single unique fabrication process, but rather a broad definition that includes numerous techniques. Three common types of rapid solidification processes are melt-spinning, droplet, and surface melting. In these processes, a molten metal is cooled at a high rate (up to 10^6 K/s) [32]. The rapid solidification process most commonly used for the production of titanium MMCs is the melt spinning approach [31]. In melt spinning, small amounts of a metal alloy and reinforcements are placed inside a crucible that is surrounded by an induction coil. The induction coil has a high current, which will cause the crucible to reach high temperatures and melt. Once melted, the composite slurry will be ejected through inert gas pressurization onto a rotating wheel at high speeds (in the range of 5,000 to 7,000 rpm). This inert gas pressurization step is known as atomization. These high speeds are what cause the rapid solidification rates to occur; the high rotational speed will quickly freeze the molten liquid into a solid amorphous state [32]. This amorphous solid is the titanium MMC, however further machining and/or post-processing will be required in order to produce a usable part from this step.

Rapid solidification has multiple advantages over other forms of producing titanium MMCs; perhaps the most important of these benefits is the low cost of rapid solidification when compared to other fabrication methods. Because rapid solidification is a direct and simple process and only requires a melt-spinner machine, the investment cost

to make titanium MMCs with this method is much lower comparatively. Additionally, the fast cooling rates associated with rapid solidification can lead to the formation of nonequilibrium phases [32]. This can lead to smaller grain size and shapes, which in turn reduces dislocation motion and increases the overall tensile strength of the final product.

Rapid solidification's main disadvantage is that this fabrication method has inherent limitations in terms of what types of ceramics can be added to the titanium matrix. If the reinforcement density is significantly different from the density of titanium, the atomization process will result in separation between the titanium matrix and the added reinforcements, which in turn will lead to agglomerates of the reinforcements [31]. These agglomerates will result in a non-uniform distribution of ceramics in the final MMC, which in turn can lead to poor mechanical properties such as brittle regions. Another downside is that the input heat required for the melt-spinning is high, and this can be prohibitive for some applications. A final downside is the atomization process requires a well-maintained machine, or else impurities can be introduced into the final composite at that step in the process [31].

Powder metallurgy is a complex multi-step process that can be used to create a discontinuous fiber titanium MMC. Powder metallurgy begins with powder metal alloy, and uses some form of mixing or blending to add the desired reinforcement to the powder. This mixing may be purely physical in nature; however mechanical alloying through processes such as HEBM may be conducted as well depending on the end goal for the composite powder. Once the desired amount of reinforcement particle distribution has been achieved, die compacting is used to condense the powder and eliminate porosity. The die compacting step is followed by a sintering step, where the composite power is sintered then cooled into a solid metal structure such as an ingot. These composite ingots will then undergo re-pressing or optional secondary manufacturing as needed in order to produce the ring, disc, blade, shaft, etc., that is desired. It is important to note that there are two distinct types of powder metallurgy: *ex situ* processing and *in situ* processing. In *ex situ* processing, the reinforcements do not react with the metal matrix and retain their original particle size and morphology. This will result in a composite that has superior mechanical properties such as increased tensile strength and temperature resistance, as well as improved wear

resistance. However, the fact that the reinforcement did not form any new compounds can lead to issues such as poor bonding between the reinforcements and the metal matrix. *In situ* processing is different in that it utilizes the high natural reactivity of titanium in order to form new compounds. Additives such as TiB_2, B_4C, Cr_3C_2, and Si_3N_4 will react with the titanium matrix during sintering to form new compounds such as TiB [31]. These new compounds often have whisker grain shapes, and lead to better interfacial bonding compared to composites produced with *ex situ* processing. *In situ* processing can lead to higher specific tensile strength, a higher elastic modulus, higher creep resistance, and higher oxidation resistance when compared to composites produced via *ex situ* processing. It should be noted, however, that uncontrolled *in situ* reactions can actually lead to interfacial defects which negate any of these potential benefits. *In situ* processing can also be performed via self-propagating high temperature synthesis (see [33]) and additive manufacturing (see [34]). Fabrication of additively manufactured titanium MMCs will be discussed in more depth in Section C below.

Powder metallurgy is widely considered the preferred process for making particle reinforced titanium MMCs due to its ability to produce composites with a uniform, isotropic microstructure. Other important advantages of powder metallurgy include its significantly lower cost than any of the continuous fiber reinforcement fabrication techniques and its ability to easily scale up to high production volumes [31]. Downsides of traditional powder metallurgy include comparative design limitations—traditional powder metallurgy requires molds, dies, or sacrificial mandrels in order to be made into complex shapes and features. Thus, these end products are not as easily transformed into curved GTE components when compared to components made via additive manufacturing techniques. Another design limitation of powder metallurgy is that large continuous structures cannot be created easily via this technique due to the size limitations imposed by the die-compacting and sintering steps [31].

3. Titanium MMCs Ultimate Tensile Strength

The ultimate tensile strength of titanium MMCs depends on what ceramics are added to the titanium metal matrix, and whether they are added as continuous fibers or as

discontinuous particles. Figures 9 and 10 illustrate the general increase in ultimate tensile strength exhibited by composite materials. In Figure 9, the ultimate tensile strengths were measured such that the loading direction was in line with the fiber axis—the tensile strength would be markedly lower if measured perpendicular to the reinforcement axis. The reduction in strength in the off-axis orientation can largely be attributed to the weak interface region between the ceramic fibers and the titanium metal matrix [35]. The ultimate tensile strength of $\alpha+\beta$ alloys such as Ti-6Al-4V is approximately 1100 MPa at room temperature, and decreases to less than 500 MPa at 600 degrees Celsius [31]. When silicon carbide reinforcement fibers are added to create a continuous fiber titanium MMC, this ultimate tensile strength increases dramatically to 2300 MPa at room temperature and 1700 MPa at 600 degrees Celsius [35]. The increase in ultimate tensile strength is not nearly as dramatic for discrete particle reinforced titanium MMCs as it is for continuous fiber MMCs, but it is still large enough to make these discontinuous fiber titanium MMCs more desirable in many applications that the base metals. For instance, the addition of Ti-C particulates to Ti-6Al-4Voffers minimal tensile gains at room temperature, but can increase the ultimate tensile stress of this material from 500 MPa at 400 degrees Celsius to above 650 MPa at 400 degrees Celsius. Since the mechanism for this increase in strength is dispersion-hardening from the ceramic constituents, this gain in tensile strength is isotropic in nature. Dispersion-hardening decreases dislocation motion throughout the grain structure of the composite material [31]. Thus, components fabricated from discontinuous fiber MMCs will realize these tensile strength gains in all directions. In addition to increased tensile strength, the elastic modulus will generally increase for all types of MMCs. When as little as 4% by volume of ceramic fibers are added discontinuously, the elastic modulus can increase by up to 25% [36].

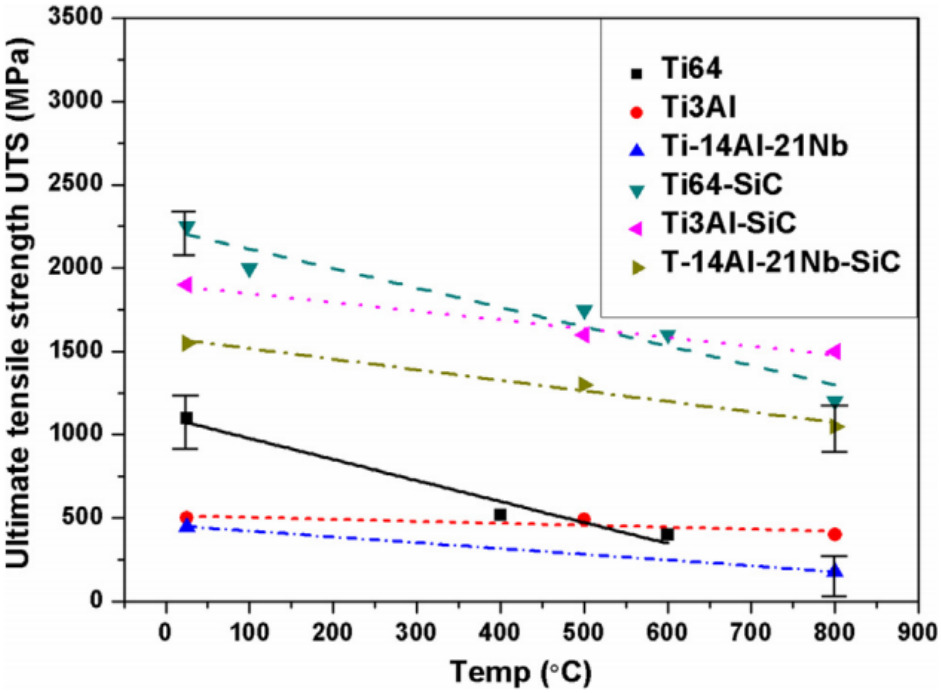

Figure 9. Ultimate Tensile Strength vs. Temperature for Continuous Fiber Titanium MMCs. Source: [31].

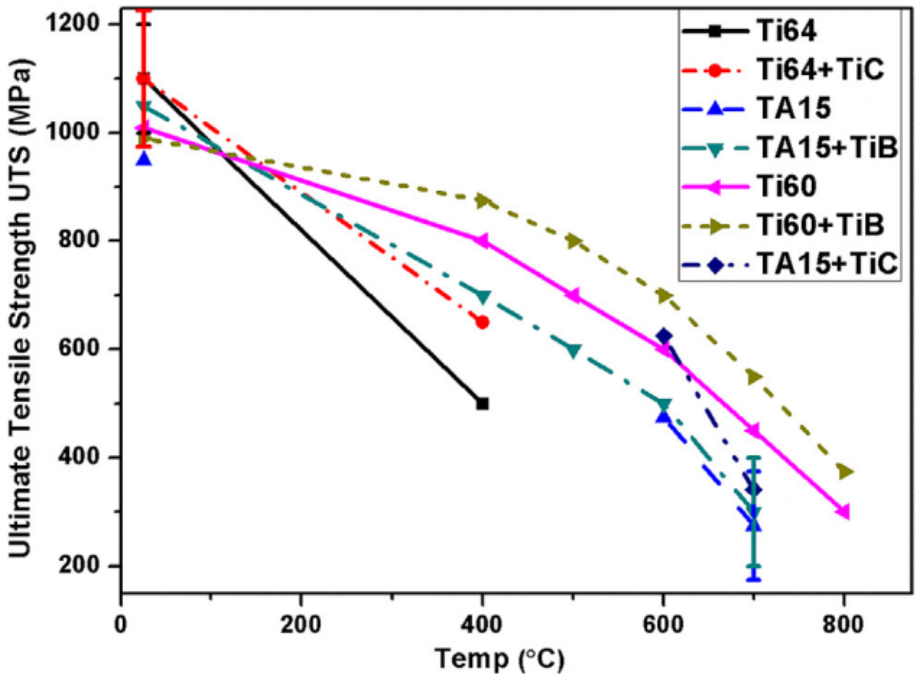

Figure 10. Ultimate Tensile Strength vs. Temperature for Discontinuous Fiber Titanium MMCs. Source: [31].

4. Titanium MMCs Oxidation Behavior

Just as ultimate tensile strength in titanium metal matrix composites has a high dependence on both the constituents added and the fabrication method used, these factors can result in wide variations in oxidation behavior. For example, titanium boride (TiB) and titanium carbide (TiC) reinforced Ti-6Al-4V were shown to have increased oxidation resistance as the volume fraction of reinforcements was increased when tested at atmosphere at 873 to 1073 Kelvin [37]. By contrast, titanium composites with silicon carbide (SiC) fiber reinforcements often do not exhibit increased oxidation resistance, as silicon dioxide (SiO_2) forms only immediately following short-term exposure—titanium dioxide (TiO_2) dominates when exposed to an oxidation environment at high temperatures for a longer duration of time [38]. The mechanism for oxidation differs for each constituent, and will ultimately determine whether the titanium MMC has increased performance relative to a pure metal matrix.

B. OXIDE REINFORCED MMCS

Up to this point, almost all of the MMCs considered have used reinforcing constituents of silicon, carbon, or boron. However, these are not the only materials that could be used in metal matrix composites. There is potential for the use of oxides such as alumina (Al_2O_3) (see [39]) and tantalum pentoxide (Ta_2O_5) (see [40]) in metal matrix composites, as these novel ceramic materials have the potential to high corrosion resistance and fracture resistance while maintaining or increasing the ultimate tensile strength of the resulting metal matrix composite. Specifically, metal oxide reinforced MMCs are being researched for use by the aerospace and automotive industries, the pharmaceutical industry, and for use in wear-resistant tools [41].

1. Fabrication Techniques

As with all MMCs, composites reinforced with oxides have widely varying material properties that are highly dependent upon the microstructure of the composites, and the interactions between the base metal matrix and the reinforcing constituents. Issues such as porosity, uneven distribution of reinforcement material, and the shapes that the reinforcement material takes on within the matrix can lead to poor mechanical properties.

These microstructural characteristics are highly dependent on the fabrication technique, meaning that even two samples with the same base metal and reinforcing oxide can have greatly different mechanical properties if they were fabricated using different methods [39]. For example, aluminum-alumina composites made via traditional powder metallurgy demonstrated higher yield strength, ultimate tensile strength, and percent elongation than aluminum-alumina samples with identical volume fractions of the reinforcing constituents that were fabricated via casting [39]. All the fabrication techniques described above in Section A: Titanium Metal Matrix Composites still apply: oxides can be added as continuous fibers (see [42]) or as discrete particles (see [43]) just as other ceramics can. The main difference for oxide reinforced MMCs is that even small variations in processing method steps can result in composites with highly different mechanical properties. One study in particular demonstrated that a slight variation in traditional powder metallurgy steps (whether the sample was die compacted as a paste with organic binder that was later removed, or whether the sample was compacted in a dry powder form) could result in a difference in elastic modulus of up to 15 GPa [39]. This extreme variation depending on fabrication method means that in order for production scale manufacturing of oxide reinforced MMCs, the fabrication process would need to be highly repeatable. This is one of the main reasons why additive manufacturing in particular is attractive to produce these advanced composite materials.

2. Impact on MMC Mechanical Properties

Adding oxides such as Al_2O_3 or Ta_2O_5 results in great increases in ultimate tensile strength for the final MMC. The young's modulus of alumina is 394 +/- 6 GPa (see [43]), and the young's modulus of pure titanium is approximately 120 GPa (see [16]). Cermets created from alumina and titanium that were 75% ceramic by volume and 25% titanium by volume had a young's modulus of 326 +/- 9 GPa [43]. One of the main reasons ceramics like alumina cannot be used in most applications is due to their brittle failure behavior, which can lead to failures without warning. Oxides added to titanium reduce ductility, but the overall toughness of the resultant MMC can be double that of the base ceramic [43]. See Figure 11 for a comparison of the toughness between monolithic ceramics and an alumina-titanium composite. Perhaps the most important impact that results from adding

oxides is that these reinforcements can result in drastically improved mechanical properties at high temperatures. The ultimate tensile strength of aluminum-silicon-copper alloy reinforced with 4% alumina by weight was only 10 MPa greater than the alloy without alumina (200 MPa instead of 190 MPa) at room temperature, but when subjected to a tensile test at an elevated temperature of 300 degrees Celsius, the alumina composite has a markedly better performance. The aluminum alloy has an ultimate tensile strength of just 62 MPa at this elevated temperature, whereas the aluminum alloy composite with 4% alumina by weight has an ultimate tensile strength of 88 MPa [44].

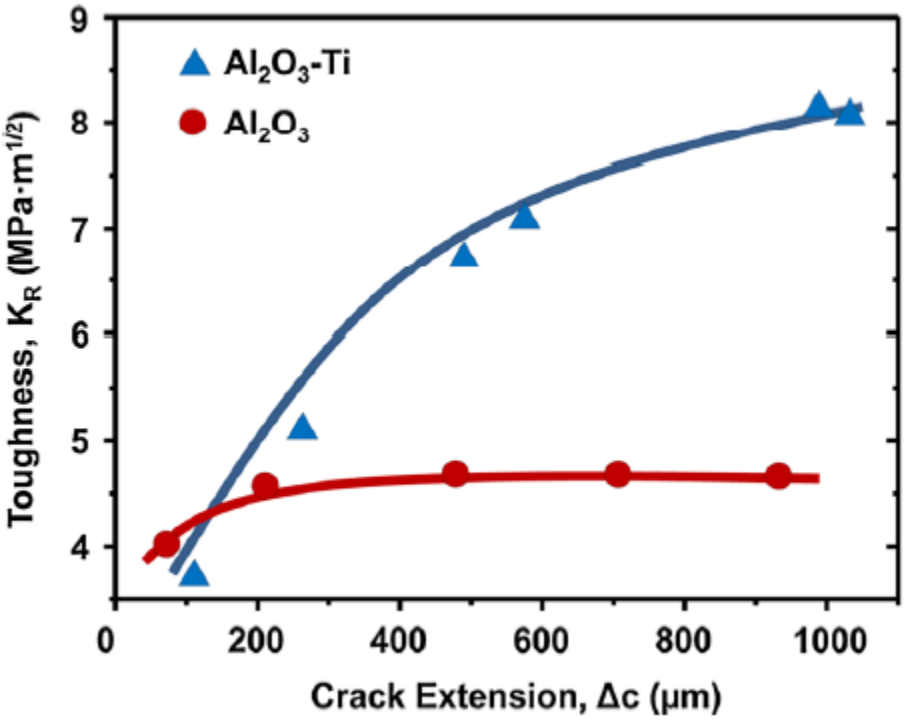

Figure 11. Comparison of Toughness between Monolithic Alumina and Alumina-Titanium Composites. Source: [43].

3. Impact of Oxide Reinforced MMCs on Oxidation Behavior and Corrosion Resistance

In addition to improved mechanical properties, metal oxides such as Al_2O_3 and Ta_2O_5 can theoretically be added to metal alloys in order to improve their corrosion resistance and reduce how much they oxidize. When Ta_2O_5 is added to titanium to create

an MMC through the sol gel process, it has been shown that it significantly increases the free potential of titanium and thus leads to significant decreases in corrosion, as seen below in Figure 12 [45]. This has led to the adoption of tantalum oxide coatings on titanium alloys used in biomedical applications [40]. When alumina is added to a metal alloy in order to create an MMC, it can result in greatly reduced oxidation rates, particularly at high temperatures. One study in particular demonstrated than the weight gain per area for a Zirconium alloy stabilized with alumina was significantly lower than for the same alloy lacking alumina when undergoing cyclic oxidation at 1000 degrees Celsius for 240 hours [46]. This study hopes to repeat these results by decreasing the oxidation rates area by adding alumina and tantalum pentoxide to Ti-6Al-4V.

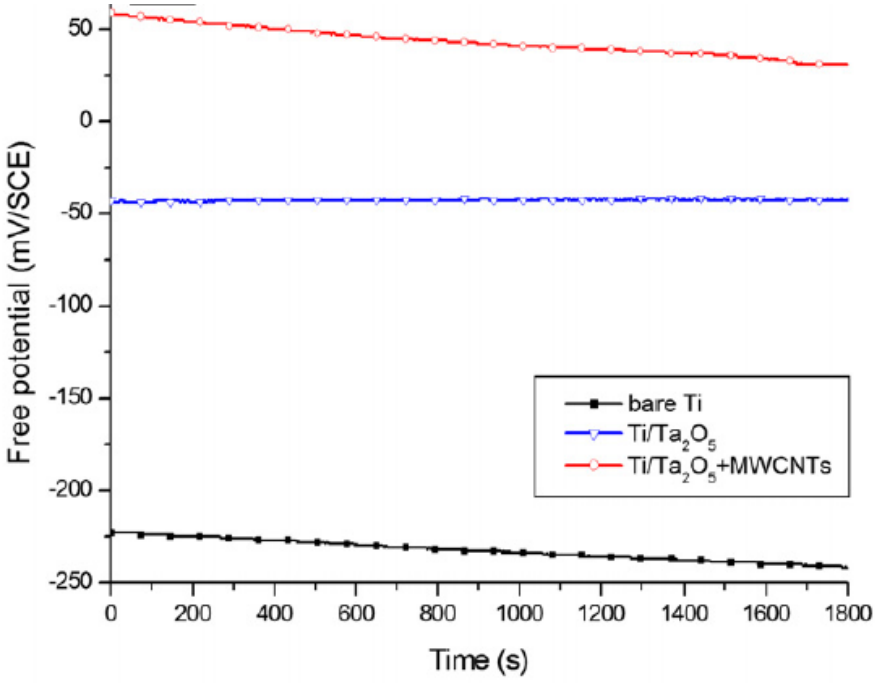

Figure 12. Free Potential of Titanium and Titanium MMCs; Measurements Performed in NaCl 0.9%. Source: [45].

C. ADDITIVE MANUFACTURED TITANIUM ALLOY COMPOSITES STATE OF THE ART

This is the first study that has attempted to measure the mechanical properties and oxidation behavior of titanium MMCs reinforced with alumina or tantalum oxide.

However, in the past five years there have been a multitude of studies regarding the mechanical properties of titanium matrix composites produced via additive manufacturing. Most of these studies either added borides (see [47] for TiB, [48] for TiB-Ti, [49] for TiB, and [50] TiB-Ti) or carbides (see [51] for TiC and [52] for Ni-TiC-C). These studies have revealed many of the potential obstacles that must be overcome in order to produce final products that have beneficial material properties via additive manufacturing.

Another major issue commonly encountered when additively manufacturing titanium MMCs is that the resulting structures often have higher porosity when compared to MMCs fabricated using traditional methods. This occurs when the laser settings result in melt instability—meaning that the melt pool is not fully molten due to the energy density of the laser being below required levels [53]. To avoid this issue, higher energy density can be achieved by either increasing the laser power, decreasing the laser scan speed, decreasing the layer thickness, or decreasing the hatching distance. However, decreasing layer thickness or hatching density potentially have drawbacks as it will can potentially result in the energy density becoming high enough to affect more than the current layer of powder, and numerous cycles of melting and solidifying can lead to the formation of a heat-affected zone similar to in the welding process, and thereby result in poor mechanical properties [54]. MMCs can potentially result in final structures with higher porosity than a structure additively manufactured from pure metal or an alloy due to issues with the solidification of dissimilar materials within the meltpools. Additionally, issues with melt pool instability can arise due to the differences in solidification rates for areas with different ceramic and metal compositions [53].

Finally, additive manufacturing titanium MMCs has an additional challenge in that no titanium composite feedstock powder exists commercially, and thus all working in this field need to create their feedstock powders from scratch. This can be particularly challenging as the ceramic reinforcements added to the titanium matrix have melting temperatures that are significantly greater than those of titanium, meaning the optimal laser settings for SLM of the two materials may be different, and the optimal settings for powder mixtures with different weight percentages of reinforcements will certainly be different. To date, most studies that have tried additively manufacturing using titanium powders

reinforced with ceramics have utilized either direct powder blending or mechanical milling, as gas atomization of the powder is both cost-prohibitive for most applications and technically challenging [53]. Of these two methods, mechanical milling has shown more promise despite being a time-consuming process, as mechanical milling tends to result in feedstock composite powders that are far more homogenous than powders created by direct blending. Furthermore, milling serves to break up agglomerations that are often left intact by direct milling and can cause issues later on in the additive manufacturing process [53].

THIS PAGE INTENTIONALLY LEFT BLANK

III. FABRICATION AND PROCESSING

This chapter describes how the Ti-6Al-4V, Al_2O_3, and Ta_2O_5 commercial powders were prepared for use in SLM, and the design parameters used during the additive manufacturing process. Specifically, four composite powders were created Ti-6Al-4V reinforced with 1% by volume of Al_2O_3 (Ti-A1), Ti-6Al-4V reinforced with 3% by volume of Al_2O_3 (Ti-A3), Ti-6Al-4V reinforced with 1% by volume of Ta_2O_5 (Ti-Ta1), and Ti-6Al-4V reinforced with 3% by volume of Ta_2O_5 (Ti-Ta3).

A. AS RECEIVED POWDERS

Three commercially available powders were used to create four titanium-based MMCs. The three commercially available powders used were: spherical Ti-6Al-4V powder procured from the EOS Corporation with the following maximum amounts of contaminants O < 2000 ppm, N < 500 ppm, C < 800 ppm, H < 120 ppm, and Fe < 2500 ppm for a 99.6% overall purity with an average particle size between 20 to 80 microns; Al_2O_3 gamma phase powder procured from the MTI Corporation with 99.0% purity with an 80 nm average particle size, and Ta_2O_5 powder procured from NOAH Technologies Corporation with 99.9% purity with a less than 10 micron average particle size.

1. Ti-6Al-4V Powder

The Ti-6Al-4V powder used was the standard powder recommended for use by the manufacturer for the EOS 100M SLM machine used in this experiment. The EOS 100M SLM machine is described in more depth below in Section D: Additive Manufacture of Cube Specimen. As mentioned above, the Ti-6Al-4V powder was reported by the manufacturer to consist of particles between 20 to 80 microns. As seen in Figures 14 and 15, imaging in the scanning electron microscope (SEM) revealed that the Ti-6AL-4V powder consists primarily of uniform spheres on the scale of 30 microns, and this matched the description of the powder given by the manufacturer. Figure 15 highlights some of the smaller spheres of titanium alloy powder, which range in scale from two to five microns. Another noteworthy feature of the Ti-6Al-4V powder is the large amount of spacing between individual spheres; this lower density when compared to either the Al_2O_3, or the

Ta_2O_5 powder results in much greater flowability for the Ti-6Al-4V powder than either of the two ceramic powders. Finally, the Ti-6Al-4V powder does have some irregular shaped powder particles, but these particles never form agglomerates larger than 40 microns. Again, this lack of agglomerates results in improved flowability for this powder.

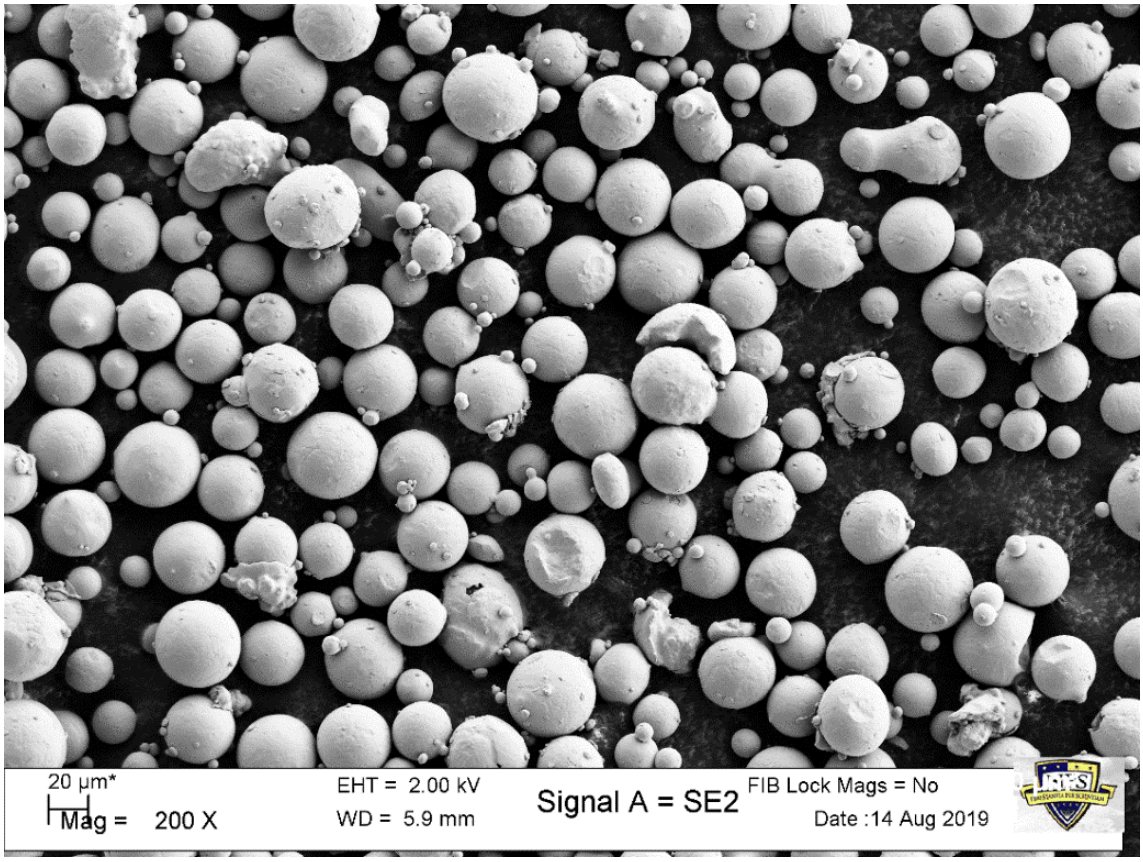

Figure 13. Low Magnification SEM Image of As-Received Ti-6Al-4V Powder

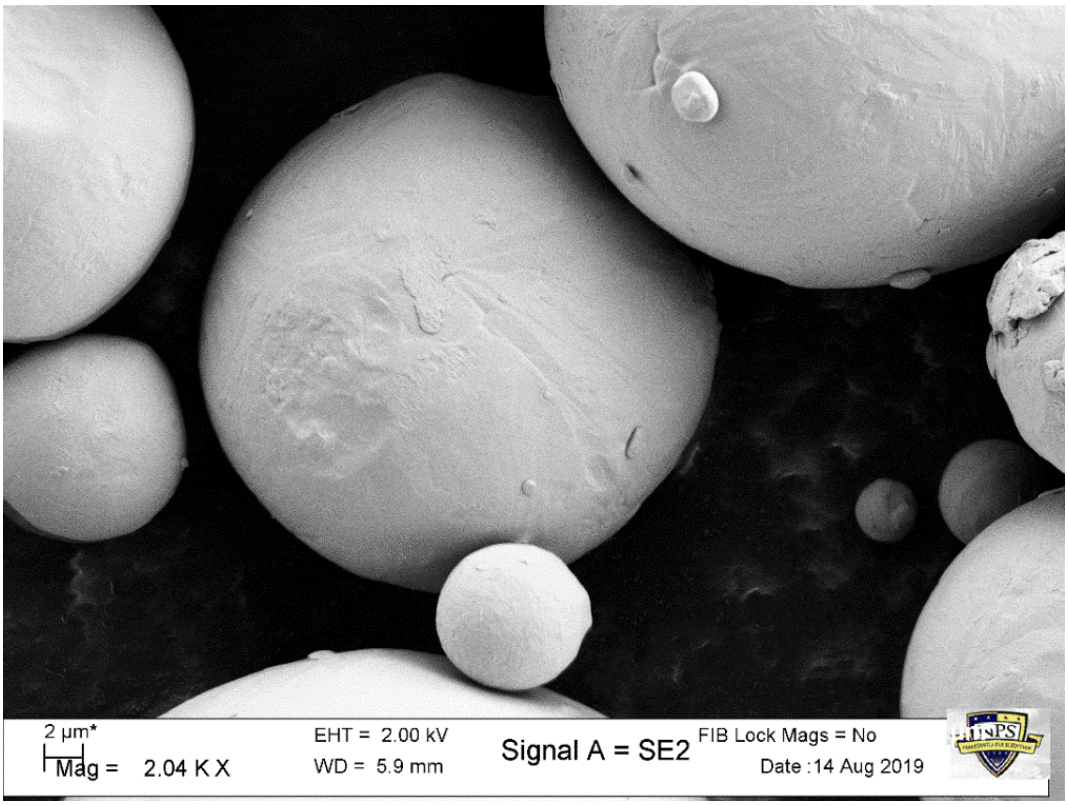

Figure 14. High Magnification SEM Image of As-Received Ti-6Al-4V Powder

2. Al_2O_3 Powder

The as-received Al_2O_3 powder was revealed to be markedly different from the titanium powder when observed using the SEM. As seen in Figure 15, the Al_2O_3 powder had some spheres like the Ti-6Al-4V powder, but spherically shaped powder particles were the exception rather than the rule. Instead, most of the powder had irregular shapes of varying sizes. Individual particles ranged from spheres on the scale of 25 microns to fragments smaller than 0.25 microns. This was interesting, as the manufacturer listed the particle size as 0.8 microns. The small particle sizes of the Al_2O_3 powder meant that the powder was able to pack much closer together when compared to the titanium powder, which resulted in decreased flowability. Figures 17 and 18 in particular highlight how closely packed the Al_2O_3 powder was due to the smaller irregular fragments of powder. However, this did not result in the formation of any large agglomerates—the largest were still on the scale of 30–35 microns, similar to those in the Ti-6Al-4V powder.

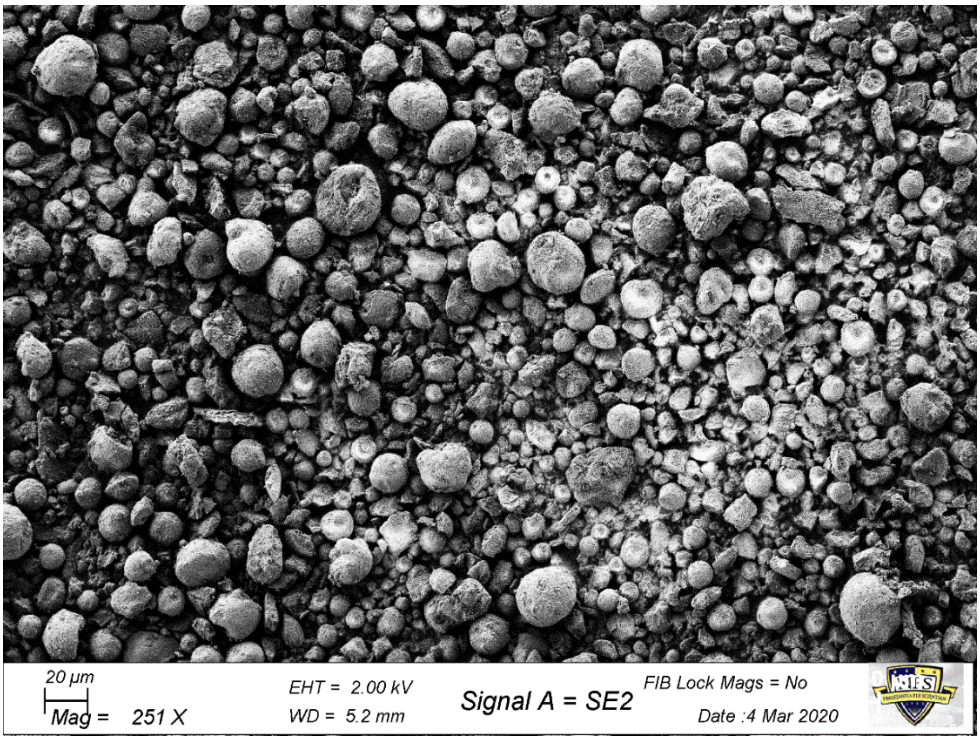

Figure 15. SEM Image of As-Received Al_2O_3 Powder

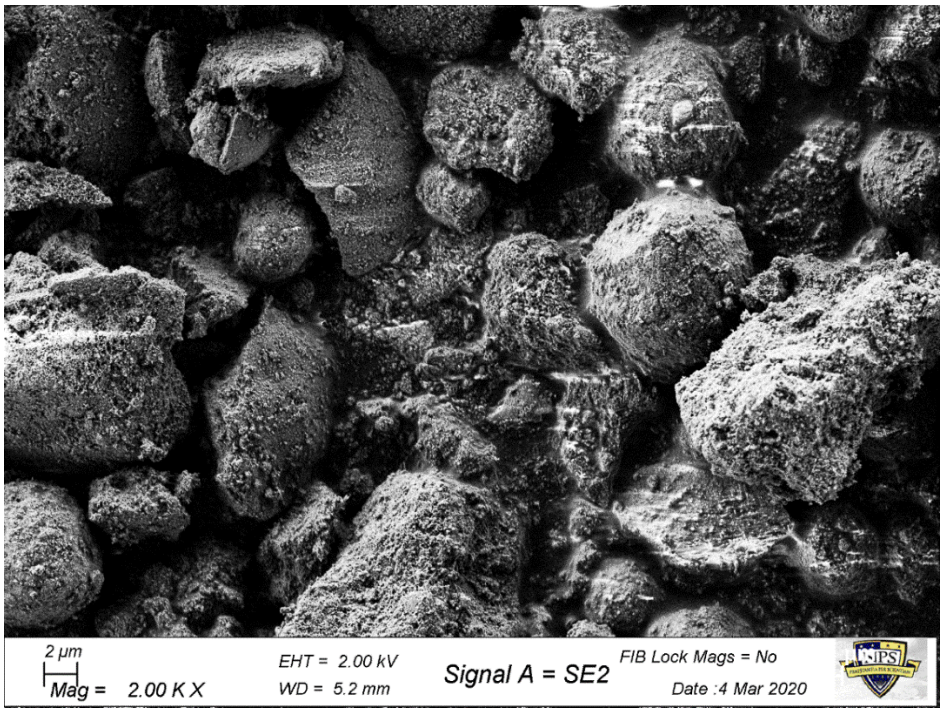

Figure 16. SEM Image of As-Received Al_2O_3 Powder Agglomerates

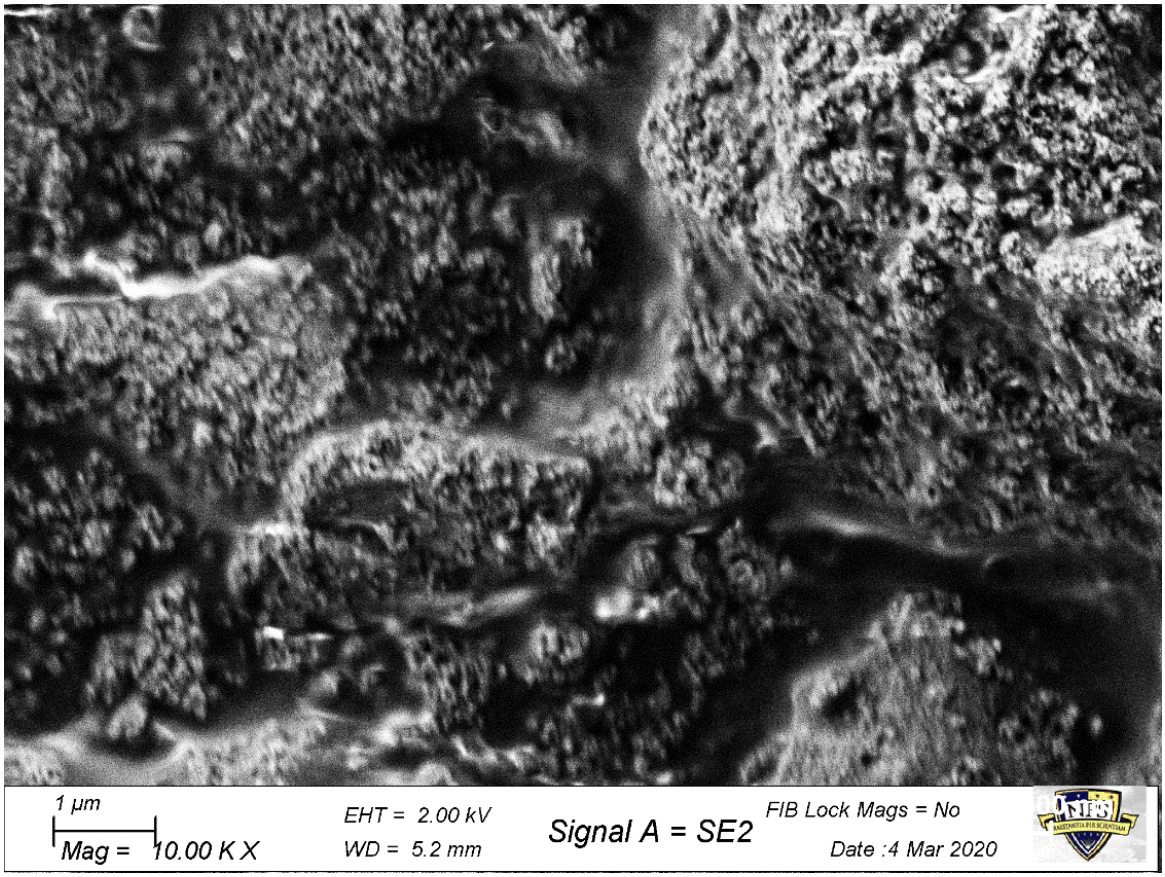

Figure 17. High Magnification Image of As-Received Al_2O_3 Powder to View Individual Nanopowders

3. Ta_2O_5 Powder

The commercial Ta_2O_5 powder had massive agglomerates of Ta_2O_5 particles. These agglomerates were up to an order of magnitude larger than any of the agglomerates in either the titanium or alumina powders, and were measured at sizes of up 150 microns. Figure 18 highlights one of these large agglomerates. As seen in Figure 19, these large agglomerates formed because the Ta_2O_5 powder was actually composed of much smaller fragments that exhibited high amounts of cohesion. According to the manufacturer, these particles were on average smaller than 10 microns. One of the main hopes for the HEBM process was that these agglomerates could be successfully broken up in order to disperse the Ta_2O_5 particles evenly throughout the titanium powder.

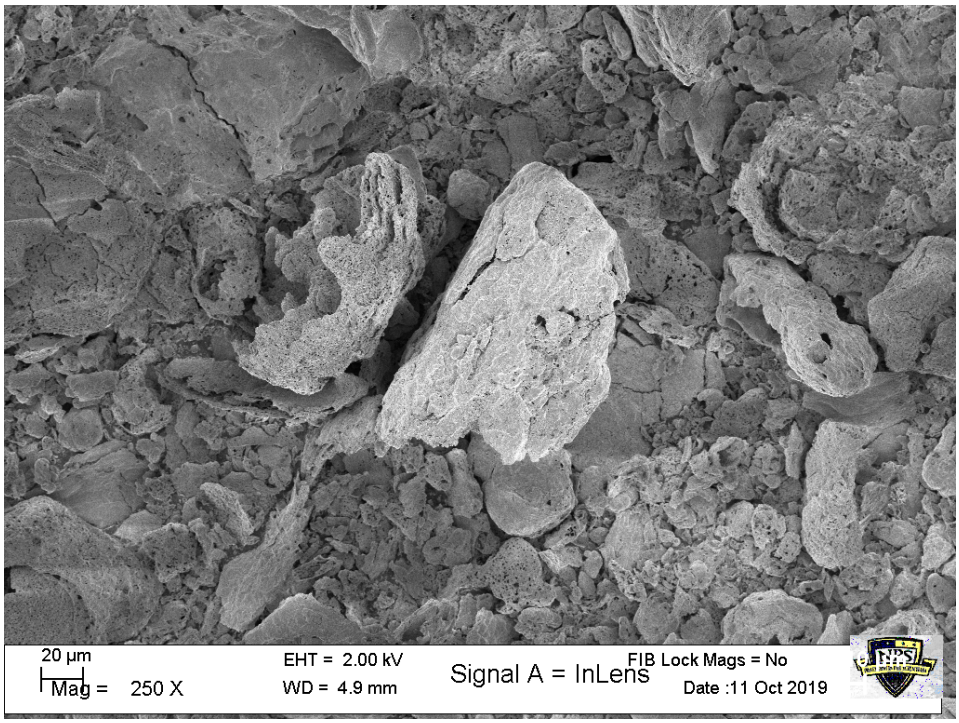

Figure 18. SEM Image of Ta_2O_5 Powder Agglomerates

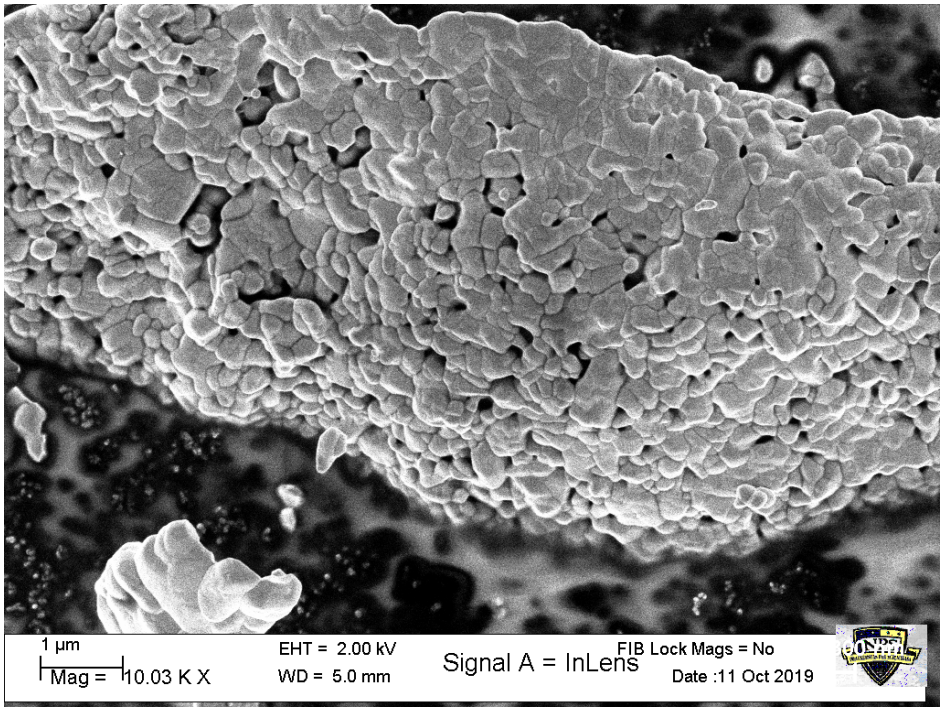

Figure 19. High Magnification SEM Image of Ta_2O_5 Powder to Highlight Nanoparticles

B. COMPOSITE POWDER SYNTHESIS

1. HEBM

The SEM imaging of the Al_2O_3 powder and the Ta_2O_5 powder revealed both powders had agglomerates of particle fragments, and this led to the determination that simply blending the ceramic powders with the commercial grade Ti-6Al-4V powder would not be enough to insure good distribution of the reinforcements. For this reason, it was decided to use HEBM to insure good distribution of the ceramic powder. Prior work experience using the HEBM machine at the Naval Postgraduate School had indicated that if alloying was not desired, cycles of two minutes of active HEBM followed by five minutes of rest could be repeated to achieve good dispersion of reinforcement material with limited or no chemical reactions occurring in the powder blend between the reinforcement material and the metal base powder. Ultimately, ten cycles of this two minutes on five minutes off were used in the HEBM apparatus. The HEBM machine used in this study was a SPEX Sample Prep 8000M Mixer/Mill machine (see Figure 20). Stainless steel milling balls were used; again, previous experience indicated that these milling balls would not be a source of contamination and energy-dispersive X-ray spectroscopy (EDS) analysis later confirmed that there were no significant amounts of either iron or carbon in the resulting composite powder.

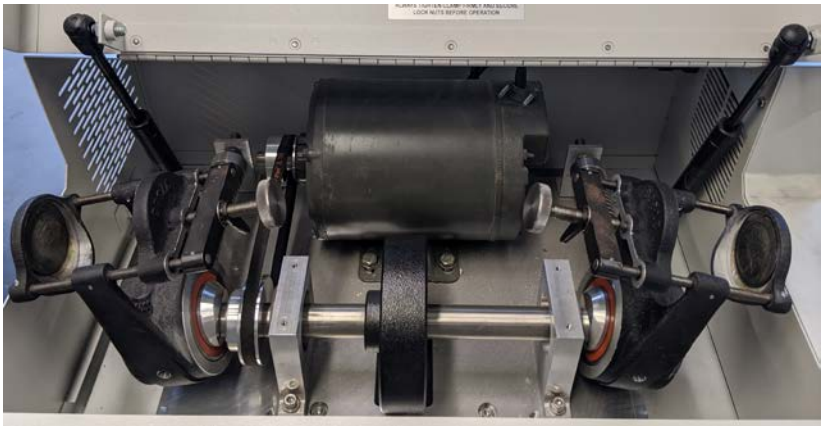

Figure 20. HEBM Apparatus

2. Flowability Concerns

As explained below in Section C: Composite Powder Imaging, the HEBM process was largely successful in that it resulted in a good dispersion of the reinforcing ceramics and broke up most, if not all, large agglomerates of the ceramics. However, the resulting composite powder had greatly reduced flowability when compared to the base Ti-6Al-4V powder. Flowability is a nebulous concept that is particularly difficult to quantify; this study limited measurements of flowability to the following comparison: when the commercially pure Ti-6Al-4V powder was poured through a 425-micron sieve, the powder would flow easily without assistance. The composite powders required aggressively shaking the 425-micron sieve in order to get all of the powder to flow through the sieve. The Ti-6Al-4V Ta_2O_5 powder had worse flowability compared to the Ti-6Al-4V Al_2O_3 powder, and required noticeably more agitation to get it to pass through the 425-micron sieve comparatively.

C. COMPOSITE POWDER MORPHOLOGY

1. Ti-6Al-4V Ta_2O_5 1%

The Ti-Ta1 powder is pictured in Figure 21 and Figure 22. This powder was characterized by lower flowability than the either of the Ti-6Al-4V Al_2O_3 powders. As seen in Figure 21, there were agglomerates made solely of Ta_2O_5. However, these agglomerates were much smaller than they were in the pure Ta_2O_5 powder, indicating that the HEBM process had achieved the desired results. Furthermore, the vast majority of Ta_2O_5 particles were actually well cohered to Ti-6Al-4V powder spheres, indicating that the powder had achieved good distribution of ceramic reinforcements. For this reason, the decision was made to move forward in the additive manufacturing process and attempt to perform SLM using this composite powder as the feedstock powder—further cycles of HEBM did not appear necessary. Furthermore, more of the Ti-6Al-4V spheres appeared to have been impacted and to have lost their spherical shape than with the as-received commercial Ti-6Al-4V powder as seen in the bottom right-hand corner of Figure 21. More HEBM could have exacerbated this issue and actually decreased the performance of this composite powder.

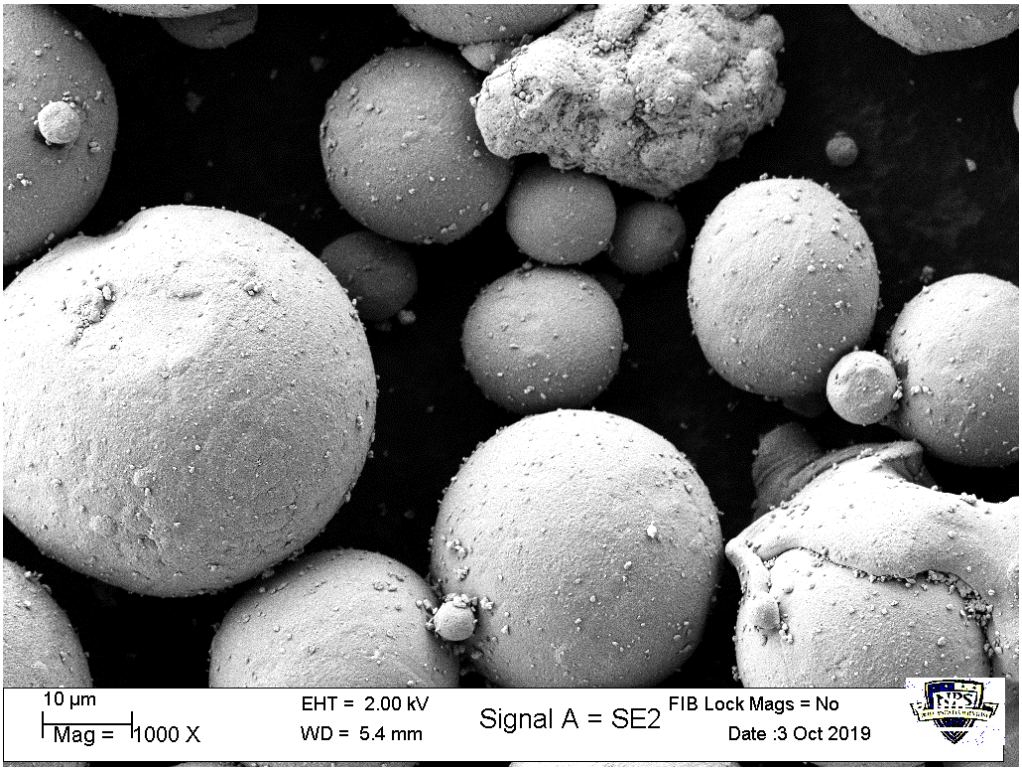

Figure 21. High Magnification SEM Image of Ti-Ta1 Powder

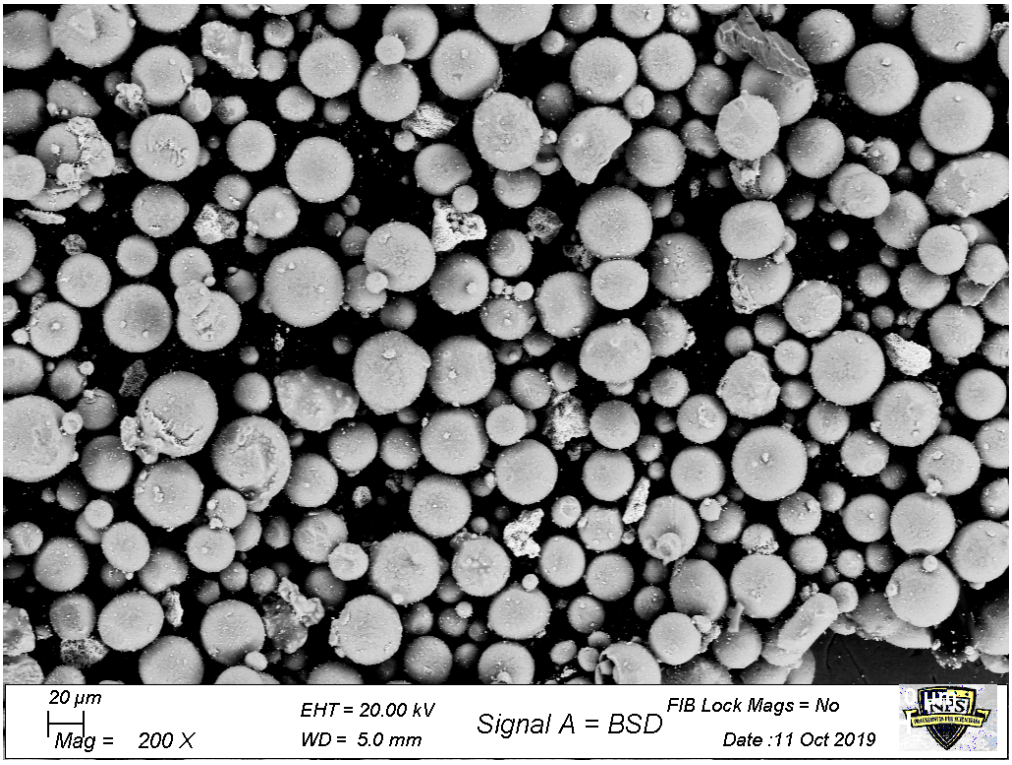

Figure 22. Low Magnification SEM Image of Ti-Ta1 Powder

2. Ti-6Al-4V Ta_2O_5 3%

The Ti-Ta3 had no noticeable decrease in flowability when compared to the Ti-Ta1 powder. However, under the SEM this powder was revealed to have considerably worse ceramic reinforcement distribution than the Ti-Ta1 powder. Specifically, as seen in Figure 23, the small Ta_2O_5 fragments were not as evenly dispersed as they were in the 1% powder. This had the potential to impact additive manufacturing negatively, as it created the potential for pockets with different amounts of reinforcing ceramic to occur in the final part. On a more positive note, the amount of large agglomerates of Ta_2O_5 was not increased in the 3% composite powder when compared to the 1% powder (see Figure 24). This was expected, as both powders underwent the same amount of HEBM cycles.

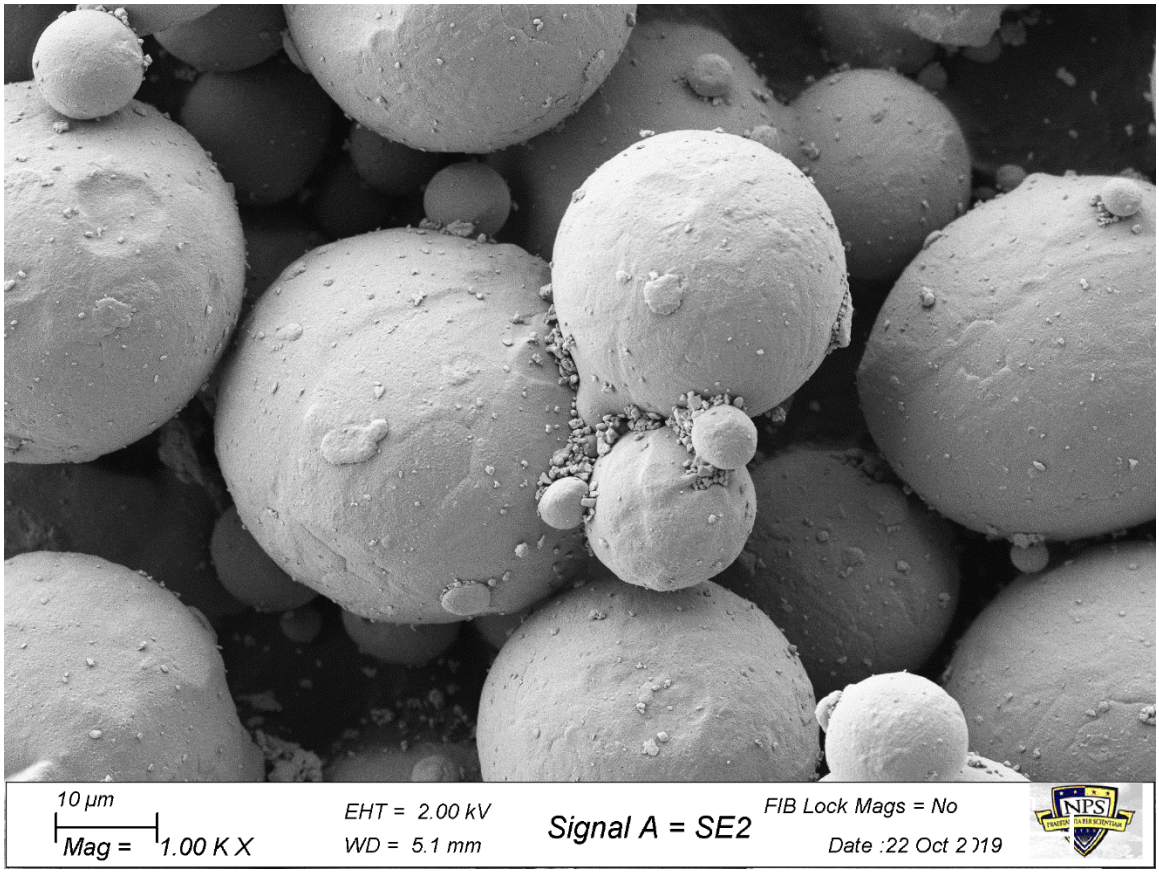

Figure 23. High Magnification SEM Image of Ti-Ta3 Powder

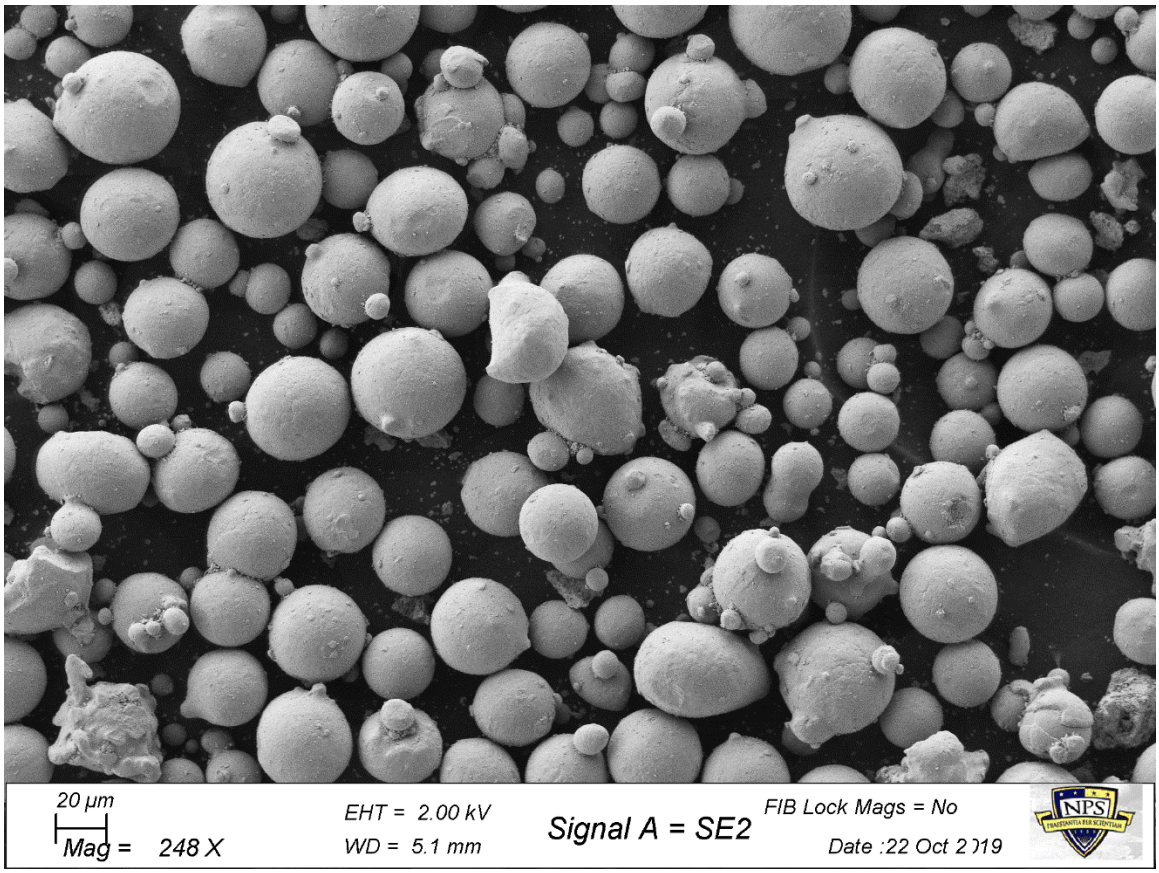

Figure 24. Low Magnification SEM Image of Ti-Ta3 Powder

3. Ti-6Al-4V Al_2O_3 1%

As mentioned above, the Ti-Al1 powder had markedly better flowability than the either of the Ta_2O_5 composite powders. The Al_2O_3 powder also did not have large agglomerates of Al_2O_3, indicating that the HEBM process was largely successful. As seen in Figure 25, the Al_2O_3 was well cohered to the Ti-6Al-4V particles. Figure 26 shows that neither the addition of Al_2O_3 nor the HEBM process appeared to result in large changes to the composition of the titanium—roughly the same number of imperfect spheres were visible in the post HEBM composite powder as in the as received titanium powder. As a result, this was the powder that the research team expected would perform best in the EOS 100M SLM machine.

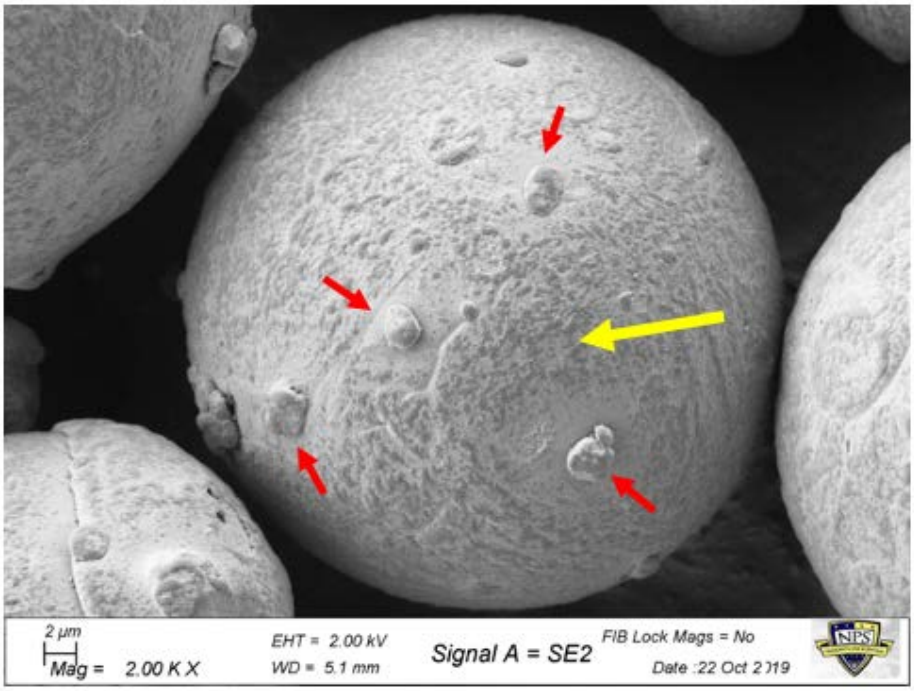

Yellow arrow highlights a region of well-dispersed Al_2O_3; red arrows highlight Al_2O_3 agglomerates

Figure 25. High Magnification SEM Image of the Ti-Al1 Powder

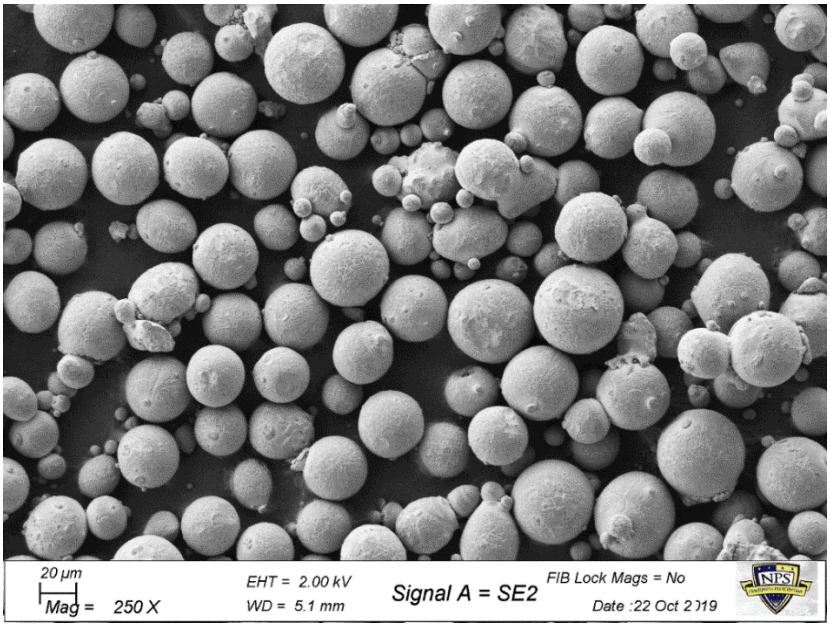

Figure 26. Low Magnification SEM Image of the Ti-Al1 Powder

4. Ti-6Al-4V Al_2O_3 3%

The Ti-Al3 powder had no visual decrease in flowability readily apparent when compared to the Ti-Al1 powder. However, imaging using the SEM made it obvious that even just two percent increase in volume percent of Al_2O_3 had a large impact on the overall composition of the composite powder. For example, Figure 27 highlights an area were a misshapen titanium sphere resulted in a large grouping of Al_2O_3 particles. Regions such as these were more common in the Ti-Al3 powder than they were in the 1% powder. Thus, the increase in Al_2O_3 had a negative overall impact on the distribution of the ceramic reinforcements within the composite powder. That said, the HEBM process was still sufficient to eliminate any large agglomerates of Al_2O_3, as seen in Figure 28.

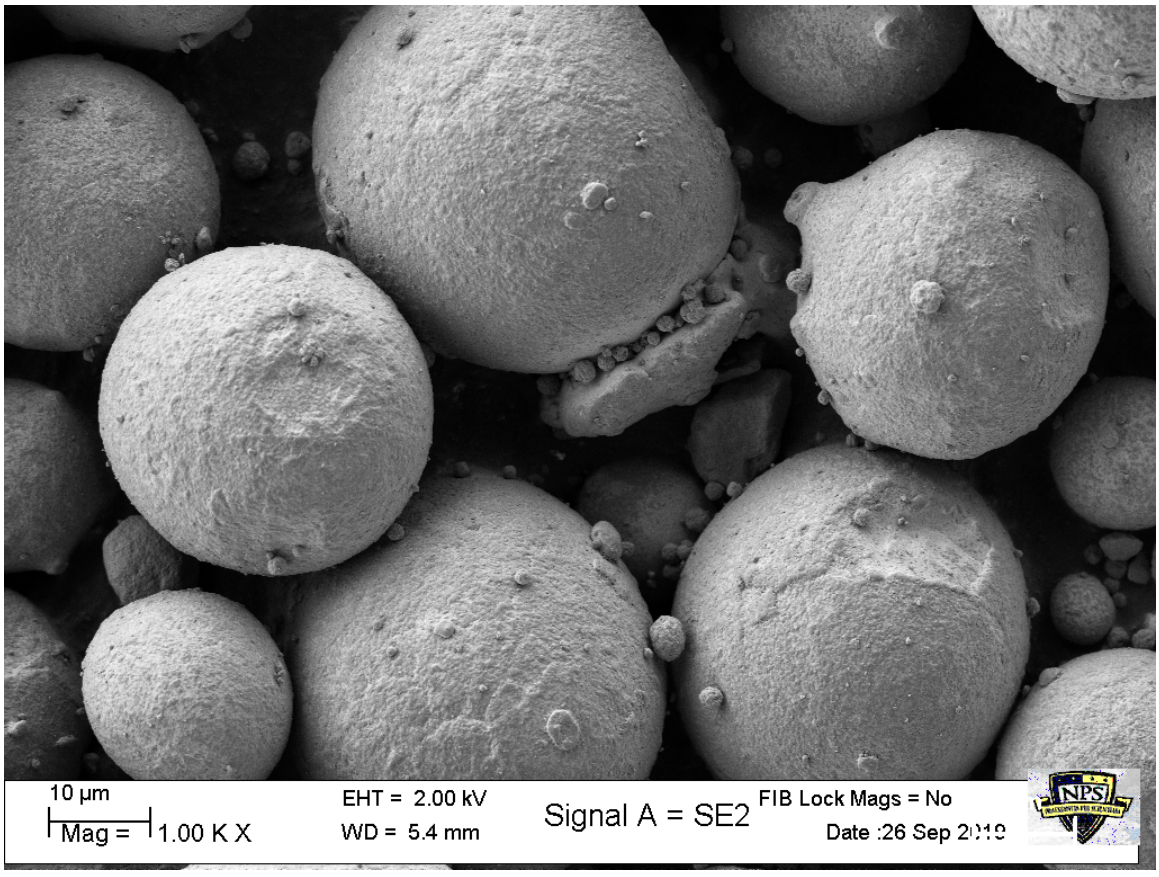

Figure 27. High Magnification SEM Image of the Ti-Al3 Powder

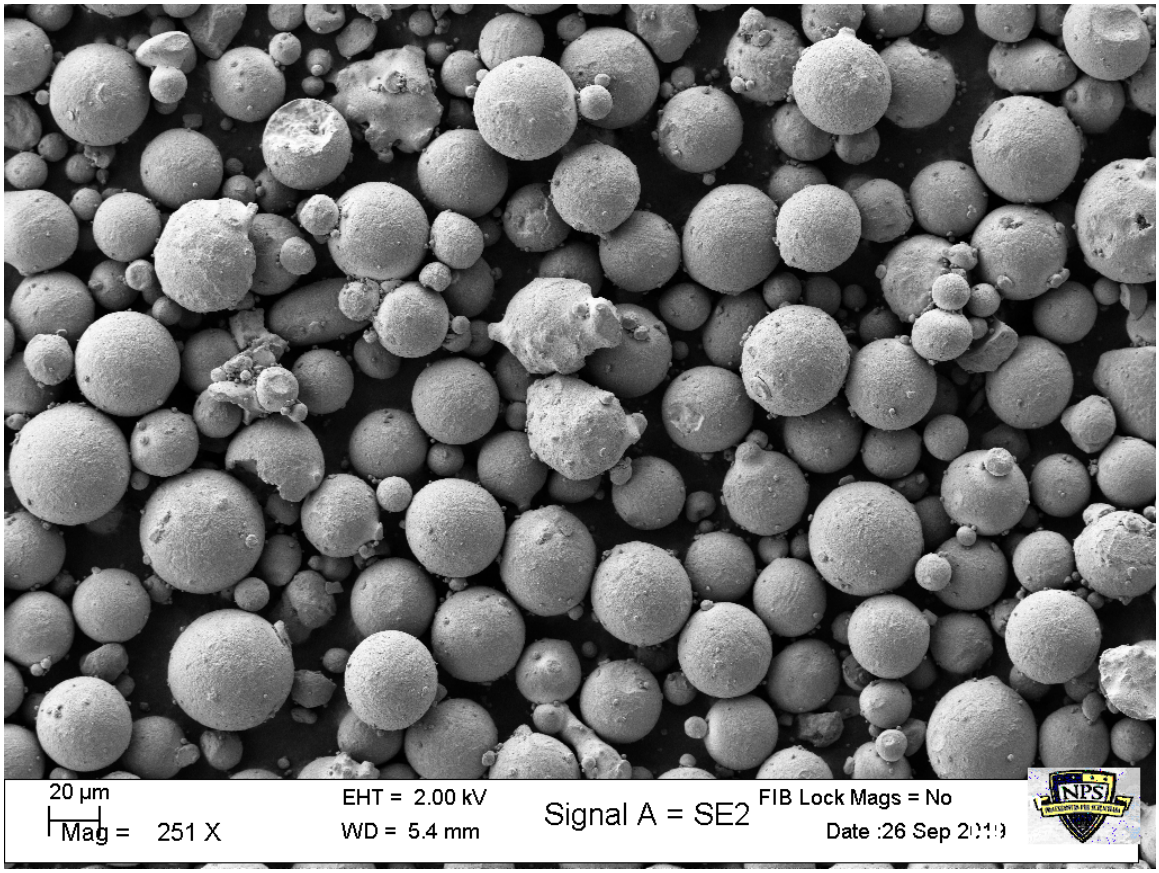

Figure 28. Low Magnification SEM Image of the Ti-Al3 Powder

D. ADDITIVE PROCESSING OF CUBOID SPECIMENS

The cube specimens were additively manufactured using the Naval Postgraduate School Mechanical and Aerospace Engineering Department's EOS M 100 Printer (see Figure 29). The EOS M 100 printer is an entry level model for SLM of metal materials such as Ti-6Al-4V. If the cube specimens could be successfully fabricated in this machine, they could easily be scaled up for commercial use in larger, more customizable SLM printers. The EOS M 100 Printer uses a Yb-fiber laser with a maximum power of 200 watts, has a maximum rastering speed of 7 meters per second, and a focus diameter of 40 micrometers. It requires a power supply of 240 volts, and has a maximum power consumption of 1.7 kilowatts. The EOS M 100 also requires an inert gas supply of 4,000 hectopascals at 50 liters per minute [55]. The maximum building volume for the printer is a cylinder with a 100-millimeter diameter and a 95-millimeter height.

Figure 29. EOS M 100 Printer. Source: [55].

The decision was made to use the manufacturer's recommended default settings for SLM for Ti-6Al-4V powder for all four composite samples. This meant that the laser for printing was set to 100 watts and that the rastering speed was 1000 millimeters per second. Cubes of four millimeters by ten millimeters by ten millimeters were designed in SolidWorks then imported to the Materialise Magics software in order to turn them into STL files. Originally, Materialise Magics default support cross hatching was used; however difficulty getting the composite powder to adhere to the supports once building of the actual cubes commenced led to the use of much thicker, custom made cylindrical supports be utilized instead. Specifically, large cylindrical support structures were added to around the edges of the cube, in addition to automated matrix of cylindrical supports generated by default by the Materialise Magics software (see Figure 30). An image of the final build file produced in the Materialise Magics software is included as Figure 31. This was an STL file, meaning that it included information for each individual layer that would be built in the EOS M 100 printer.

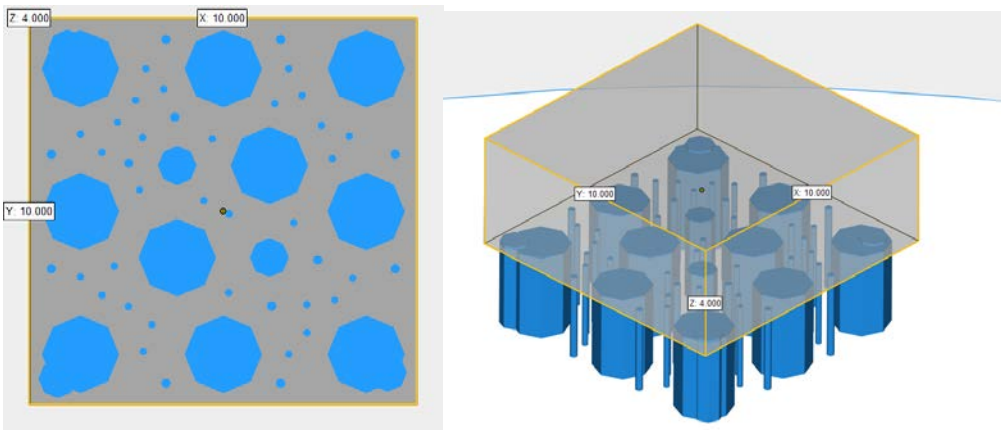

Figure 30. Images of Customized Supports

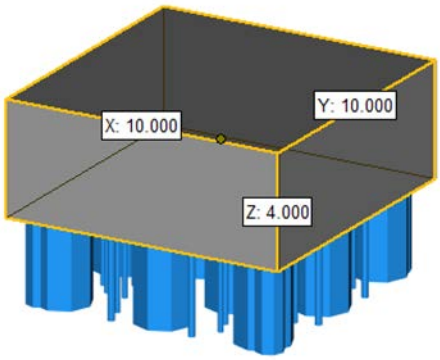

Figure 31. Cube Specimen Build File Image from Materialise Magics Software

Once the STL build file and supports were completed using the Materialise Magics software, they were then imported into the EOS M 100's native EOS print software (see Figure 32). From here, an array of 16 cubes was created so that all the test specimens required for a single composite powder would be constructed in the same run to mitigate potential processing differences between the different cubes as much as possible. The laser was programed to raster beginning from the top left cube, then moving right across the first row, finishing an entire row before moving down to next row in order to minimize any potential re-melting or cross contamination that could arise from the laser passing over certain regions multiple times. A final completed cube specimen is included below as Figure 33.

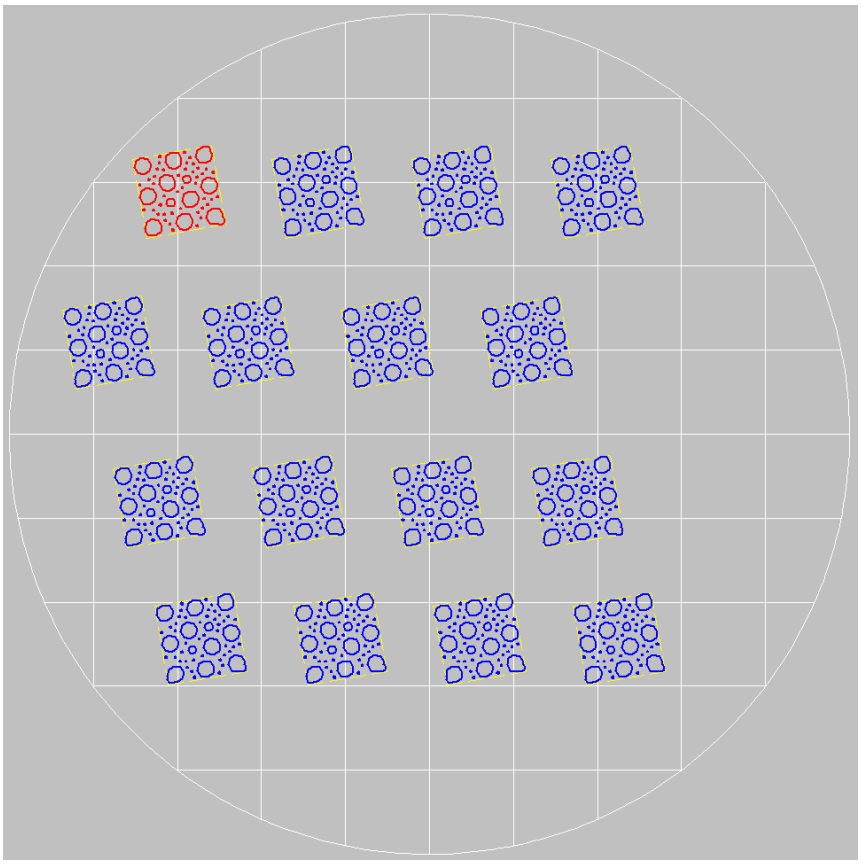

Figure 32. EOS Batch Run File

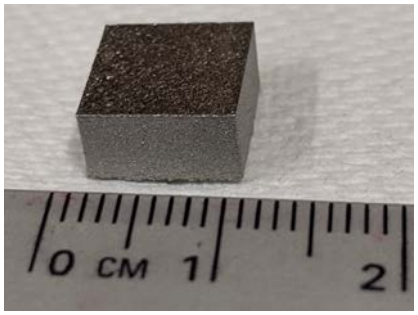

Figure 33. Completed Cube Specimen

As mentioned above, SEM imaging of the various powders and flowability observations lead to the hypothesis that the Ti-Al1 powder would perform best in the SLM process as this powder had the highest flowability, the smallest agglomerates of the ceramic reinforcements, and the best dispersion of the reinforcement material throughout the titanium powder. However, this was not the case. Out of the four composite powders, only

the Ti-Ta1powder was able to print successfully. The other three powders failed to completely print cube specimens, as their high porosity and poor flowability prevented the individual additively manufactured layers from properly adhering to the previously built layers and/or the support structure, as well as due to reactivity issues that arose for some of the powders. The Ti-Al1 powder in particular failed primarily due to reactivity between the powder and the laser. The Ti-3A powder failed due to reactivity and possible dispersion. Finally, the Ti-Ta3 powder failed due to poor powder dispersion and low flowability. Enough material was deposited from all four powders to analyze their microstructure via SEM, and enough material was deposited to allow for nanoindentation tests to be conducted on the Ti-Al1 in addition to the successfully completed Ti-Ta1sample. Oxidation tests required completed cube specimens; thus oxidation tests were only performed on the control material and the Ti-Ta1samples.

E. MICROSTRUCTURE OF PRINTED CUBE SPECIMENS

The microstructure of completed additively manufactured composite cubes was observed using the SEM and compared to the microstructure of a control cube made solely from the commercial grade Ti-6Al-4V powder. These samples were etched with a solution that was 10 percent by volume HF, 5 percent by volume HNO_3, and 85 percent water in order to make the α and β phases more easily visible under the SEM. Additionally, these samples were subjected to the nanoindentation tests before being placed under the SEM. For more information regarding the results from the indentation tests, please refer to Chapter IV Section A. Nanoindentation Testing.

1. Ti-6Al-4V (Control Sample)

As mentioned above, a control sample made solely from the commercial grade Ti-6Al-4V was fabricated via SLM to allow for comparison between the microstructure and mechanical properties of the base material and the composite materials. The microstructure of this control sample was first examined under the SEM without etching, as seen below in Figure 34. However, this was not sufficient to reveal which phases of titanium were present, and was only useful to learn about the porosity and uniformity of the sample. This

did demonstrate that this Ti-6Al-4V sample had very low porosity and was mostly uniform, as expected, which in turn would lead to high tensile strength.

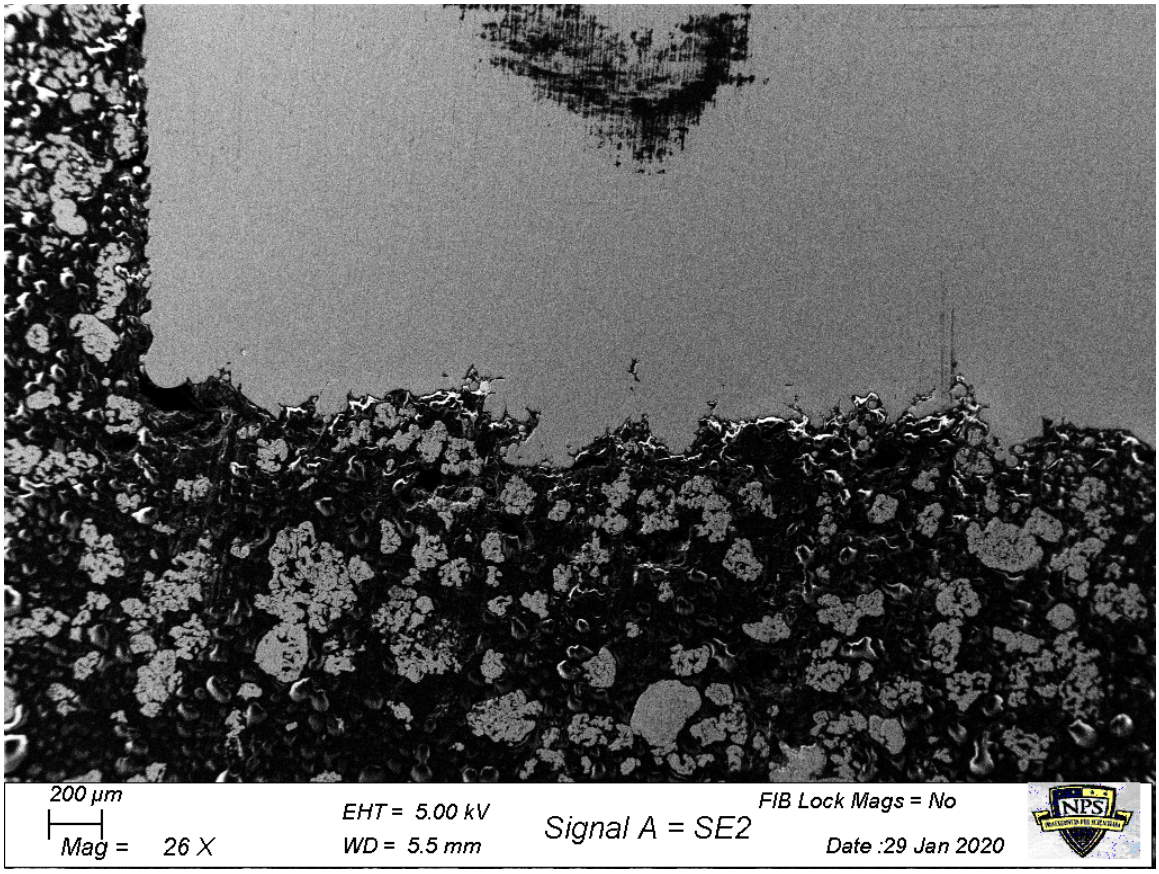

Figure 34. SEM Image of Control Ti-6Al-4V Sample

As seen in Figure 35 and Figure 36, etching the control sample revealed a great deal of information regarding the phases present in the microstructure of the titanium. Both of these images highlight the presence of α and β phases throughout the microstructure, as expected given that Ti-6Al-4V is an α+β titanium alloy. The β phase is stable at temperatures above 882 degrees Celsius, and the laser clearly melted the titanium at temperatures higher than this. The β regions are the darker regions, and the α grains appear as the lighter, linear regions in Figure 35 . The fact that there are α grains oriented in numerous different directions indicates that the imaged cross-section is likely isotropic in nature, and thus will have similar mechanical properties across all directions. One of the

key observations from Figure 36 is that the β regions are not perfectly uniform or evenly dispersed throughout the control sample—the sample was ‘mostly’ uniform, as mentioned above, but there were certainly regions where only one phase was phase present. This observation was important as it indicates that the composite sample did not need to be entirely uniform in order to exhibit better mechanical properties than the control sample—as long as they were mostly uniform, they could potentially exhibit the same amount of isotropic behavior as the cube specimens constructed from the commercial Ti-6Al-4V.

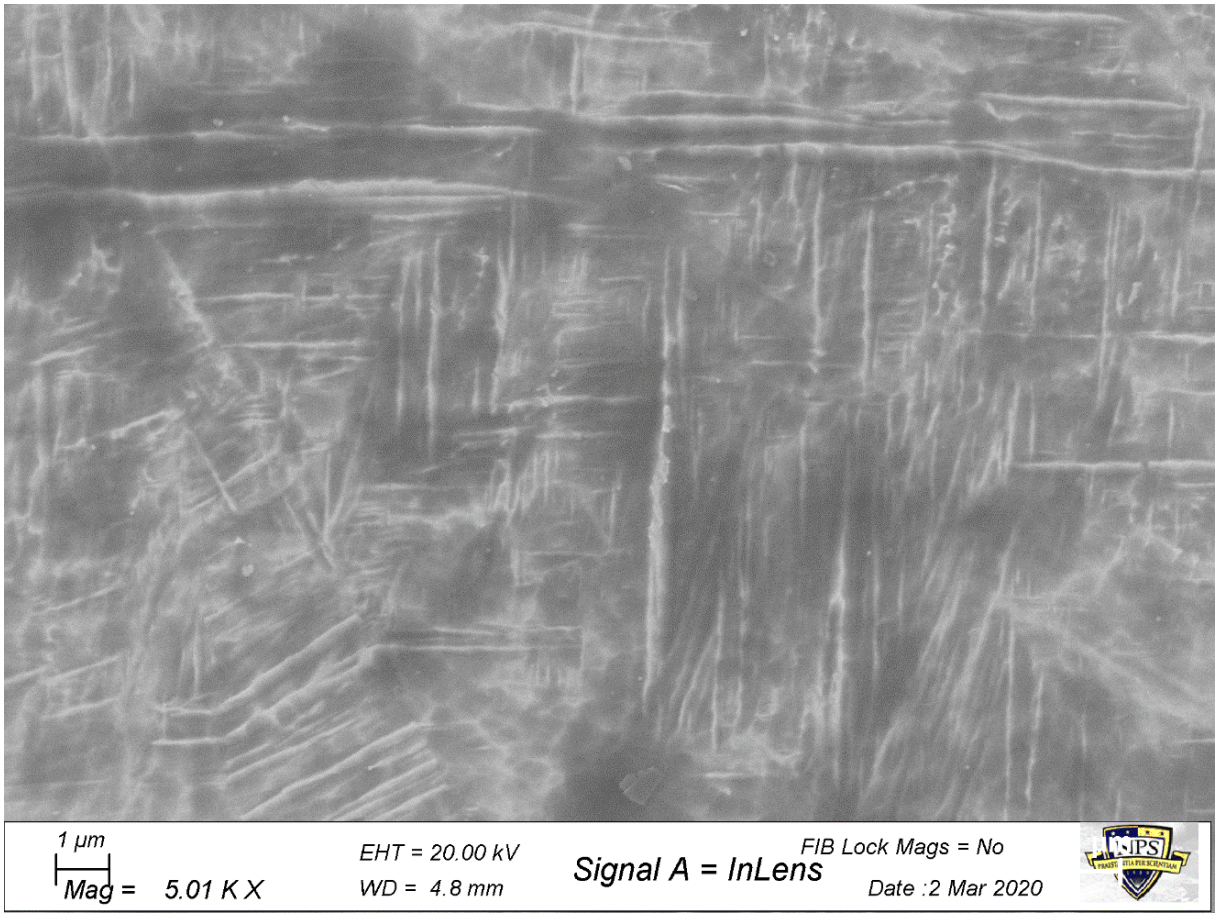

Figure 35. High Magnification SEM Image of Ti-6Al-4V Microstructure from Etched Sample

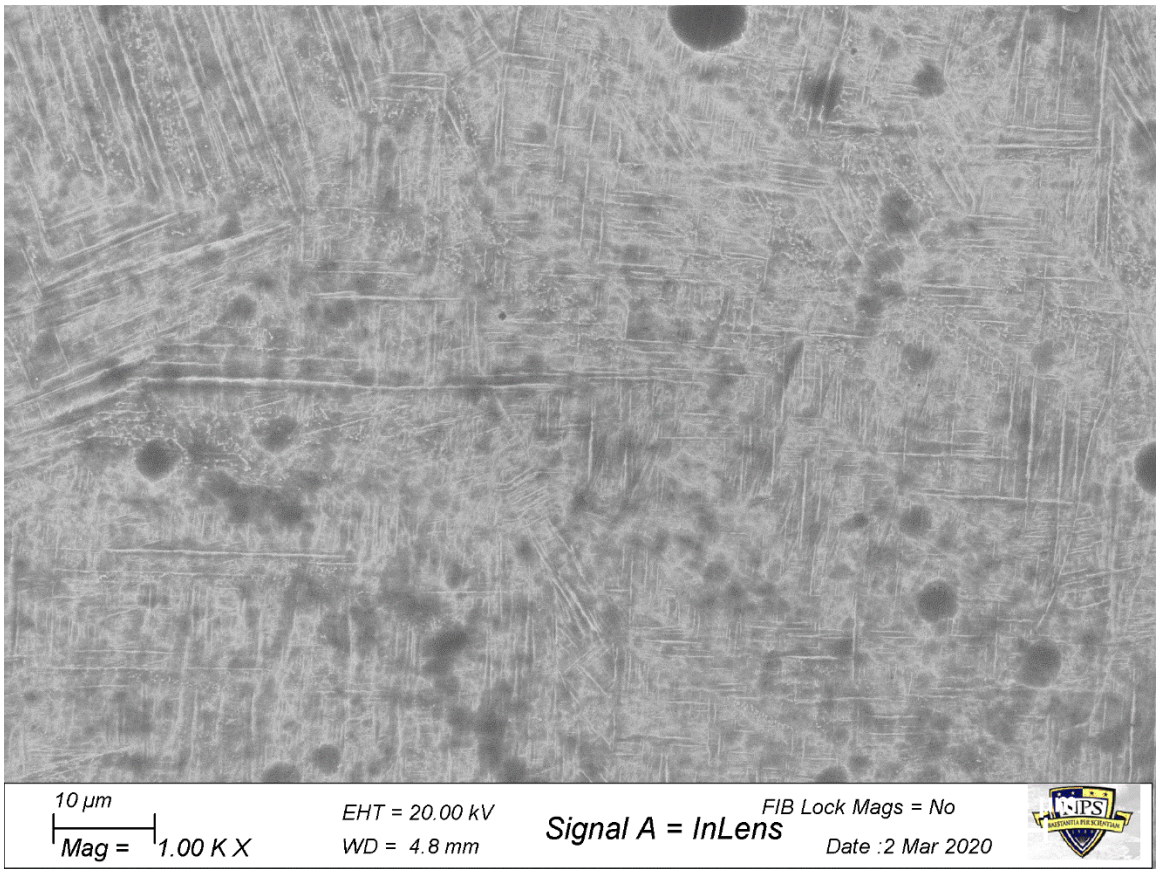

Large dark circular features are likely etching artifacts

Figure 36. Low Magnification SEM Image of Ti-6Al-4V Microstructure from Etched Sample

2. Ti-6Al-4V Ta_2O_5 1%

There were 16 cube specimens of Ti-Ta1 successfully additively manufactured via SLM. From these samples, 15 were used in oxidation studies while one was subjected to nanoindentation testing and had its microstructure analyzed via the SEM as received from the EOS 100 M SLM machine. In addition, energy-dispersive X-ray spectroscopy (EDS) was performed on this sample to locate the tantalum pentoxide reinforcements and determine how these tantalum particles were added to the titanium matrix. Figure 37 is an image of this sample taken prior to etching. The highlighted region was an area of interest, as the lighter particle on the surface was believed to be a tantalum conglomerate that

retained its form. As seen in Figure 38, EDS analysis confirmed that this was indeed an agglomerate of Ta_2O_5.

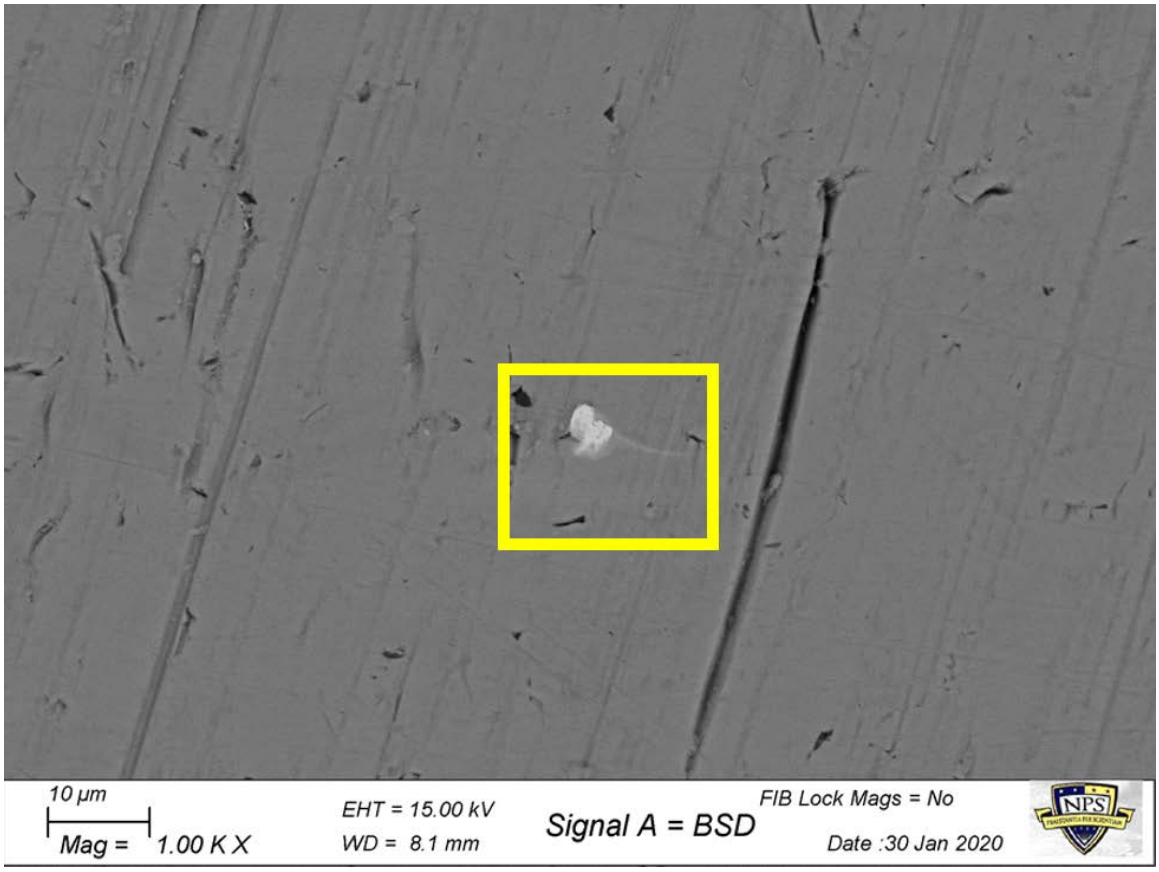

Figure 37. 1000x SEM Image of Untreated Ti-Ta1Sample with Ta_2O_5 Particle Highlighted

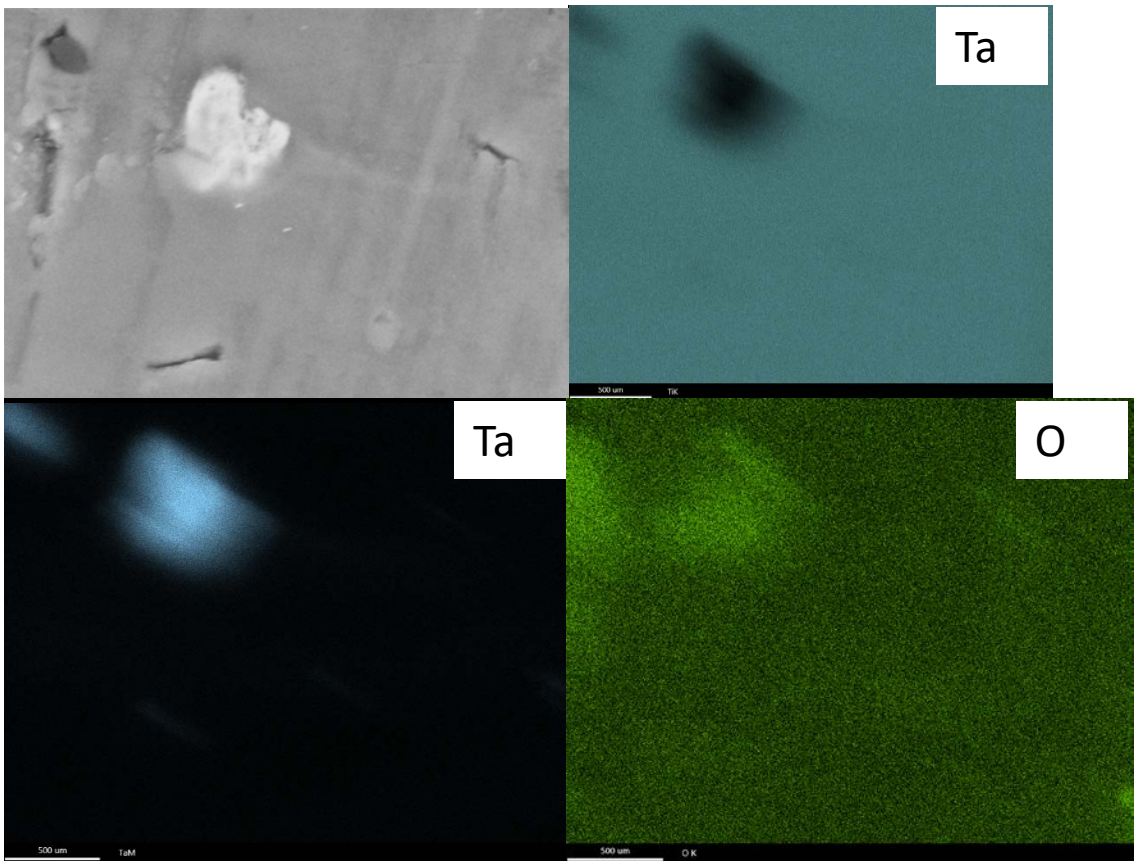

Figure 38. Elemental Overlay Conducted via EDS

These Ta_2O_5 agglomerates were readily apparent at many different locations in the microstructure, and the amount of Ta_2O_5 particles that mixed with the titanium matrix appeared to be limited. Figure 39 and Figure 40 are SEM images of the etched specimen. Again, both the α and β phases of titanium were readily apparent, as was expected. Also important to notice are the numerous agglomerates of Ta_2O_5; these agglomerates are distinct as they appear as white particles that are separate from the underlying titanium matrix. Additionally, the distribution of these Ta_2O_5 is random and not uniform in anyway; rather there appear to be groupings of Ta_2O_5 particles. That said, the tantalum did not have any negative impact on the phases of titanium—the α phases are oriented in all directions just as they were for the control sample, indicating that this sample should have mechanical properties that are just as isotropic as the specimen produced solely from the pure Ti-6Al-4V powder.

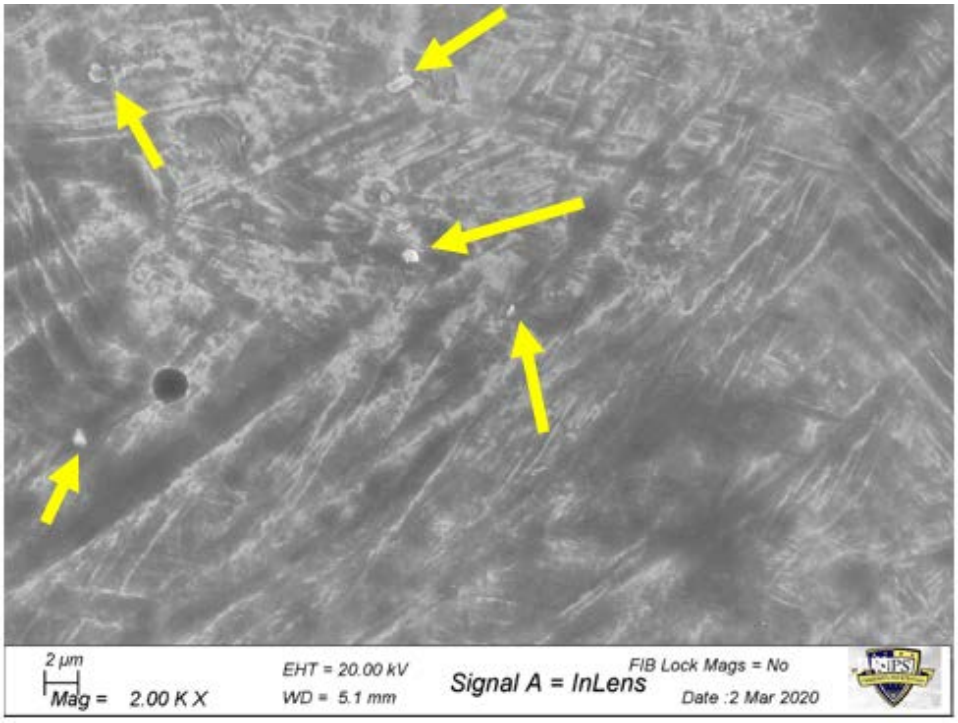

Figure 39. High Magnification SEM Image of Etched Ti-Ta1
Arrows Indicate Ta_2O_5

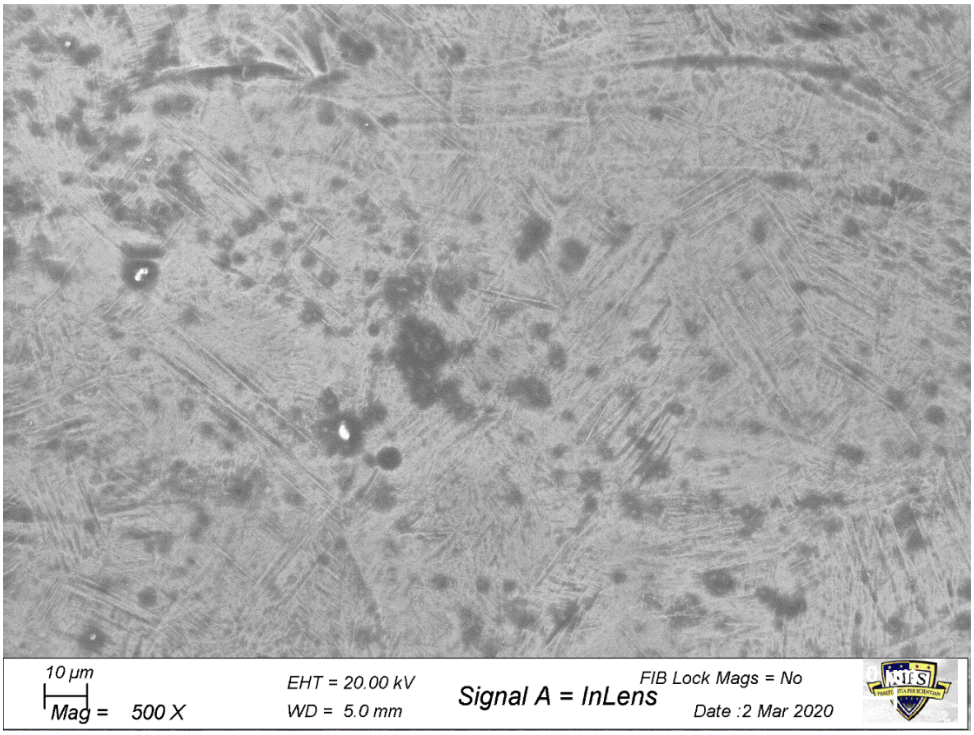

Figure 40. Low Magnification SEM Image of Etched Ti-Ta1

3. Ti-6Al-4V Ta_2O_5 3%

As mentioned previously, the Ti-Ta3 composite powder failed to successfully print cube specimens during SLM. The following SEM images were taken from partially completed additively manufactured fragments. These images revealed much higher porosity than was seen in either the control sample constructed solely from Ti-6Al-4V, or in the Ti-Ta1sample. This indicates that the EOS M 100 printer was most likely unable to fully coat the build plate during printing, an issue that can arise as a result of poor flowability from the feedstock powder. The incomplete coating will lead to the high porosity of the resulting material, as there was not enough powder available to be melted by the laser. It is believed that this was the main reason why these samples failed to print completely. Figure 41 in particular depicts some of this localized residual porosity within the microstructure of the composite material. Figure 42 is a low magnification image that helps highlight the fragmented nature of the incomplete specimen, particularly along the edges of this sample. Figure 43 is an image of an internal crack within this sample.

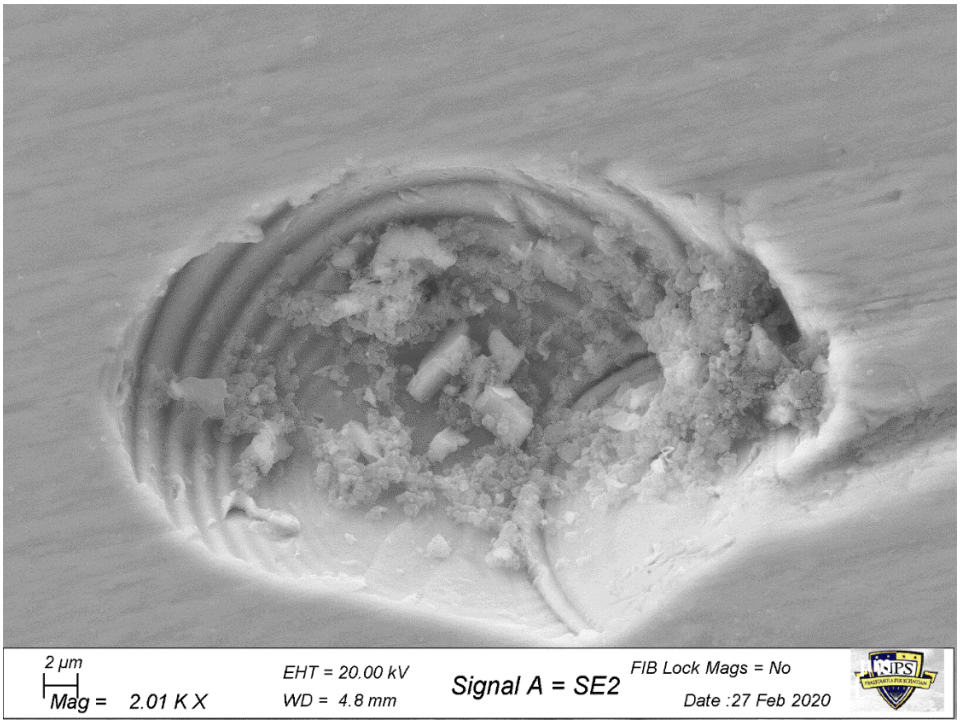

Figure 41. SEM Image of Ti-Ta3 with Localized Porosity

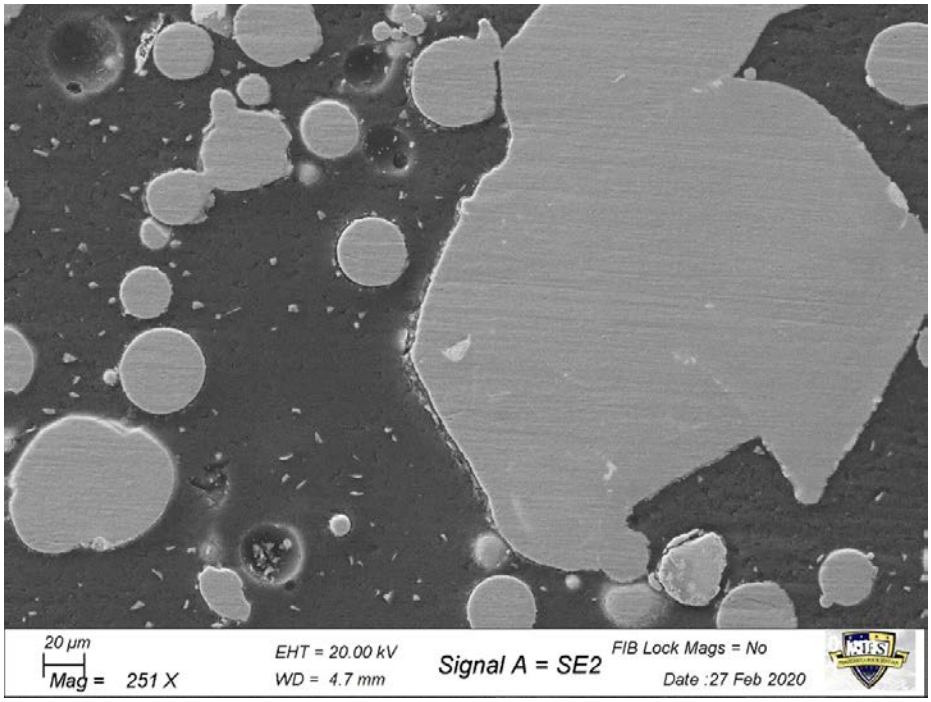

Taken at edge of sample, highlights fragmented nature of specimen, particularly at edges of sample

Figure 42. Low Magnification SEM Image of Ti-Ta3

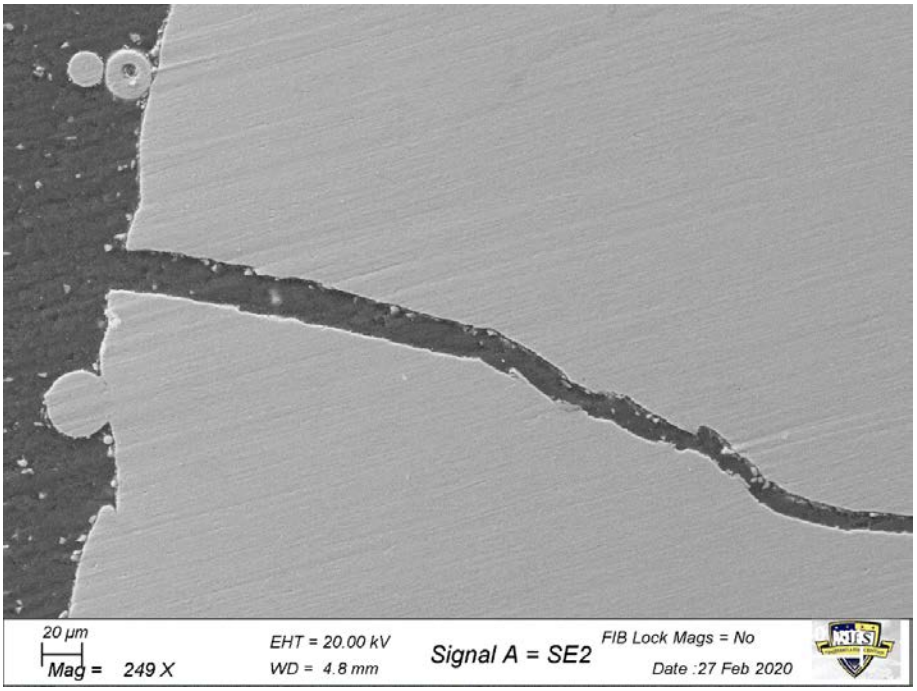

Figure 43. SEM Image of Internal Crack within Ti-Ta3 Sample

In the SEM imaging of each composite powder, it was noted that the agglomerates of ceramic reinforcements were no larger in the 3% powder than they were in the 1% powder, but that there were not nearly as well dispersed. In Figure 44 , one of the agglomerates of Ta_2O_5 was imaged at high magnification. This particle is actually very similar in size to the agglomerate of Ta_2O_5 depicted in Figure 37; the particle in the 3% composite power is approximately six microns in width while the particle in the 1% composite powder was determined to be approximately four microns in width. Thus, this observation remained true even after SLM.

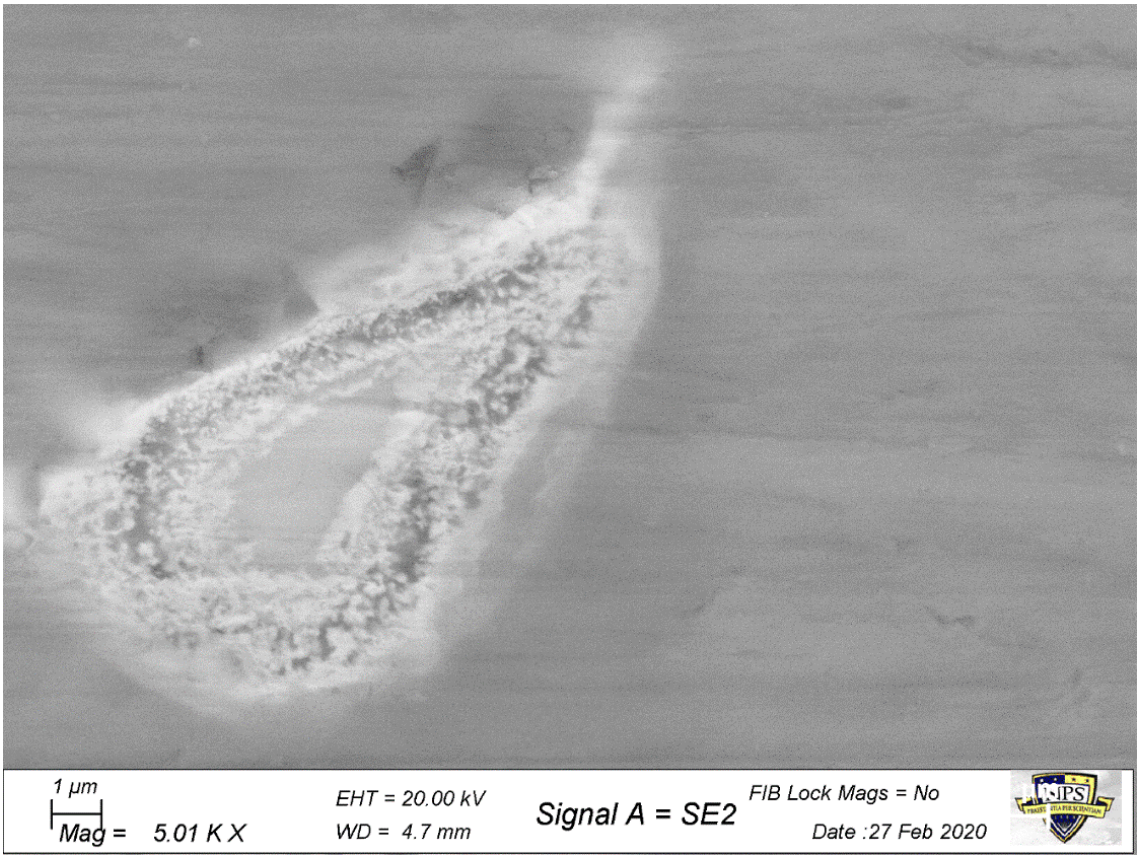

Figure 44. SEM Image of Ta_2O_5 within the Ti-Ta3 Specimen

4. Ti-6Al-4V Al_2O_3 1%

The Ti-Al1 sample also failed to print correctly. Analysis under the SEM indicated that porosity may also have been driving factor in this failure, just as it was for the tantalum

pentoxide samples. Additionally, it was noted above that reactivity was believed to be the main reason for the failure to complete the print. Figure 45 is an example of localized residual porosity found within the specimen. Although the Ti-Al1 powder had better flowability than the Ta_2O_5 powders, the alumina composite powder still had worse flowability than the base titanium powder and this could have been a driving factor that lead to the formation of localized pores. Figure 45 is an image of a cluster of nano-Al_2O_3 particles within the composite build. The survivability of a large cluster would tend to indicate that the agglomerate did not disperse well and establish adequate interfacial bonding with the titanium matrix.

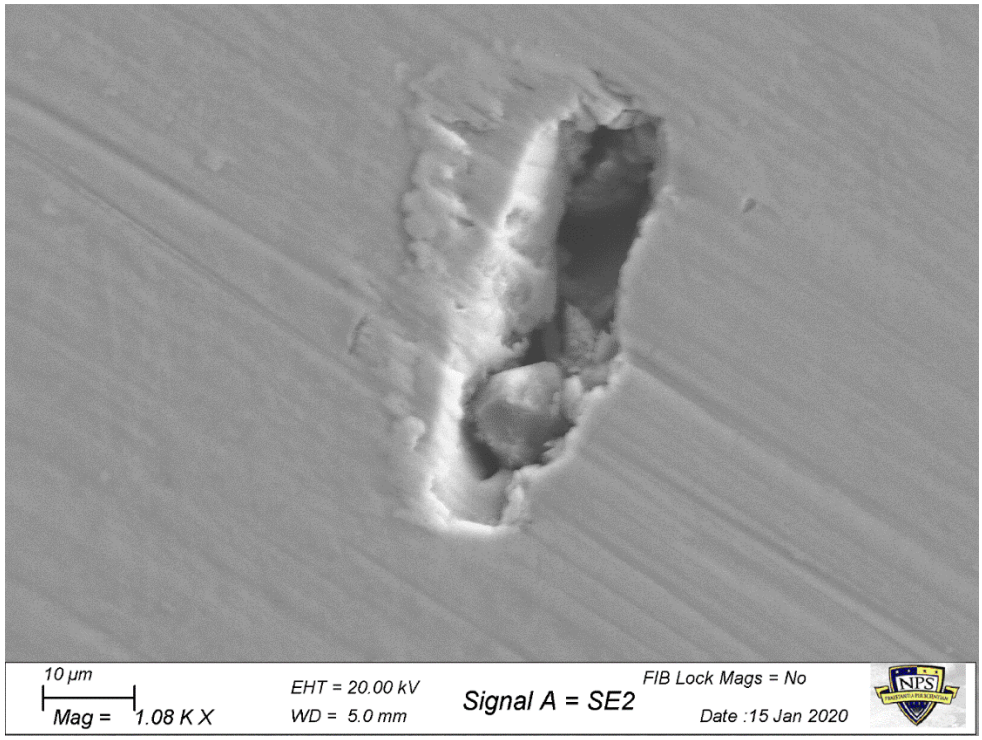

Figure 45. SEM Image of Localized Porosity within the Ti-Al1 Specimen

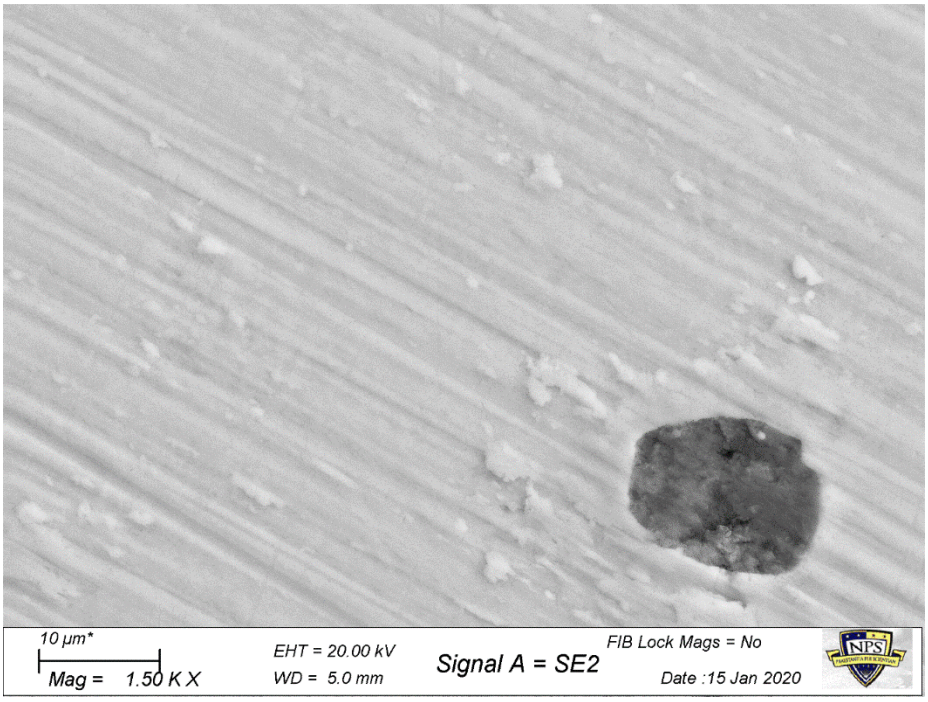

Figure 46. 1500x SEM Image of Cluster of Al_2O_3 within the Ti-Al1 Build

5. Ti-6Al-4V Al_2O_3 3%

The Ti-Al3 also failed to successfully complete a full build. As seen in Figure 47, the composite build was composed of both the α and β phases of titanium. However, the microstructure actually appears significantly different when compared to the microstructure of the etched Ti-6Al-4V Ta_2O_5 samples at the same magnification. For example, β phases within the Ti-6Al-4V Al_2O_3 sample are much wider and longer than in the Ti-6Al-4V Ta_2O_5 sample. That being said, the β phases are also less dominant and cover less percent area of sample when compared with the tantalum specimen. The etched Ti-Al3 sample was just as isotropic as the Ti-6Al-4V Ta_2O_5 sample, as it had β phases oriented in all directions. This implies that the added ceramic reinforcements did not result in the formation of unstable compounds, and that mechanical issues such as flowability were more likely the cause of the SLM processing challenges rather than any potential chemical compatibility issues between Al_2O_3 and Ti-6Al-4V.

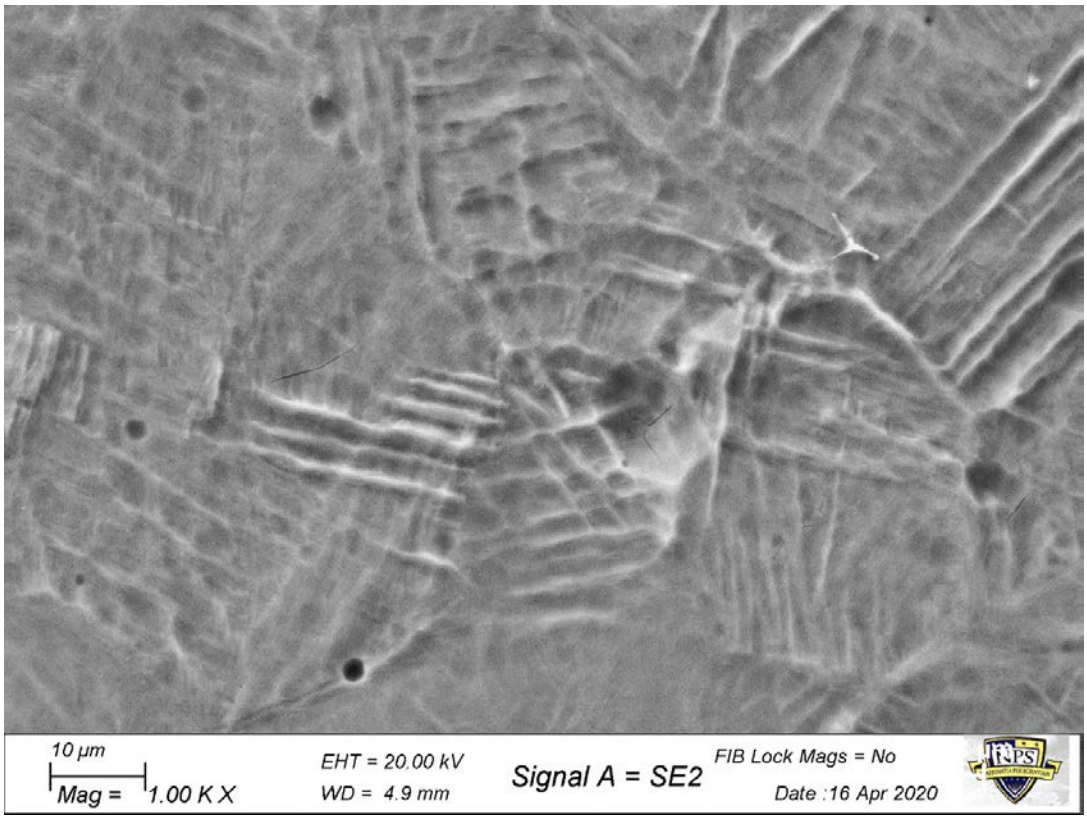

Figure 47. SEM Image of Etched Ti-Al3

Figure 48 and Figure 49 are SEM images of alumina particles within the etched Ti-Al3 sample. These images illustrate that the alumina has a high degree of survivability within the composite builds. Another important observation from these two images is that there was a substantial amount of internal cracking within the build. This internal cracking resulted in increased porosity, and thus could also be part of the reason why this composite powder failed to print successfully.

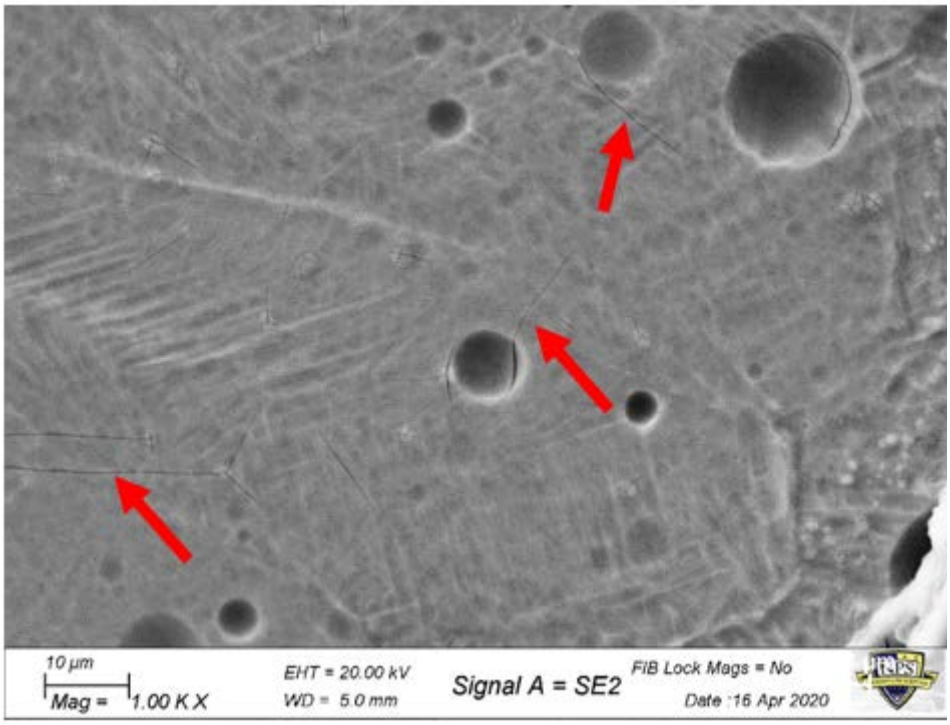

Figure 48. High Magnification SEM Image of Internal Cracking within Etched Ti-Al3 Specimen

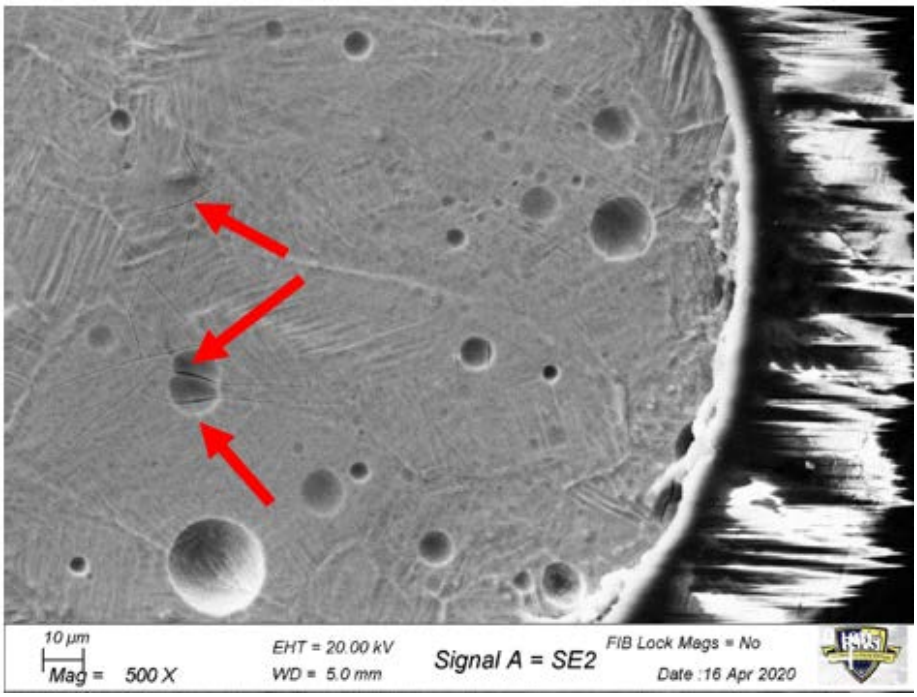

Figure 49. Low Magnification SEM Image of Internal Cracking within Etched Ti-Al3 Specimen

THIS PAGE INTENTIONALLY LEFT BLANK

IV. MECHANICAL PROPERTIES

In the second phase of this study, the material properties of each composite material were tested and compared to the properties of the control Ti-6Al-4V sample. Specifically, and indentation test was performed on each material in order to determine their hardness and elastic modulus.

A. INDENTATION TESTING

Due to the small cuboid nature of the 3D printed specimens, the best technique to measure mechanical properties such as tensile strength was via hardness testing. This study used a Berkovich diamond tipped nano-indenter at two different loading conditions: 500 mN and 3 mN. A schematic of a Berkovich tip is included as Figure 50. The rationale behind the two different load tests was that the 500 mN test would approximate a micro-indentation test due to the depth of the indentations created, whereas the 3 mN test would be a true nano-indentation test. Using a poisons ratio of 0.340 for titanium alloy (see [56]) allowed for the calculation of hardness and elastic modulus for both the composite materials and the control sample.

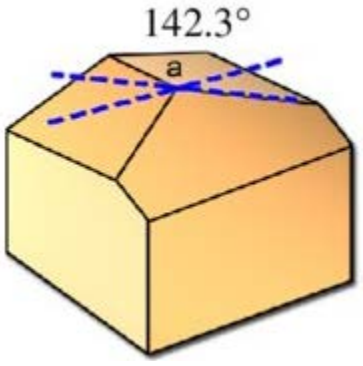

Figure 50. Nano-indenter Berkovich Tip [57]

The indenter made an array of 25 indents with 25 microns between indents for the 500 mN tests and an array of 100 indents with five microns between indents for the 3 mN tests. For each individual indentation, a peak hold time of 3 seconds was used, a time to

load of 10 seconds was used, and the percent to unload between indents was set to 100%. The surface approach velocity of the indenter tip was set to 100 nm/s and the indents were only loaded a single time. Figure 51 is an example of a single indentation test site and Figure 52 is an image taken of part of the 500 mN test array. The 3 mN test arrays made indents so small that they could not be easily found using the SEM. The main reason for using 25 tests at one loading condition and 100 tests at the other was that much more localized variation was expected for the indents conducted on the nano scale than indents conducted on the micro scale, and as a result more tests would be necessary in order to insure the data was an accurate representation of the tested materials actual mechanical properties. See Figure 53 for an example of an indent that contained a defect, leading to an erroneous result. In both tests, all results that were more than one standard deviation away from the mean were dismissed as outliers, and then a new average was calculated from the remaining values.

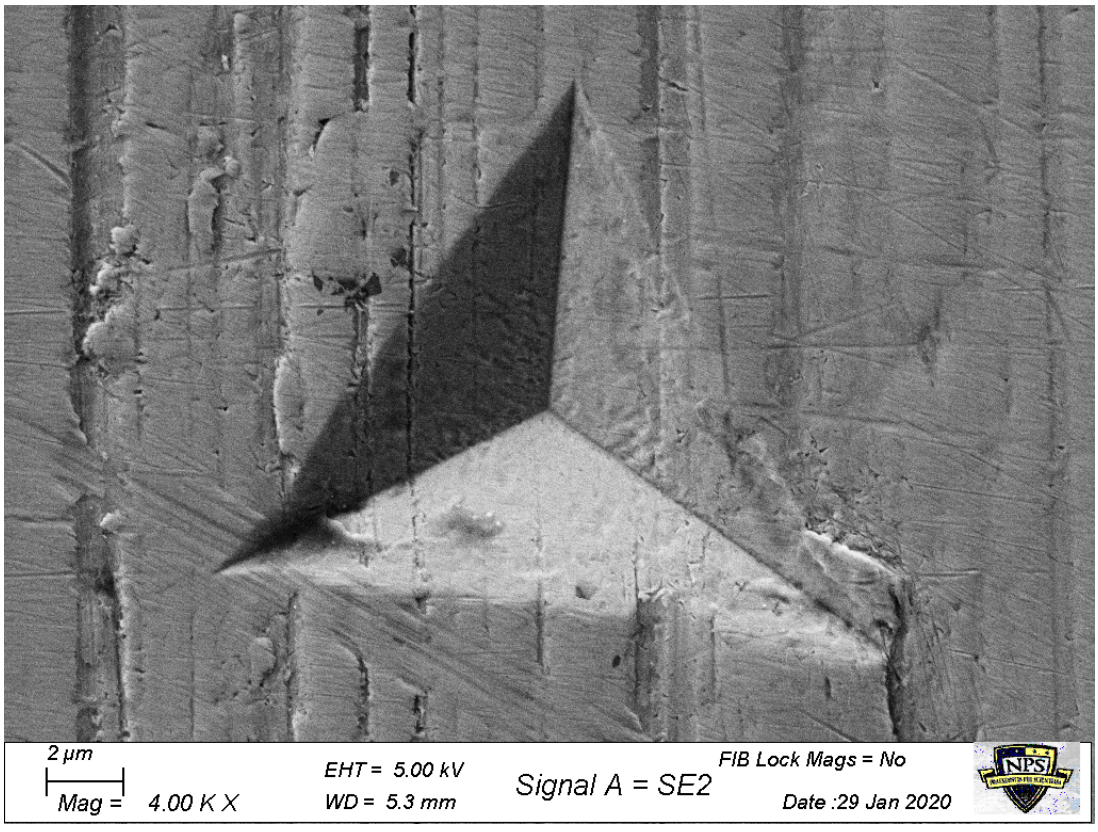

Figure 51. 500 mN Indentation Test Site on Control Sample

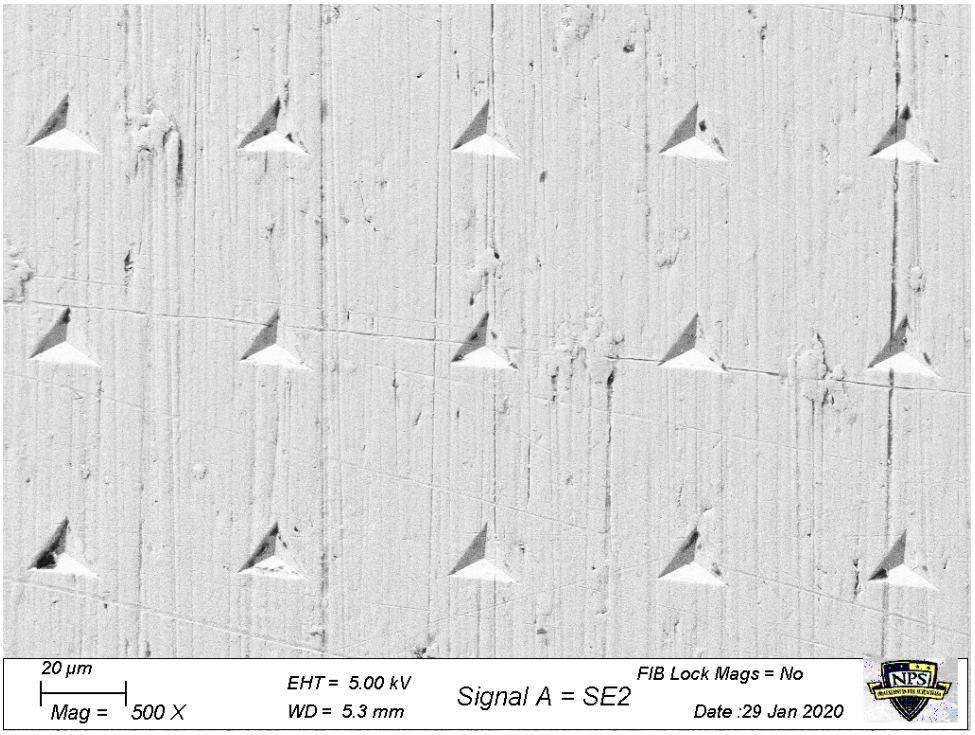

Figure 52. 500 mN Indentation Test Array on Control Sample

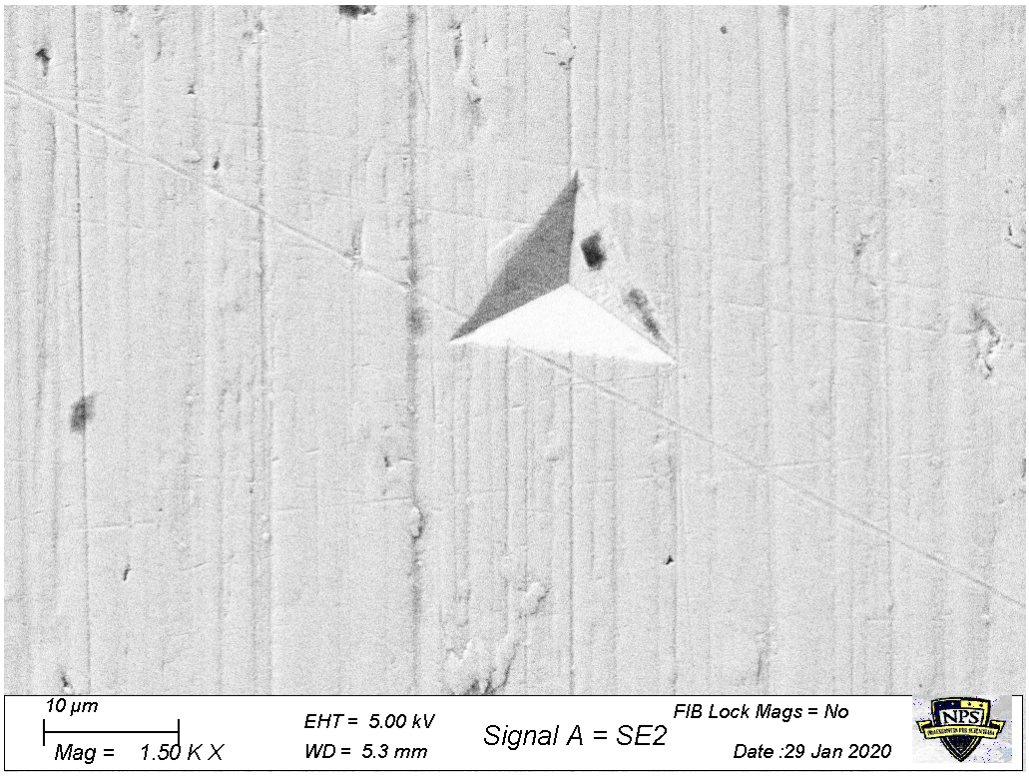

Figure 53. 500 mN Test Site on Control Sample with Defect

B. MECHANICAL PROPERTIES AND BEHAVIOR

Tabulated below in Table 3 and Table 4 are the results from the 3 mN indentation tests and the 500 mN indentation tests, respectively. The literature values obtained indicated that nano-indentation tests usually result in modulus of elasticity between 107.8 and 116.7 GPa for Ti-6Al-4V for samples with microcrystalline grains [58]. The result obtained for the control Ti-6Al-4V sample in the 500 mN indentation test was 112.662 GPa, and this fell well within the accepted literature values, indicating that the SLM processed Ti-6Al-4V alloy properties fell within the norm for this alloy. Based on the indentation test results, the addition of 1% Ta_2O_5 by volume to the Ti-6Al-4V matrix resulted in a 3.1% increase in modulus of elasticity based on the 500 mN results. This percent change nearly doubled to a 6.1% increase in the modulus of elasticity when considering using the 3 mN results. This is not surprising, as the reinforcing material can greatly increase the strength in a localized region when the Ta_2O_5 is present. It is also worth noting that the standard deviation of the modulus of elasticity for the 3 mN test was an order of magnitude larger for all samples, including the control, when compared to the standard deviation of the elastic modulus obtained during the 500 mN test. This variation was expected, and it occurred due to local variations in phases (α/β) and microstructural features such as phase morphology and localized porosity.

Both Ti-Al_2O_3 samples exhibited much lower hardness and elastic modulus when compared to the control sample. Based on these results, alumina may not be an ideal reinforcing constituent to add to additively manufactured Ti-6Al-4V and any further research would first require significant processing optimization studies. The use of nano Al_2O_3 may lead to reactions during processing that can induce poor interfacial characteristics between ceramic particulate and metal matrix, including localized micro/nano scale porosity. The Ti-Ta3 sample also exhibited a lower hardness and lower elastic modulus than either the Ti-Ta1 or the control. However, it is believed that this was due to more macroscopic porosity resulting from the failure to build properly rather and was not an indication that tantalum oxide is a poor reinforcing constituent for additively manufactured titanium since the Ti-Ta1 showed significant promising results when compared to the control sample. Improvements in powder flowability and processing can

likely overcome this and result in a build with improved structural integrity and enhanced mechanical properties.

Table 3. 3 mN Indentation Test Results

	Control	Ti-Ta1	Ti-Ta3	Ti-Al1	Ti-Al3
Mean Hardness at Max Load (GPa)	6.209	7.767	9.255	6.835	2.309
Standard Deviation of Hardness (GPa)	0.760	0.430	1.320	0.433	0.337
Mean Elastic Modulus at Max Load (GPA)	140.365	148.915	144.079	100.765	58.134
Standard Deviation of Elastic Modulus (GPa)	10.858	5.406	12.606	3.679	5.033

Table 4. 500 mN Indentation Test Results

	Control	Ti-Ta1	Ti-Ta3	Ti-Al1	Ti-Al3
Mean Hardness at Max Load (GPa)	4.459	6.070	4.227	1.522	0.408
Standard Deviation of Hardness (GPa)	0.294	0.204	0.0840	0.0671	0.0283
Mean Elastic Modulus at Max Load (GPA)	112.662	116.118	41.768	13.684	3.379
Standard Deviation of Elastic Modulus (GPa)	2.086	0.893	0.370	0.318	0.148

As seen in Figure 54-Figure 57, the addition of more reinforcing material for the composite specimens had the end result of decreased elastic modulus and strength for both the Ti-Al1 and Ti-Al3 samples. The Ti-Ta1 sample was definitely better than the control, whereas the Ti-Ta3 was only better than the control in the 3mN load case. Again, the fact that the Ti-Ta3 performed fine in the 3 mN loading but poorly in the 500mN loading leads to the conclusion that the difference in performance may have been a result of increased

macroscopic porosity due to the failed builds; this trend could potentially reverse itself if a better process to additively manufacture Ti-Ta3 composite powder was created.

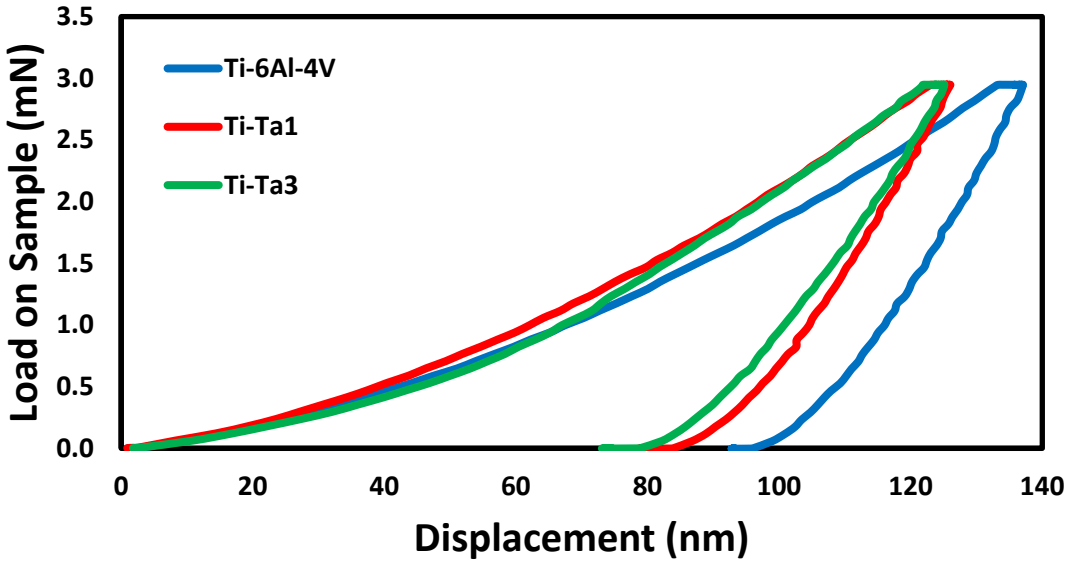

Figure 54. Load-Displacement Curve for Ti-6Al-4V and Ti-Ta_2O_5 Composites under Max Loading of 3mN

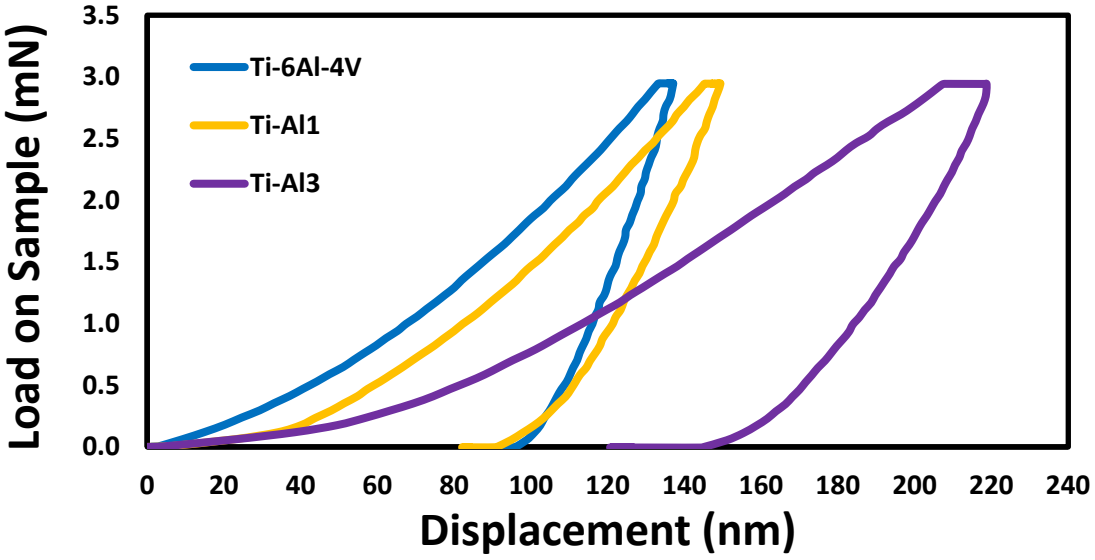

Figure 55. Load-Displacement Curve for Ti-6Al-4V and Ti-Al_2O_3 Composites under Max Loading of 3mN

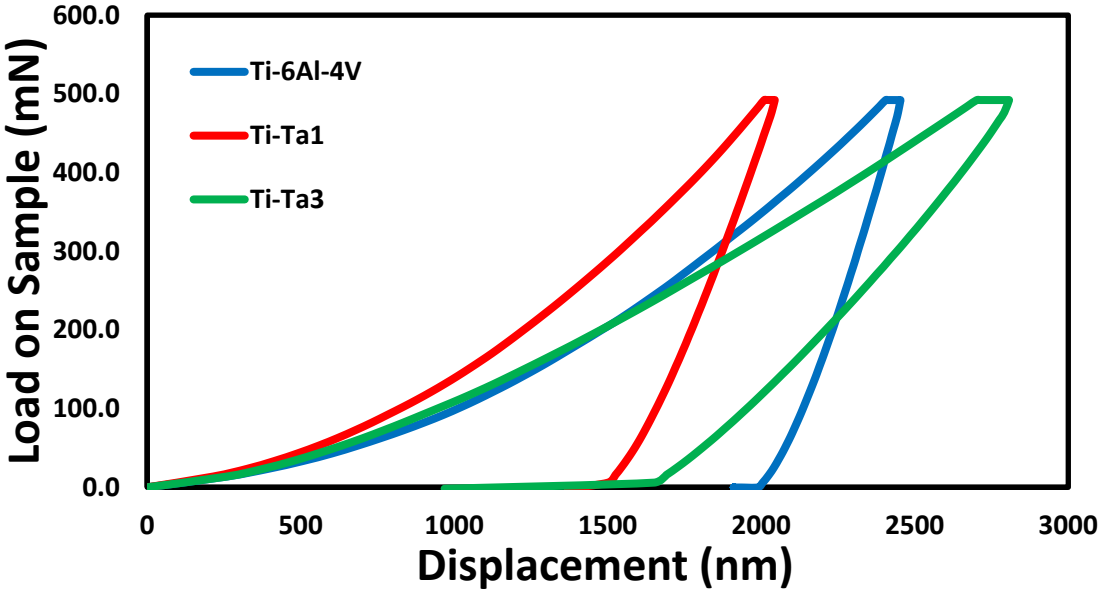

Figure 56. Load-Displacement Curve for Ti-6Al-4V and Ti-Ta_2O_5 Composites under Max Loading of 500mN

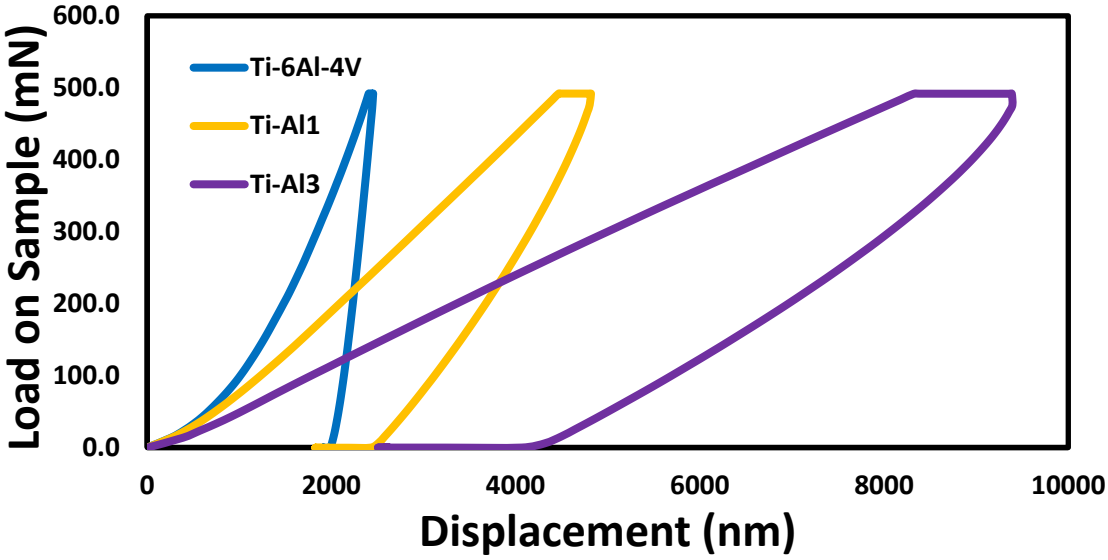

Figure 57. Load-Displacement Curve for Ti-6Al-4V and Ti-Al_2O_3 Composites under Max Loading of 500 mN

THIS PAGE INTENTIONALLY LEFT BLANK

V. OXIDATION BEHAVIOR

As mentioned previously, only the Ti-Ta1 and the control sample successfully produced cuboid specimens and were subjected to isothermal testing to measure their oxidation behavior and compare the performance with the base metal to the performance of the composite material. This chapter discusses the results of the oxidation testing.

A. ISOTHERMAL TESTING

The testing matrix for the isothermal tests was included in the background section as Table 2. To reiterate, composite and control samples were tested in atmosphere at 700, 900, and 1100 degrees Celsius for 4, 40, and 400 hours for a total of nine independent trials.

B. MASS CHANGES AND THICKNESS MEASUREMENTS

The results from the mass change measurements are tabulated in Table 5. These results were reported as grams gained per surface area. The base mass change and size measurements collected are included as Appendix A. Based on the oxidation weight change measurements alone, the Ti-Ta1 sample was determined to have increased oxidation resistance when compared to base Ti-6Al-4V at high temperatures or long exposure times. However, these weight gain measurements only give an incomplete picture of the true oxidation behavior of the composite materials, as will be demonstrated below in Section C: Evolution of Oxide Behavior. Likewise, the fact that the weight gain per surface area measurement was actually higher for the control sample than for the composite in the 40-hour 1100 degrees trial will be explained in Section C.

Table 5. Mass Change Measurements Collected from Isothermal Testing

Time (hours)	Temperature (Celsius)	Ti-6Al-4V oxidation (g/mm^2)	Ti-Ta1 oxidation (g/mm^2)
4	700	4.86E-06	6.04E-06
40	700	9.31E-06	1.62E-05
400	700	7.62E-05	6.82E-05
4	900	5.60E-05	6.14E-05
40	900	2.20E-04	1.53E-04
400	900	7.01E-04	5.17E-04
4	1100	2.30E-04	1.43E-04
40	1100	4.70E-04	6.83E-04
400	1100	1.77E-03	1.68E-03

Highlighted fields indicate which sample oxidized less in the given test. Thus, the control sample outperformed the composite at 4 hours 700 degrees, 40 hours 700 degrees, 4 hours 900 degrees, and 40 hours 1100 degrees.

C. EVOLUTION OF OXIDE STRUCTURE

After the oxidation weight change measurements were collected, the oxides were imaged under SEM and analyzed using EDS in order to learn more about how the oxidized metal formed and what it was primarily composed of. The SEM imaging led to an important observation: the composite samples actually had numerous internal cracks that oxidized, meaning that the values reported in Table 5 above are actually inaccurate portrayals of the true weight gain per surface area, since the composite materials had such high porosity that there were actually internal regions that were also exposed to the oxidizing environment. Images of some of these cracks are included below in Section 2. In particular, a large crack in the 40 hour 1100 degrees composite sample that oxidized was the reason why this sample had a higher weight gain per surface area measurement (see Table 5 and Figure 65), even though the composite clearly oxidized less when compared under SEM (see Figure 62 and Figure 63). EDS analysis lead to the conclusion that the oxide layer in the Ti-Ta1 samples had significant quantities of TaO, which may have helped contribute to the reduced total amount of oxidation.

1. Trends with Temperature and Time

The amount of oxidation correlated positively with both temperature and time of exposure, as displayed in Figure 58-Figure 61. This was the case for both the control sample and the composite. In Figure 60 and Figure 61, the 1100 degrees C 400 hour case produced an oxide so large it was unable to be completely imaged at any magnification—so the entire image in both of these two photos is in fact the oxide layer.

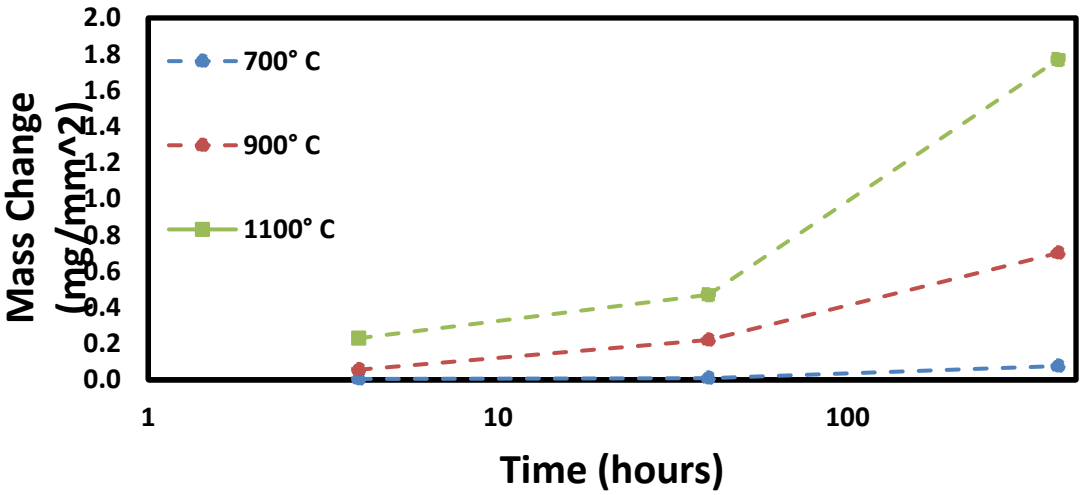

Figure 58. Ti-6Al-4V Oxidation Rate

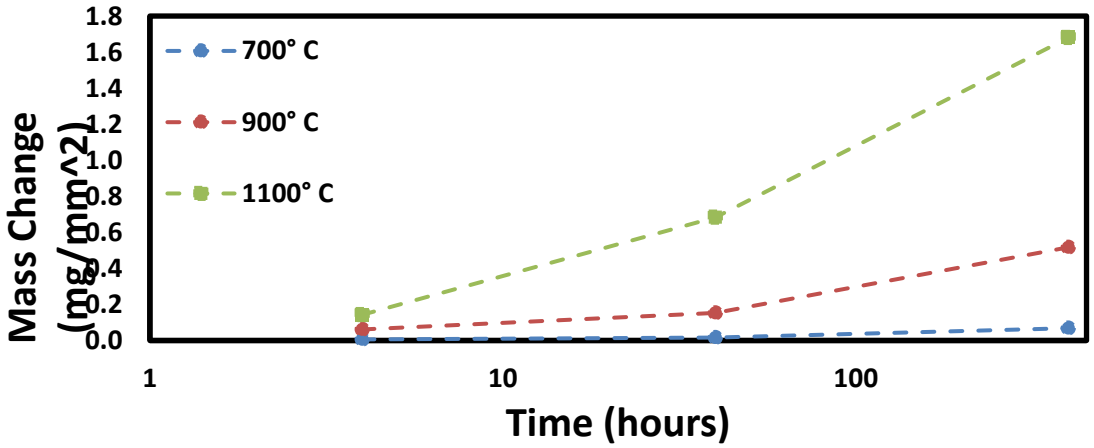

Figure 59. Ti-Ta1 Oxidation Rate

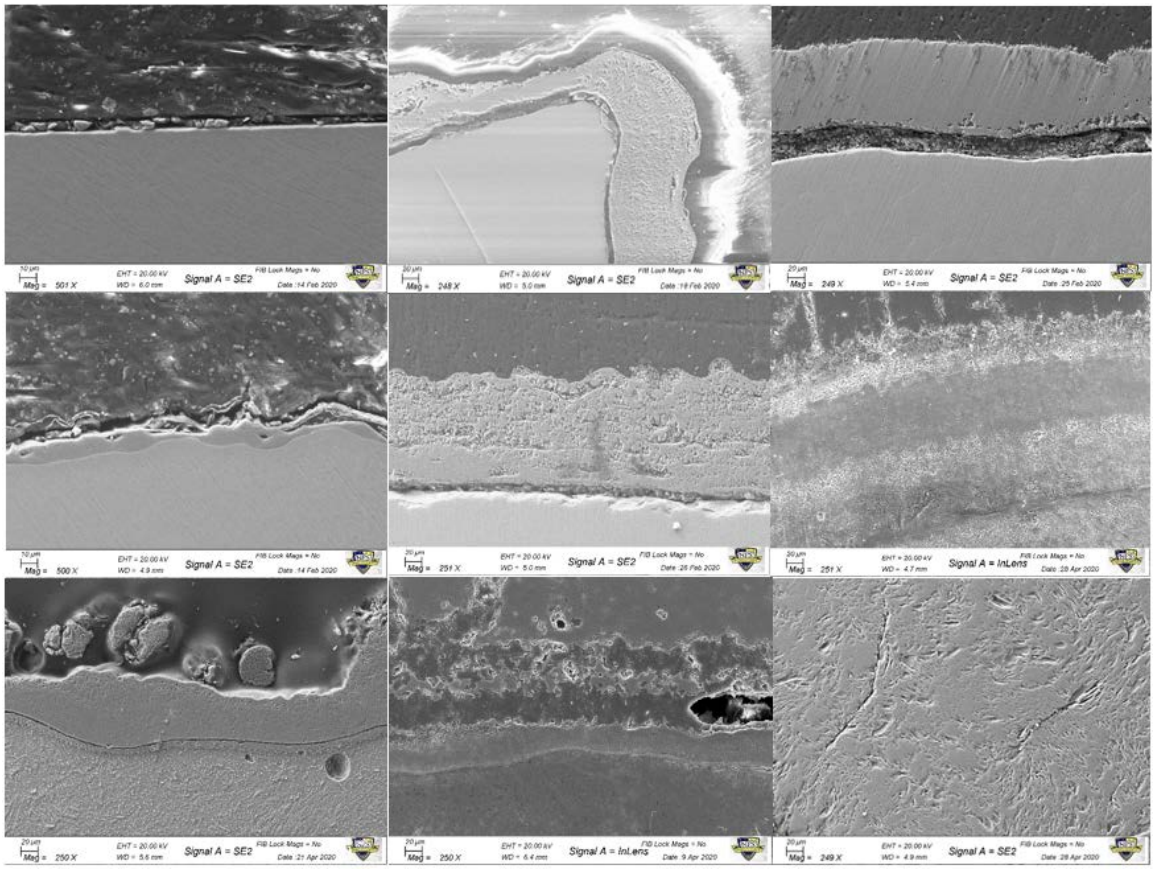

Top row: 700 degrees C, middle row: 900 degrees C, bottom row: 1100 degrees C, left column: 4 hours, middle column: 40 hours, and right column: 400 hours

Figure 60. Trends with Exposure Time and Temperature for Ti-6Al-4V

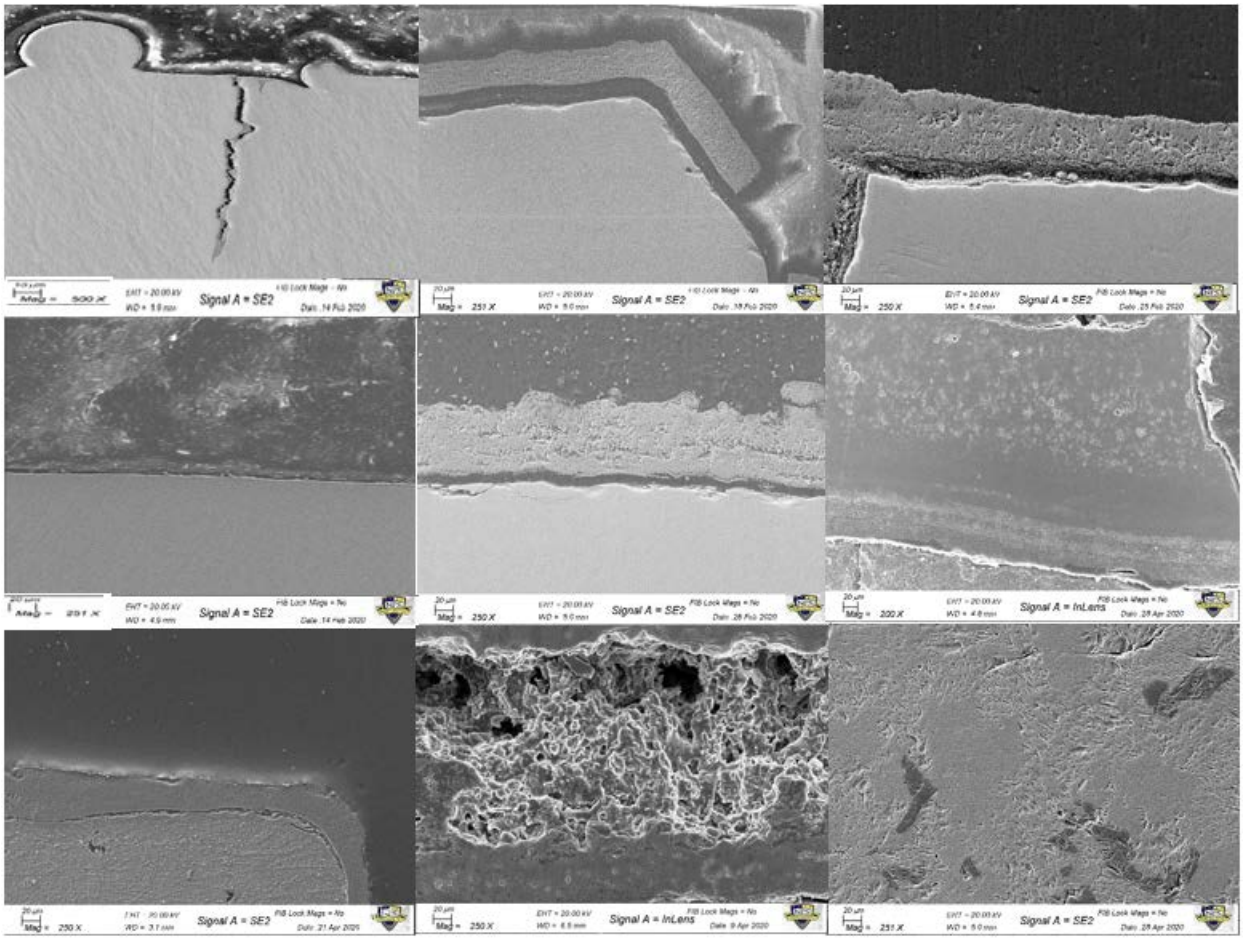

Top row: 700 degrees C, middle row: 900 degrees C, bottom row: 1100 degrees C, left column: 4 hours, middle column: 40 hours, and right column: 400 hours

Figure 61. Trends with Exposure Time and Temperature for Ti-Ta1

2. Comparison between Ti-Ta1 and Ti-6Al-4V Oxidation Behavior

The Ti-Ta1 composite specimens exhibited significantly less oxidation externally when compared to Ti-6Al-4V samples exposed to the same temperatures for the same amounts of time. Figure 62 and Figure 63 display the difference in oxidation on the external sides of the specimens. The Ti-6Al-4V oxide layer was twice as large as the oxide layer formed in the Ti-Ta1 samples. However, the weight changes were very similar or sometimes even higher for the Ti-Ta1 due to oxidation of internal cracks within the Ti-Ta1. Thus to fully realize up to a 50% oxidation reduction potentially offered by Ti-Ta1,

the internal cracking issue must first be solved through SLM processing optimization. Figure 64 and Figure 65 are images the internal cracks that oxidized in the Ti-Ta1 samples.

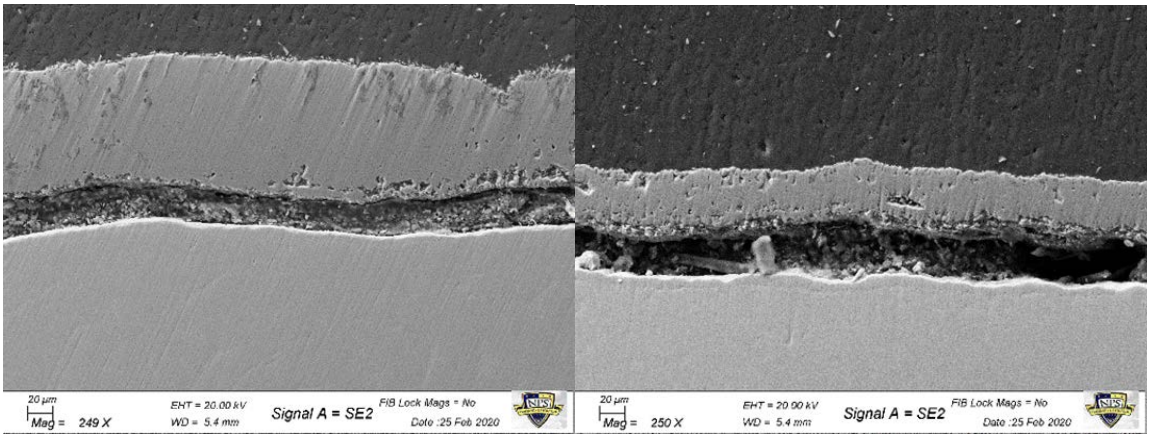

Left image is the Ti-6Al-4V oxide, right image is the Ti-Ta1 oxide

Figure 62. Comparison between Ti-6Al-4V and Ti-Ta1Oxide Formations for the 1100 Degrees C 4 Hours Specimens

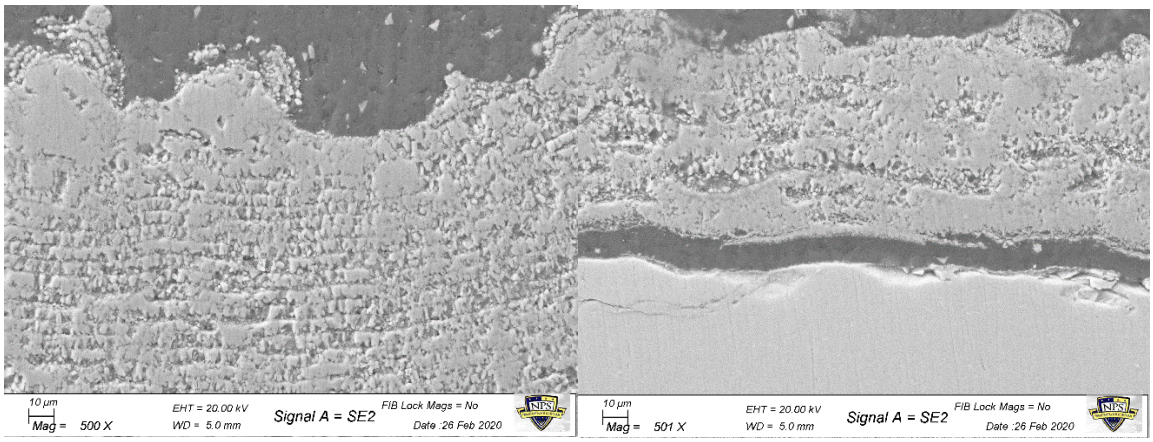

Left image is the Ti-6Al-4V oxide, right image is the Ti-Ta1 oxide

Figure 63. Comparison between Ti-6Al-4V and Ti-Ta1 Oxide Formations for the 900 Degrees C 40 Hours Specimens

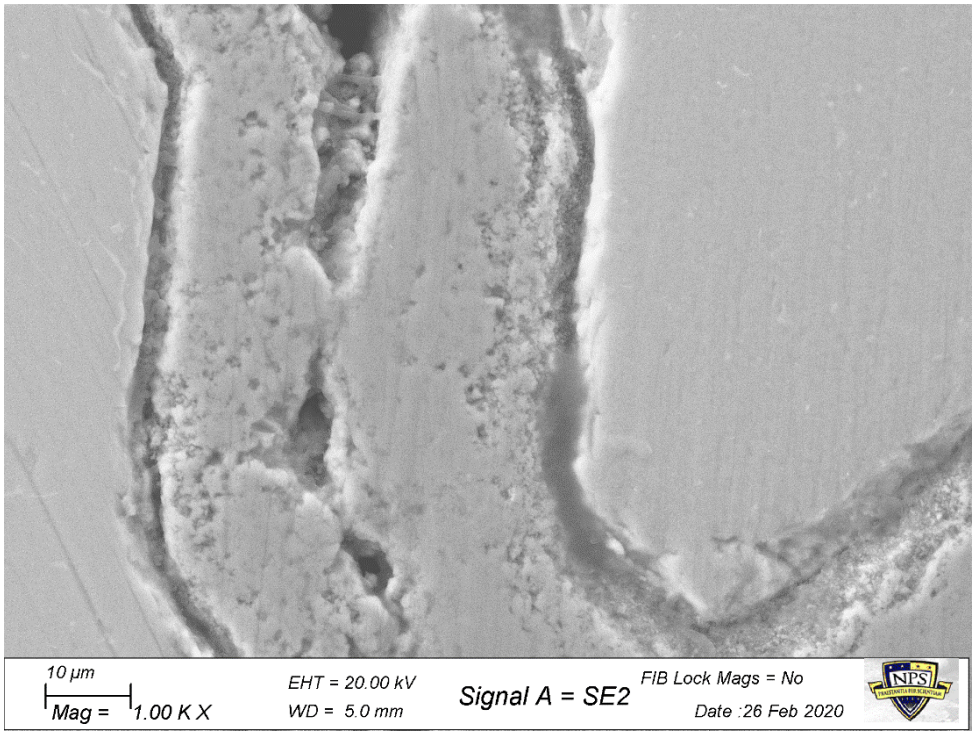

Figure 64. Internal Oxidation in 900 Degrees C 40 Hour

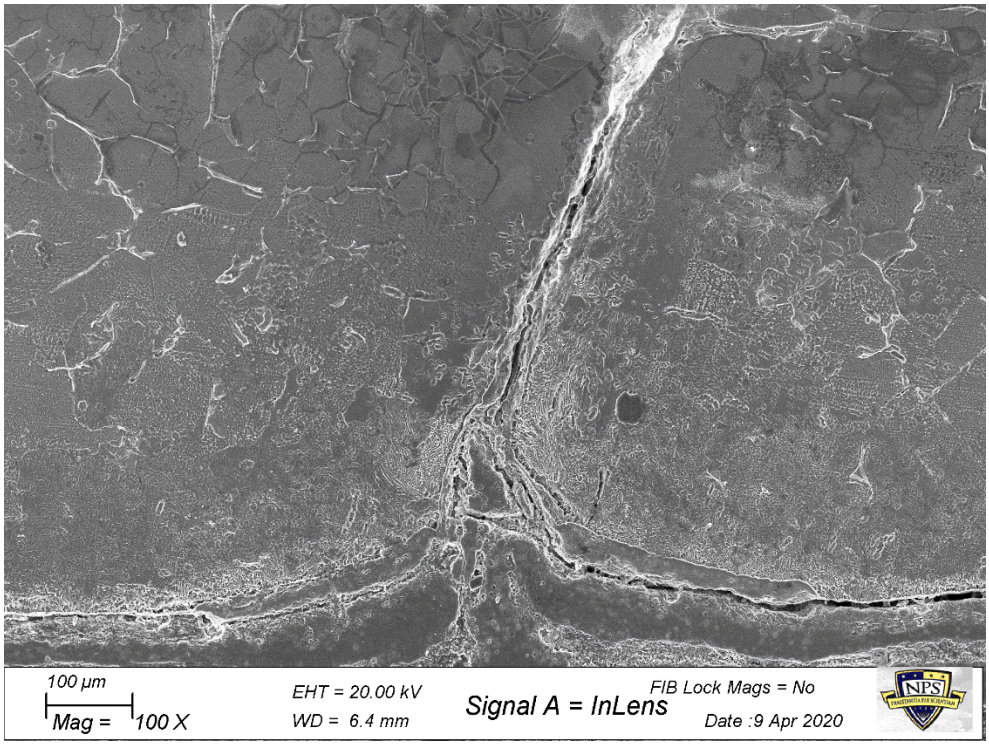

Figure 65. Massive Oxidized Internal Crack in 1100 Degrees C 40 Hour Specimen Resulting in Weight Discrepancy

3. EDS Analysis of Oxide Layer and Ti-Ta1 Oxidized Microstructure

The oxide layer within the Ti-Ta1 samples was determined to include significant amounts of tantalum via EDS, indicating that tantalum oxides were forming and partially making up the oxide layer. Interestingly, the tantalum within the oxide layer was not uniform. The tantalum was revealed to be highly segregated, as some regions were rich in well-dispersed tantalum oxides (see Figure 67), while other regions had low tantalum oxide content (see Figure 66), and other regions had only discrete tantalum particles (see Figure 68). This may be indicative of poorly dispersed tantalum within the feedstock powder; better dispersion of the reinforcing constituents could have potentially prevented this from occurring.

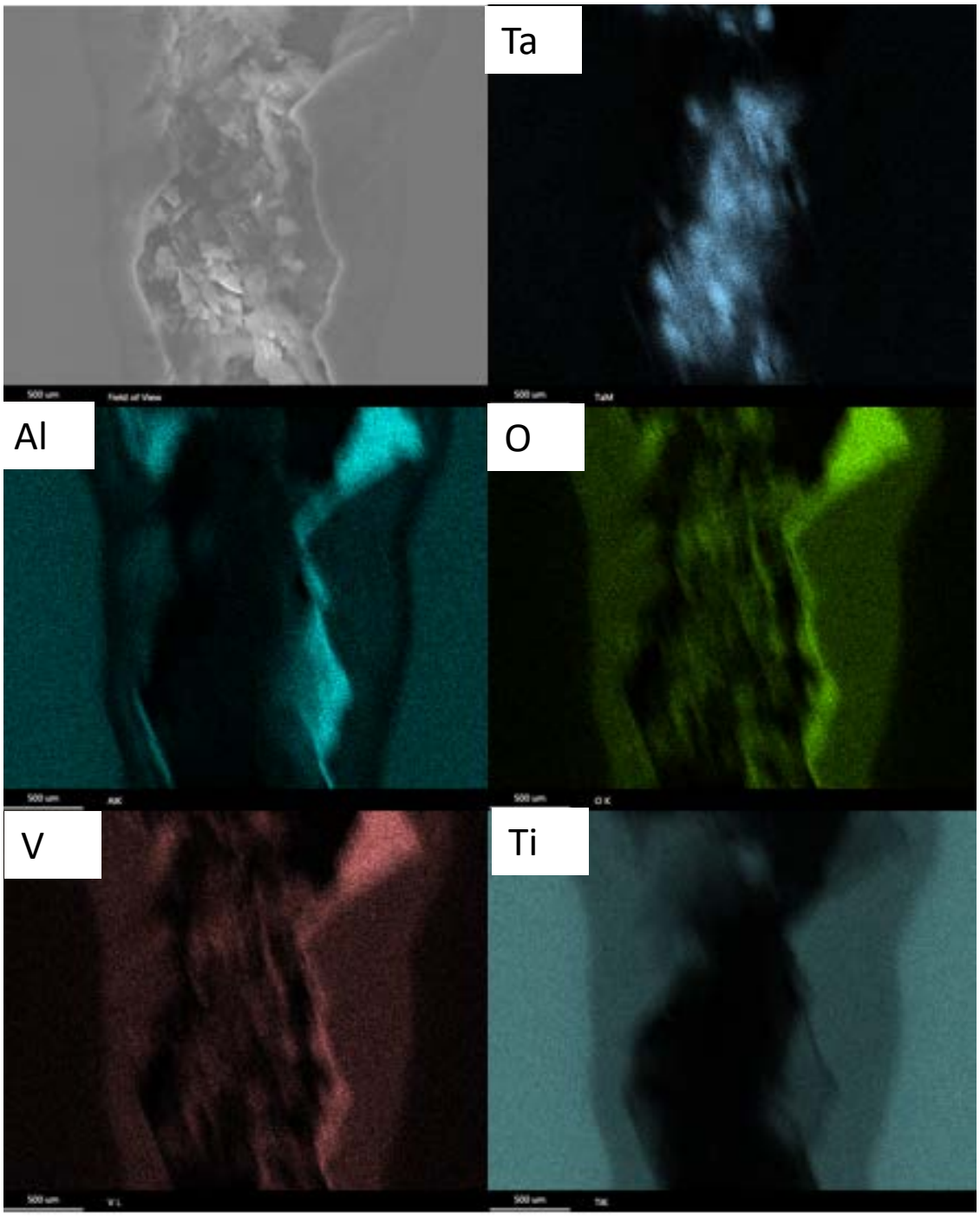

Figure 66. EDS Overlay of Well-Dispersed TaO within Ti-Ta1 700 Degrees 40 Hour Sample

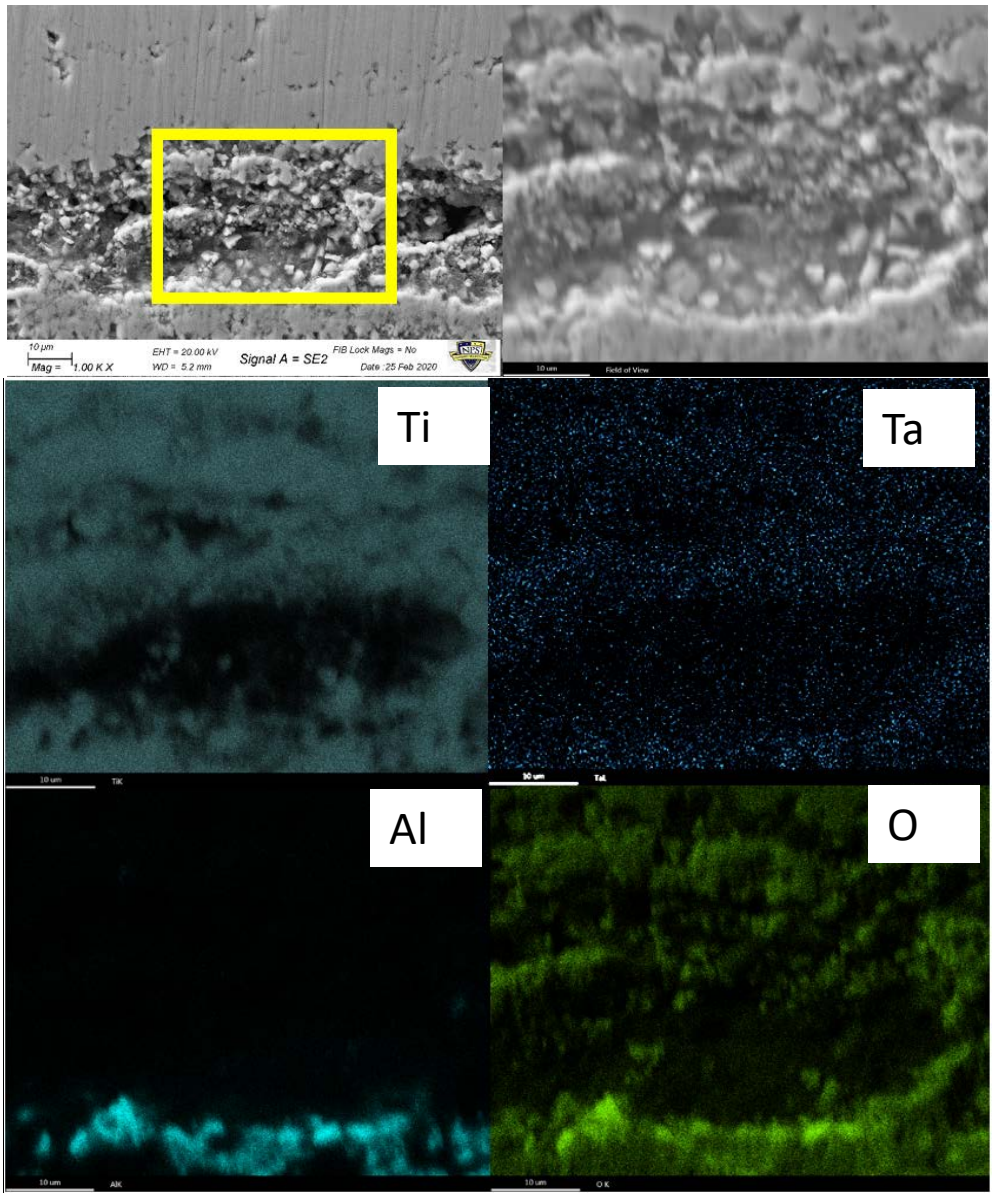

Figure 67. EDS Overlay of Oxide Layer with Low Tantalum Content within Ti-Ta1 1100 Degrees C 4 Hour Specimen

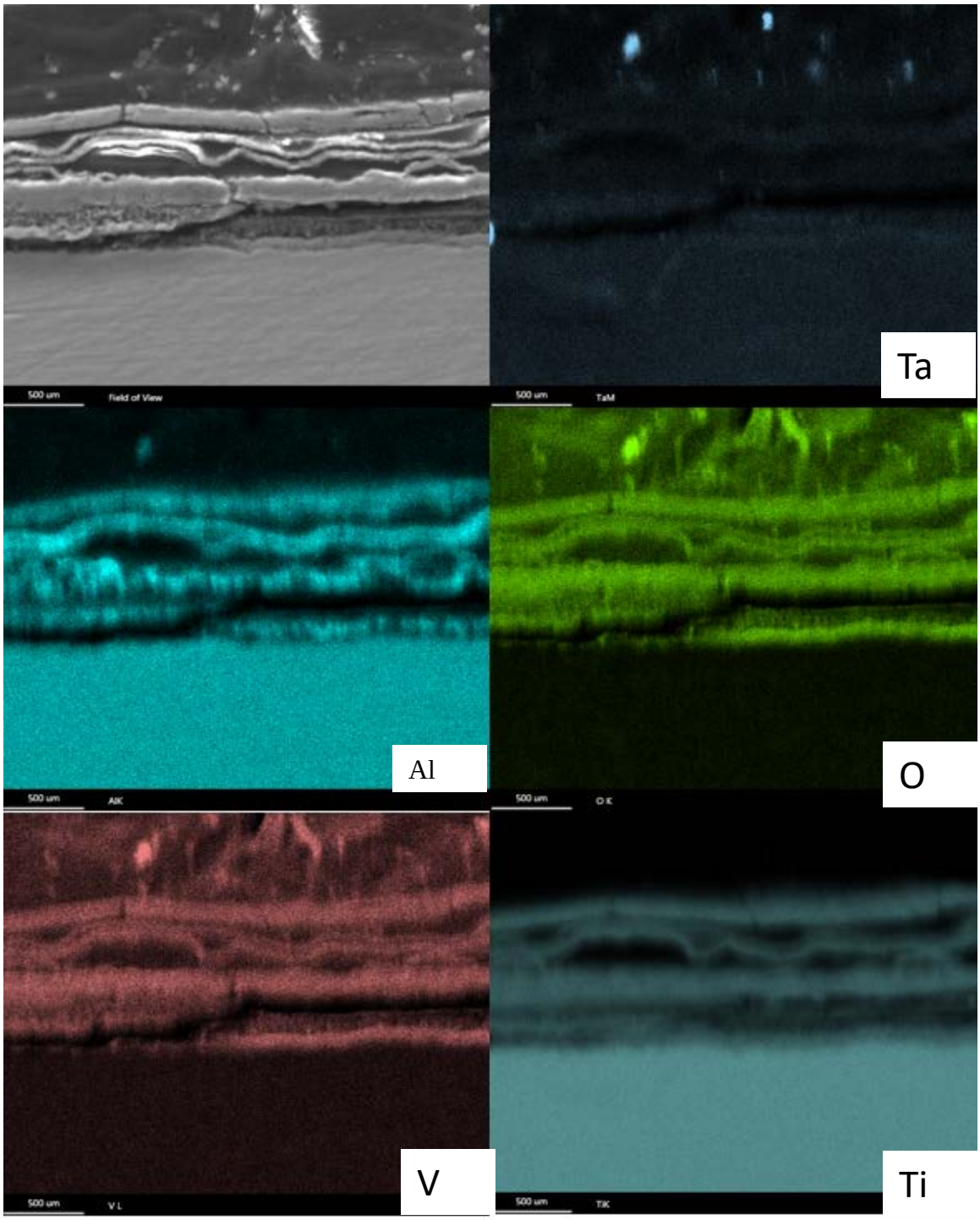

Figure 68. EDS Overlay of Concentrated Tantalum Particles within the Oxide Layer of Ti-Ta1 700 Degrees C 4 Hour Sample

Etched images of the oxidized samples (see Figure 69 and Figure 70) revealed significantly different microstructures when compared to the microstructure of the as as-

printed samples (see Figure 36 and Figure 40). The amount of α phase titanium has appeared to significantly decrease, whereas the amount β phase titanium has appeared to increase. Again, the relatively lighter, linearly patterned regions are regions of α phase titanium. This makes sense as the β phase is the BCC phase which precipitates at temperatures above 882 degrees Celsius, and these samples were oxidized at 1100 degrees Celsius. Additionally, large visible cracks are likely grain boundaries in the Ti-Ta1 sample whereas no cracks were visible within the control sample. These cracks are precursors to many of the oxidized internal cracks seen frequently in the Ti-Ta1 specimen.

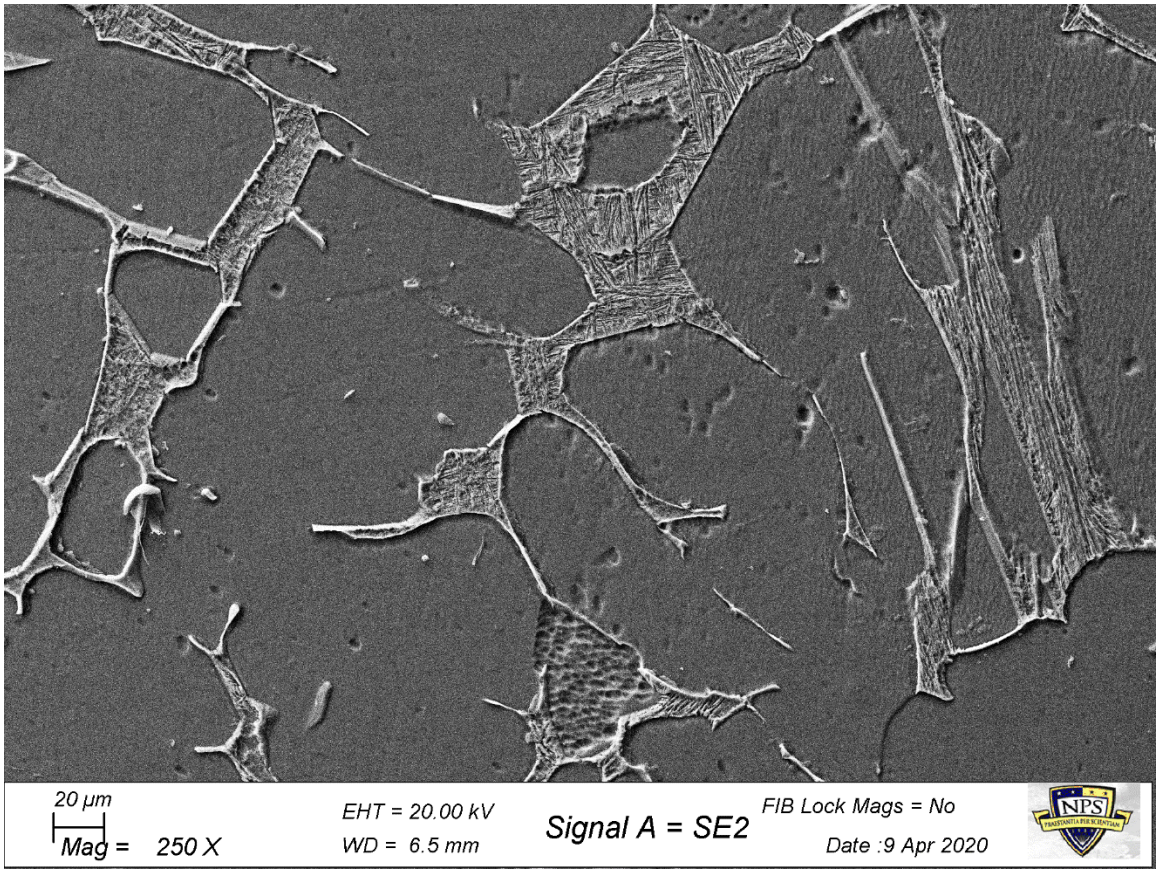

Figure 69. Microstructure within 1100 Degrees C 40 Hour Ti-6Al-4V Sample

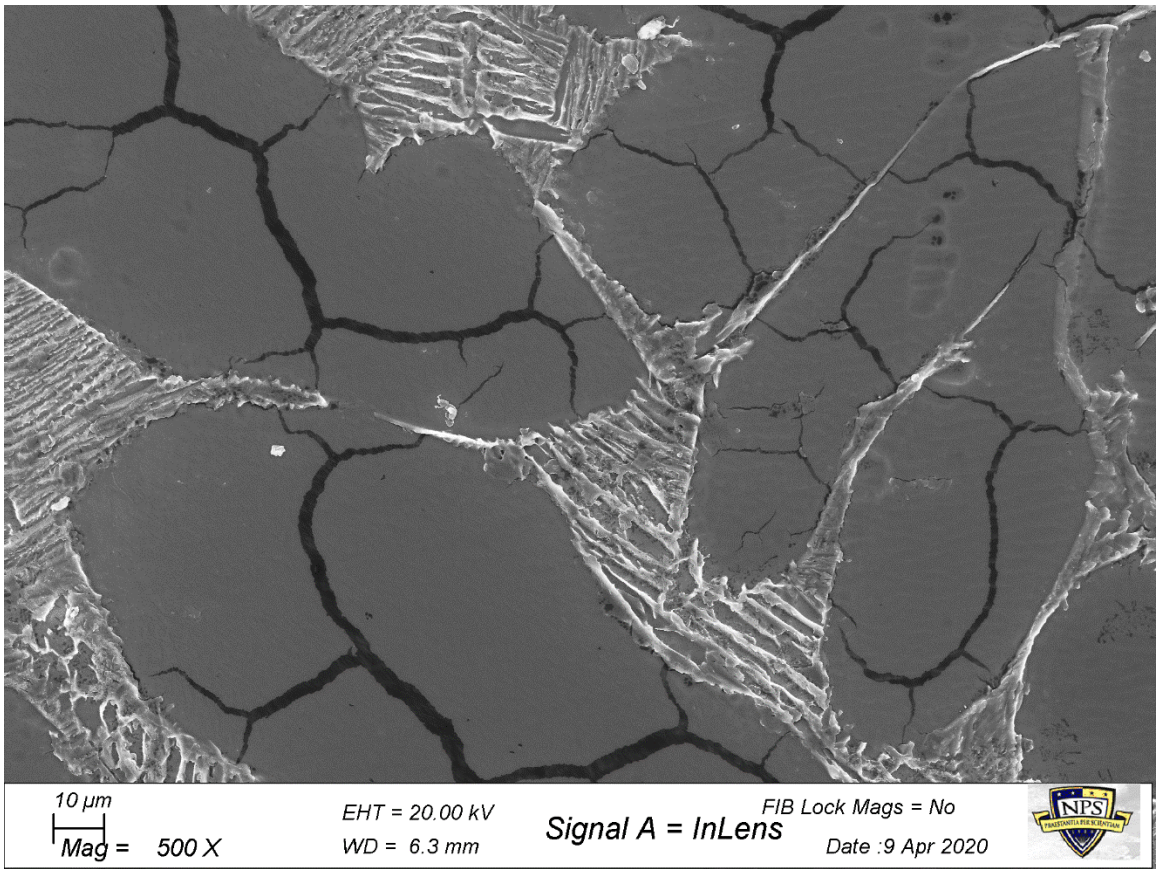

Figure 70. Microstructure within 1100 Degrees C 40 Hours Ti-Ta1 Specimen

THIS PAGE INTENTIONALLY LEFT BLANK

VI. CONCLUSIONS

A. SUMMARY OF RESULTS

This research demonstrated that SLM of the novel composite material Ti-6Al-4V reinforced with 1% by volume Ta_2O_5 produced components that exhibited better oxidation behavior and a higher elastic modulus when compared specimens produced via SLM with commercially pure Ti-6Al-4V powder, despite significant internal cracking within the novel composite material. Specifically, the Ti-Ta1 sample had almost 50% less thick oxidation layers on exposed surfaces when compared to the control Ti-6Al-4V sample, and the elastic modulus was about 3% higher on the nanoscale and 6% higher on the macroscale. Increasing the volume percentage of the reinforcing material to 3% for the titanium-tantalum oxide composite led to an incomplete build as a result of exacerbating powder flowability issues within the SLM fabrication process. Analysis of the incomplete build indicated that a Ti-Ta3 composite would need to address these processing issues to attain defect-free builds in order to realize any strengthening from the added oxide reinforcements. The Ti-Al1 and Ti-Al3 powders both resulted in incomplete builds as a result of reactivity issues and porosity on both the macro and nanoscale. Based on analysis of the incomplete builds, any future work with titanium alumina composites will require significant process optimization in order to address these issues in order to produce a sample with adequate mechanical properties.

B. SCOPE FOR FUTURE WORK

1. Optimization of Powder Flowability/Dispersion

One of the main issues noted in all four composite samples was porosity. Particularly in the Ti-Ta3 case, macro porosity led to incomplete printing of this powder. The potential for future work in this field could consist of coming up with a quantitative measurement system for powder flowability, then testing numerous HEBM settings and or other mixing techniques in order to determine which results in a composite powder with the greatest flowability. Ideally, the goal would be to produce a composite powder with flowability equal to or even higher than the commercial Ti-6Al-4V powder.

2. Optimization of Printing Parameters

Reactivity was an issue for the Ti-Al1 and Ti-Al3 samples, and this could potentially be avoided in the future through optimization of the SLM parameters. For example, a lower laser power could potentially still completely melt the titanium alloy without resulting in a reaction from the nanopowders. Furthermore, printing parameter optimization could also help eliminate the internal cracking issues within the Ti-Ta1 sample as a more complete melt would help reduce or eliminate the nanoscale porosity issues. This could eliminate the reactivity issues and allow for a complete build without significant defects such as cracks being present.

3. General Exploration of Reinforcement Materials

The promising results from the Ti-Ta1 sample suggest that SLM of titanium matrix composite materials is possible, and warrants further research into other reinforcement materials. The SLM of titanium alloy reinforced with SiC fibers or carbon nanotubes could be potential avenues for future research.

4. Scale-Up Volume Percentage of Oxide Particulates

1% and 3% by volume is a low quantity of reinforcing material. Once the processing issues have been addressed, the natural next step for this research would be to gradually increase the volume percentages of these materials and determine the resultant mechanical properties from samples built from these composite powders. It is conceivable that a final completed part could have as high as 25% by volume of the reinforcing constituent.

APPENDIX. RAW ISOTHERMAL MEASUREMENTS

Specimen Tested	side (mm)	side (mm)	width (mm)	weight (g)	%increase per surface area g/mm^2
Case 1					
Before					
Pure	9.91	10.00	3.80	1.6034	left
1% Ta	9.91	9.94	3.80	1.6163	right
After					
Pure	9.91	10.00	3.80	1.6051	0.00000486
1% Ta	9.91	9.92	3.80	1.6184	0.0000060
Case 2 Before					
Pure	9.89	9.90	3.81	1.6043	
1% Ta	9.94	9.99	3.80	1.6128	
After					
Pure	9.8	9.9	3.8	1.6075	0.000009
1% Ta	9.9	9.9	3.8	1.6184	0.000016
Case 3 Before					
Pure	9.9	9.9	3.8	1.5911	
1% Ta	9.8	9.9	3.7	1.5716	
After					
Pure	9.99	9.98	3.88	1.6181	0.000076
1% Ta	10.05	10.0	3.77	1.5957	0.000068
Case 4 Before					
Pure	9.9	9.9	3.85	1.6066	
1% Ta	9.86	9.83	3.76	1.5890	
After					
Pure	9.9	9.9	3.8	1.6212	0.000042
1% Ta	10	9.9	3.7	1.6063	0.000050
Case 5 Before					
Pure	9.8	9.8	3.7	1.6131	
1% Ta	9.8	9.8	3.7	1.5898	

After					
Pure	10.2	10.1	3.9	1.6934	0.000220
1% Ta	10.0	10.0	3.8	1.6438	0.000153
Case 6 Before					
Pure	9.8	9.9	3.8	1.6401	
1% Ta	9.8	9.8	3.6	1.5728	
After					
Pure	10.6	10.4	4	1.7586	0.000305
1% Ta	10.1	10.1	3.8	1.6746	0.000285
Case 7 Before					
Pure	9.9	9.8	3.7	1.6002	
1% Ta	9.8	9.9	3.6	1.5604	
After					
Pure	10.2	10.15	3.98	1.6815	0.000220
1% Ta	10.13	10.08	3.85	1.6176	0.000159
Case 8 Before					
Pure	9.93	9.88	3.75	1.5857	
1% Ta	9.87	9.89	3.63	1.5468	
After				*below was a bad trial, stuck to plate	
Pure*	9.98	9.98	3.72	1.6585	0.000209
1% Ta	10.8	10.8	4.33	1.8693	0.000768
Case 9 Before					
Pure	9.81	9.77	3.71	1.5954	
1% Ta	7.41	9.79	3.69	1.2279	
After					
Pure	12.79	12.65	6.26	2.7323	0.001771
1% Ta	9.95	12.17	6.09	2.0867	0.001679

LIST OF REFERENCES

[1] T. Wohlers, “History of additive manufacturing,” *Wohlers Report*, vol. 24, no. 2014, p. 118, 2014.

[2] M. Shellabear, “DMLS-Development history and state of the art,” *Laser Assisted Netshape Engineering 4, Proceedings of the 4th Lane*, pp. 21–24, 2004.

[3] Conteo AG, “Laser Sintering (LS),” Additively, 2020. [Online]. Available: https://www.additively.com/en/learn-about/laser-sintering. [Accessed September 2019].

[4] C. Noon, “GE Reports,” 19 June 2018. [Online]. Available: https://www.ge.com/reports/hot-off-press-3d-printing-pushed-turbine-new-highs/. [Accessed 5th December 2019].

[5] S. Rafi, ““Microstructures and mechanical properties of Ti6Al4V parts fabricated by selective laser melting and electron beam melting.”,” *Journal of Materials Engineering and Performance 22, no. 12*, pp. 3872–3883, 2013.

[6] T. D. Ngo, “Additive manufacturing (3D printing): A review of materials, methods, applications and challenges,” *Composites Part B: Engineering*, vol. 143, pp. 172–196, 2018.

[7] M. Norfolk, “Solid-state additive manufacturing for heat exchangers,” *JOM*, vol. 67, no. 3, pp. 655–659, 2015.

[8] M. Vaezi, “A Review on 3D Micro-additive Manufacturing Technologies,” *International Journal of Advanced Manufacturing Technology (0268-3768), 67 (5-8)*, p. p. 1721, August, 2013.

[9] H. Asgari, “On microstructure and mechanical properties of additively manufactured AlSi10Mg_200C using recycled powder,” *Materials Science and Engineering: A*, vol. 707, pp. 148–158, 2017.

[10] O. A. Quintana, “Effects of reusing Ti-6Al-4V powder in a selective laser melting additive system operated in an industrial setting,” *JOM*, vol. 70, no. 9, pp. 1863–1869, 2018.

[11] J. Allen, “An investigation into the comparative costs of additive manufacture vs. machine from solid for aero engine parts,” Rolls-Royce PLC Derby (UK), 2006.

[12] J. C. Ramme, T. Roehling et al. “Laser Intensity Profile Effects on the Solidification Microstructure of Ti-6Al-4V and Ti-5553,” Lawrence Livermore National Lab. (LLNL), Livermore, CA (United States), 2018.

[13] N. Kumbhar and A. Mulay, “Post processing methods used to improve surface finish of products which are manufactured by additive manufacturing technologies: A review,” *Journal of The Institution of Engineers (India): Series C,* vol. 99, no. 4, pp. 481–487, 2018.

[14] V. A. R. Henriques, P. P. d. Campos, C. A. A. Cairo and J. C. Bressiani, “Production of titanium alloys for advanced aerospace systems by powder metallurgy,” *Materials Research,* vol. 8, no. 4, pp. 443–446, 2005.

[15] R. Pederson, “Microstructure and phase transformation of Ti-6Al-4V,” Luleå tekniska universitet, 2002.

[16] Kyocera, “Titanium Microstructure,” Solid Carbide Tools, 2020. [Online]. Available: https://kyocera-sgstool.co.uk/titanium-resources/titanium-information-everything-you-need-to-know/titanium-microstructure/. [Accessed 12 March 2020].

[17] A. C. Karaoglanli, “Thermal shock and cycling behavior of thermal barrier coatings (TBCs) used in gas turbines,” *Progress in Gas Turbine Performance*, pp. 237–260, 2013.

[18] J. Gilbert, “The uses of titanium,” *Materials Science and Technology*, vol. 1, no. 4, pp. 257–262, 1985.

[19] T. Clyne and P. Withers, An introduction to metal matrix composites, Cambridge University Press, 1995.

[20] S. Suresh, Fundamentals of metal-matrix composites, Elsevier, 2013.

[21] Endeavor Business Media LLC, “Metal-Matrix Composites,” Machine Design, 15 November 2002. [Online]. Available: https://www.machinedesign.com/materials/article/21812641/metalmatrix-composites. [Accessed 14 March 2020].

[22] W. Hunt, “Metal Matrix Composites,” *Mechanical Engineering-New York and Basel-Marcel Dekker-*, pp. 293–300, 1997.

[23] A. V. Rane, “Methods for synthesis of nanoparticles and fabrication of nanocomposites,” in *Synthesis of Inorganic Nanomaterials*, Elsevier, 2018, pp. 121–139.

[24] M. S. El-Eskandarany, “Recent developments in the fabrication, characterization and implementation of MgH 2-based solid-hydrogen materials in the Kuwait Institute for Scientific Research,” *RSC Advances*, vol. 9, no. 18, pp. 9907–9930, 2019.

[25] N. Govindaraju, “Synthesis and properties of boron nitride nanotubes,” in *Nanotube Superfiber Materials*, Elsevier, 2014, pp. 243–265.

[26] T. Barrett, “The Future of Metal Is in Matrix Composites,” Machine Design, 1 June 2017. [Online]. Available: https://www.machinedesign.com/materials/article/21835569/the-future-of-metal-is-in-matrix-composites. [Accessed 14 March 2020].

[27] R. M. Hunt, “Selective laser sintering of MA956 oxide dispersion strengthened steel,” *Journal of Nuclear Materials*, vol. 464, pp. 80–85, 2015.

[28] S. e. a. Kundu, “Direct metal laser sintering of TiN reinforced Ti6Al4V alloy based metal matrix composite: Fabrication and characterization,” *The International Journal of Advanced Manufacturing Technology*, vol. 97, no. 5–8, pp. 2635–2646, 2018.

[29] Malcolm Ward-Close, “Titanium metal matrix composites,” in *Aerospace Materials*, Boca Raton, CRC Press, 2001, pp. 241–252.

[30] B. Vasile, A. Birca, V. Surdu, I. Neacsu and A. Nicoară, “Ceramic Composite Materials Obtained by Electron-Beam Physical Vapor Deposition Used as Thermal Barriers in the Aerospace Industry,” *Nanomaterials*, vol. 10, no. 2, p. 370, 2020.

[31] M. D. Hayat, “Titanium metal matrix composites: An overview,” *Composites*, vol. 121, pp. 418–438, 2019.

[32] M. S. El-Eskandarany, “Introduction,” in *Mechanical Alloying (Second Edition)*, William Andrew Publishing, 2015, pp. 1–12.

[33] R. Ayers, “The Application of Self-Propagating High-Temperature Synthesis of Engineered Porous Composite Biomedical Materials,” *Materials and Manufacturing Processes*, vol. 22, no. 4, pp. 481–488, 2007.

[34] W. E. Frazier, “Metal Additive Manufacturing: A Review.,” *J. of Materi Eng and Perform*, vol. 23, pp. 1917–1928, 2014.

[35] C. Leyens, “Continuous fiber reinforced titanium matrix composites: fabrication, properties, and applications,” *Advanced Engineering Materials*, vol. 5, no. 6, pp. 399–410, 2003.

[36] B. McWilliams, “Mechanical response of discontinuous ceramic fiber reinforced metal matrix composites under quasi-static and dynamic loadings,” *Materials Science and Engineering: A,* vol. 590, pp. 21–29, 2014.

[37] G. Yi, “Oxidation behavior of in situ synthesized (TiB TiC)/Ti–6Al–4V composites from Ti–B4C–C and Ti–TiB2–TiC systems,” *Journal of Materials Research,* vol. 34, no. 10, pp. 1762–1772, 2019.

[38] L. Yang, “Oxidation of Ti3SiC2at 1000°CinAi,” *Oxidation of Metals,* vol. 59, no. 1, pp. 155–165, 2003.

[39] M. Pradeep Gudlur, “On characterizing the mechanical properties of aluminum-alumina composites,” *Materials Science & Engineering A,* vol. 590, pp. 352–359, 2014.

[40] A. Maho, S. Detriche, Delhalle and Joseph, “Sol–gel synthesis of tantalum oxide and phosphonic acid-modified carbon nanotubes composite coatings on titanium surfaces,” *Materials Science and Engineering C,* vol. 33, pp. 2686–2697, 2013.

[41] E. Schlenther, “Fracture toughness and corrosion behaviour of infiltrated,” *Materials Science & Engineering A,* vol. 590, pp. 132–139, 2014.

[42] R. Tressler, T. Moore and R. Crane, “Reactivity and interface characteristics,” *Journal of Materials Science,* vol. 8, pp. 151–161, 1973.

[43] C. F. Gutierrez-Gonzalez and E. Fernandez-Garcia, “Processing, spark plasma sintering, and mechanical behavior,” *Journal Of Material Science,* vol. 49, pp. 3823–3830, 2014.

[44] M. Hoseini and M. Meratian, “Tensile properties of in-situ aluminium–alumina composites,” *Materials Letters,* vol. 59, no. 27, pp. 3414–3418, 2005.

[45] A. Maho, S. Linden and S. Detriche, “Tantalum oxide/carbon nanotubes composite coatings on titanium, and their functionalization with organophosphonic molecular films: A high quality scaffold for hydroxyapatite growth,” *Journal of Colloid and Interface Science,* vol. 371, pp. 150–158, 2012.

[46] C. Zhu, A. Javed and P. Li, “A study of the microstructure and oxidation behavior of alumina/yttria-stabilized zirconia (Al2O3/YSZ) thermal barrier coatings,” *Surface and Coatings Technology,* vol. 212, pp. 214–222, 2012.

[47] Y. Hu, “Laser deposition-additive manufacturing of in situ TiB reinforced titanium matrix composites: TiB growth and part performance,” *The International Journal of Advanced Manufacturing Technology,* vol. 93, no. 9–12, pp. 3409–3418, 2017.

[48] Y. Hu, W. Cong, X. Wang and Y. Li, “Laser deposition-additive manufacturing of TiB-Ti composites with novel three-dimensional quasi-continuous network microstructure: effects on strengthening and toughening,” *Composites Part B: Engineering,* vol. 133, pp. 91–100, 2018.

[49] N. Kang, P. Coddet and Q. Liu, “In-situ TiB/near α Ti matrix composites manufactured by selective laser melting,” *Additive Manufacturing,* vol. 11, pp. 1–6, 2016.

[50] E. Sheydaeian and E. Toyserkani, “A new approach for fabrication of titanium-titanium boride periodic composite via additive manufacturing and pressure-less sintering,” *Composites Part B: Engineering,* vol. 138, pp. 140–148, 2018.

[51] A. Levy, A. Miriyev and A. Elliott, “Additive manufacturing of complex-shaped graded TiC/steel composites,” *Materials & Design,* vol. 118, pp. 198–203, 2017.

[52] J. Mogonye and A. Srivastava, “Solid/self-lubrication mechanisms of an additively manufactured Ni–Ti–C metal matrix composite,” *Tribology Letters,* vol. 64, no. 3, p. 37, 2016.

[53] H. Attar and K. Damon, “Recent developments and opportunities in additive manufacturing of,” *International Journal of Machine Tools and Manufacture,* vol. 133, pp. 85–102, 2018.

[54] R. M. Mahamood and E. T. Akinlabi, “Heat affected zone Relationship with processing parameter in Additive Manufacturing Process,” *Materials Today: Proceedings,* vol. 5, no. 9, pp. 18362-18367, 2018.

[55] Electro Optical Systems, “EOS M 100 - Ideal entry level model for industrial 3D printing,” October 2018. [Online]. Available: https://www.eos.info/eos-m-100. [Accessed 14 April 2020].

[56] M. Fukuhara and A. Sanpei, “Elastic moduli and internal frictions of Inconel 718 and Ti-6AI-4V as a function of temperature,” *Journal of Materials Science Letters,* vol. 12, pp. 1122–1124, 1993.

[57] W. Ashraf, J. Olek and V. Atakan, “Chemo-Mechanical Comparison of the Carbonation and Hydration Reaction Products of Synthetic Tricalcium Silicate (C3S),” in *Brittle Matrix Composites 11*, Warsaw, Poland, 2015.

[58] K. Trofimov, ““Elastic properties of the titanium alloy Ti-6Al-4V.”,” *Письма о материалах* , vol. 5, no. 1, pp. 67–69, 2015.

[59] D. Ziental, “Titanium Dioxide Nanoparticles: Prospects and Applications in Medicine,” *Nanomaterials,* vol. 10, no. 2, p. 387, 2020.

[60] National Research Council, Metal-Matrix Composites: Status and Prospects, Washington, DC: The National Academies Press, 1974.

[61] H. Tang, “Effect of powder reuse times on additive manufacturing of Ti-6Al-4V by selective electron beam melting,” *JOM*, vol. 67, no. 3, pp. 555–563, 2015.

[62] W. Koop, “Metal matrix composites structural design experience,” in *26th Joint Propulsion Conference*, Orlando, 1990.

[63] S. Luo, “Recent Advances in the Design and Fabrication of Strong and Ductile (Tensile) Titanium Metal Matrix Composites,” *Advanced Engineering Materials*, vol. 21, no. 7, p. 1801331, 2019.

[64] B. Lee, “ “Oxidation of Titanium and Ti/(TiB+TiC) Composite”,” *Adv. Technol. Innov.*, vol. 2, no. 4, pp. 130–132, 2017.

[65] A. S. Namini and M. Azaadbeh, “Microstructural characterisation and mechanical properties of spark plasma-sintered TiB2-reinforced titanium matrix composite,” *Powder Metallurgy*, vol. 60, no. 1, pp. 22–32, 2017.

INITIAL DISTRIBUTION LIST

1. Defense Technical Information Center
   Ft. Belvoir, Virginia

2. Dudley Knox Library
   Naval Postgraduate School
   Monterey, California